REINFORCED EARTH

Reinforced Earth

T. S. INGOLD

BSc, MSc, PhD, DIC, MICE, MIHE,
MASCE, MSocIS(France), FGS

Chief Engineer, Ground Engineering Ltd
Visiting Professor, Department
of Civil Engineering, The
Queen's University, Belfast

Thomas Telford Ltd, London, 1982

Published by Thomas Telford Ltd, Telford House, PO Box 101,
26–34 Old Street, London EC1P 1JH

ISBN: 0 7277 0089 8

Photoset, printed and bound in Great Britain by
Redwood Burn Limited, Trowbridge, Wiltshire

Publishers' Note

The writer of the foreword to this book, M. H. Vidal, the French architect and civil engineer, is the grantee of various UK patents relating to the construction of REINFORCED EARTH structures. Additionally, and subsequent to the grant of M. Vidal's principal patents, patents relating to the design and construction of internally mechanically stablized earth structures have been granted to a variety of other people and organizations.

At the time of publication, REINFORCED EARTH is the trade name of Reinforced Earth Company Limited, and the term REINFORCED EARTH is the subject of a British trademark application by that company which is M. Vidal's exclusive licensee in Britain.

Finally, thanks are due to M. Vidal and his licensees for permission to reproduce the following figures based on his and their published works: Figures Nos 2, 22–27, 34–39, 57–66, 69–71, 75 and 76.

Contents

Preface

Reinforced Earth is a composite construction material in which the strength of engineering fill is enhanced by the addition of strong inextensible tensile reinforcement in the form of strips. The basic mechanism of Reinforced Earth involves the generation of frictional forces between the soil and the reinforcement. These forces are manifested in the soil in a form analogous to an increased confining pressure which enhances the strength of the composite. Additionally the reinforcement has the ability to unify a mass of soil that would otherwise part along a failure surface. Reinforced Earth is potentially a very versatile material; however, the vast majority of applications to date involve walls in various forms. These structures embody two basic components, namely engineering fill and reinforcement as well as some form of facing which prevents surface erosion and gives an aesthetically pleasing finish. In analysing these walls consideration must be given both to internal and external stability. The latter consideration presents no problem since the reinforced mass forming the wall may be considered as a gravity retaining wall whence conventional design methods can be employed to check bearing capacity, base sliding and overall stability. The assessment of internal stability is somewhat more complicated, however; in essence this involves designing the reinforcement against failure by either tensile fracture or pull-out from the main body of the fill.

PREFACE

In the late fifties, Henri Vidal, a French architect and engineer, investigated the frictional effects of reinforcement in soil with the aim of improving the mechanical properties of the soil in the direction in which the soil is subject to tensile strain. As a result of these investigations Vidal launched a new civil engineering material known as Reinforced Earth. Subsequently patents were granted to Henri Vidal on his invention in many countries throughout the world.

The subsequent years witnessed intensive worldwide research with particular emphasis on the performance of model and full-scale walls. The first fundamental research of wall behaviour and design methods started at the Laboratoire Central des Ponts et Chaussées (LCPC) in 1967. Within 5 years similar research had commenced both in the United States of America and the United Kingdom. The end of 1976 heralded a bonanza of research with publication of the proceedings of the international symposium 'New Horizons in Construction Materials', held at Lehigh University, Pennsylvania. This was rapidly followed in 1977 by the international conference 'The Use of Fabrics in Geotechnics', and the Transport and Road Research Laboratory (TRRL)/Heriot-Watt University symposium 'Reinforced Earth and other Composite Soil'. Two international symposia took place in 1978: the American Society of Civil Engineers (ASCE) spring convention symposium 'Earth Reinforcement', held in Pittsburgh, and the New South Wales University/Institute of Technology symposium 'Soil Reinforcing and Stabilising Techniques', held in Sydney. A further international conference, 'Soil Reinforcement', was held in Paris in 1979. In the same year session eight of the seventh European conference on soil mechanics and foundation engineering was devoted to 'Artificially Improved Soils' with a speciality session 'Reinforced Earth' being incorporated in the sixth Panamerican conference on soil mechanics and foundation engineering held in Peru.

The resulting deluge of information has prompted the publication of this slender volume which seeks to review developments and applications as well as introducing design and construction

methods. Before this, however, an attempt is made to shed light on some of the basic mechanisms involved and to illustrate the potential versatility of this phenomenon.

1

Mechanisms and Concepts

Walking across a dry sandy beach soon reveals that soil is an inherently weak material. If the same beach sand is sealed in a simple jute sack it will resist the weight of several men without showing signs of failure. A similar observation was made by Henri Vidal, a French architect, who found that roughly formed mounds

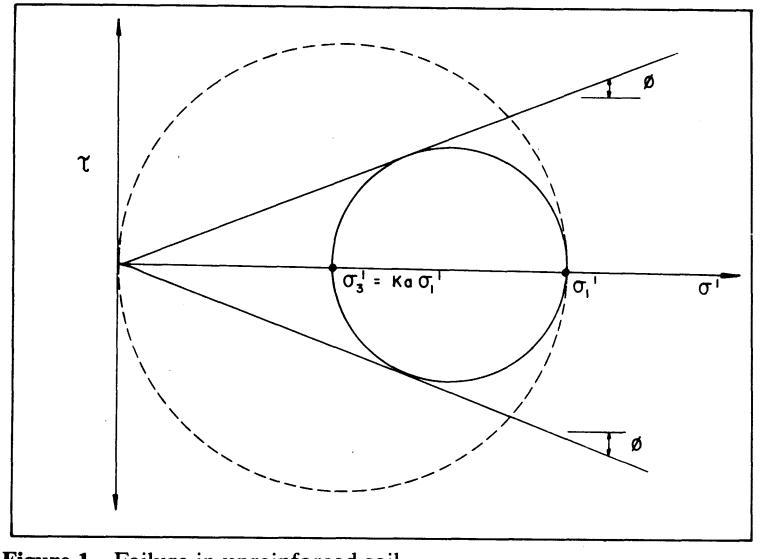

Figure 1 Failure in unreinforced soil

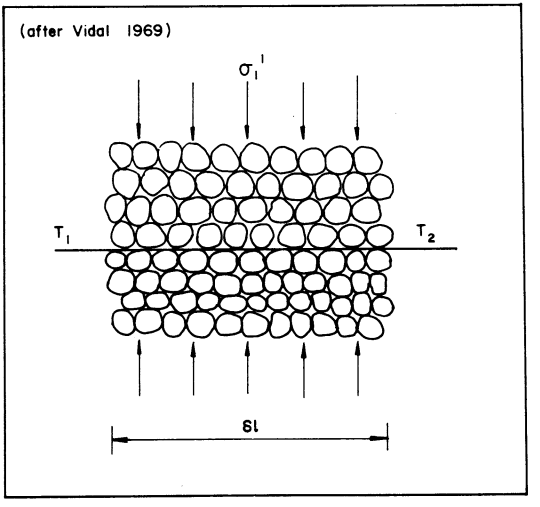

Figure 2 The effects of reinforcement

of dry sand could be made to stand at a steeper angle after the addition of horizontal layers of pine needles. The basic conclusion reached by Vidal (1966) was that when dry granular soil is combined with a rough material having tensile strength the resulting composite material is stronger than soil alone.

THE WORK OF HENRI VIDAL

In his early work Vidal (1966, 1969a, 1969b) accurately identified and explained a fundamental mechanism of Reinforced Earth. It was pointed out that unreinforced soil obeys the Mohr–Coulomb failure criterion which for a cohesionless soil may be simply defined by two linear failure envelopes inclined at $+\phi$ and $-\phi$ to the normal stress axis (Fig. 1, where ϕ is the internal angle of shearing resistance of the soil). If such a soil is loaded by a vertical principal stress σ_1' then for the soil not to fail there must also be a lateral confining stress σ_3' acting on the soil. The minimum value of σ_3' consistent with stability is $K_a\sigma_1'$ where K_a is the coefficient of active

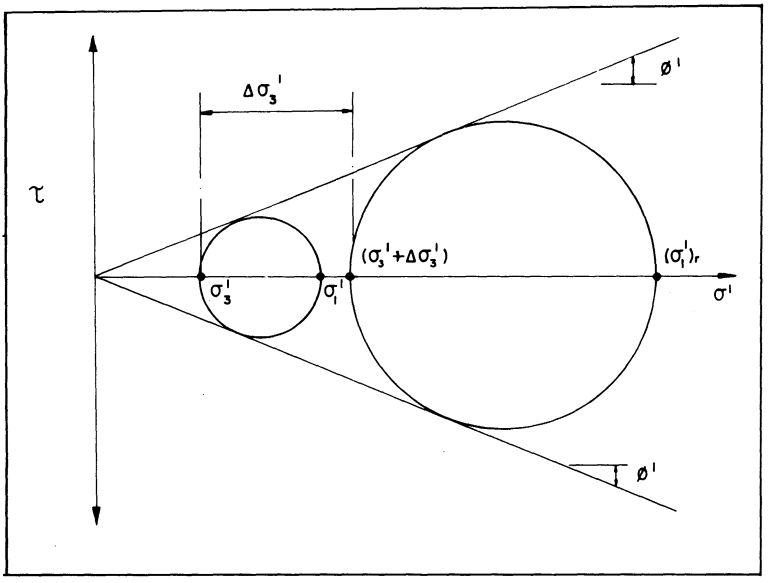

Figure 3 Improvement in strength

earth pressure. This limiting condition is represented by the Mohr stress circle shown in solid line in Fig. 1. If the externally applied confining pressure σ_3' is reduced to zero then under the action of σ_1' the stress circle, shown with a broken line in Fig. 1, would fall outside the Mohr–Coulomb envelope, thus indicating failure in the soil.

Vidal next considered the effects of introducing a strip of horizontal reinforcement of width b to an unconfined mass of soil (Fig. 2). If a steadily increasing normal stress, σ_1', is then applied there would be lateral movement induced in the soil which would generate a frictional force between the soil and the reinforcement. Considering an element of reinforcement of embedded length δl having a coefficient of soil/reinforcement friction f the change in tensile force generated under the action of the normal stress is:

$$\delta T = 2\sigma_1' bf\delta l \tag{3}$$

For there to be no failure by slippage between the soil and the reinforcement:

$$dT/2\sigma_1' bdl < f \tag{4}$$

Reference to Fig. 2 readily reveals that the quantity δT is simply the difference between the tensile forces T_1 and T_2 generated at the two ends of the element. A more general expression was later derived by Behnia (1972, 1973).

As the action of loading the element of reinforced soil induces a tensile force in the reinforcement so there is a corresponding compressive lateral stress generated in the soil. This induced confining stress $\Delta\sigma_3'$ is analogous to an externally applied confining pressure σ_3' and provided that $\Delta\sigma_3' \not< K_a\sigma_1'$ there is no failure in the soil (Fig. 1). This concept may be more readily understood by reference to Fig. 3. The left-hand stress circle represents an unreinforced soil under the action of a confining stress σ_3'. Failure occurs under a major principal stress σ_1'. If the same soil were reinforced then during the process of loading the confining pressure increases to $(\sigma_3' + \Delta\sigma_3')$ and failure occurs at a much higher stress level of $(\sigma_1')_r$. Failure ultimately occurs by bond, that is slippage between the soil and reinforcement, or by tensile failure of the reinforcement. In later work Vidal (1972) digressed from his original notion and firmly subscribed to the 'anisotropic cohesion concept.'

THE ANISOTROPIC COHESION CONCEPT

An experimental and theoretical investigation verifying the mechanism of Reinforced Earth was carried out at the Laboratoire Central des Ponts et Chaussées (LCPC) in a programme organized by Henri Vidal and François Schlosser, reported in 1969. This investigation employed the triaxial apparatus in which cylindrical samples of reinforced sand were tested under axisymmetric stress conditions.

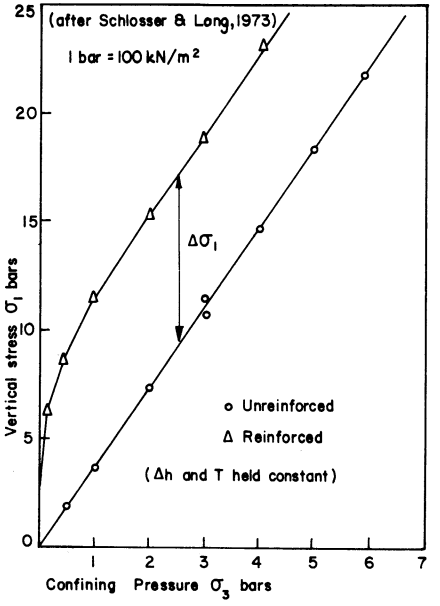

Figure 4 Reinforcement-induced cohesion

Several years later a similar investigation was undertaken at the New South Wales (NSW) Institute of Technology. Although both schools subscribed to the so-called cohesion concept it is convenient to consider the resulting hypotheses separately.

The LCPC test results

In 1972 Long, Guegan & Legeay published the results of a series of triaxial tests carried out in the hope of defining the mechanism of Reinforced Earth. The tests were carried out on 100 mm dia. samples of dry Fontainebleau sand ($d_{50} = 0{\cdot}15$ mm, $U = 1{\cdot}6$), compacted to a mean dry density of $1{\cdot}67$ Mg/m^3. Cell pressure was

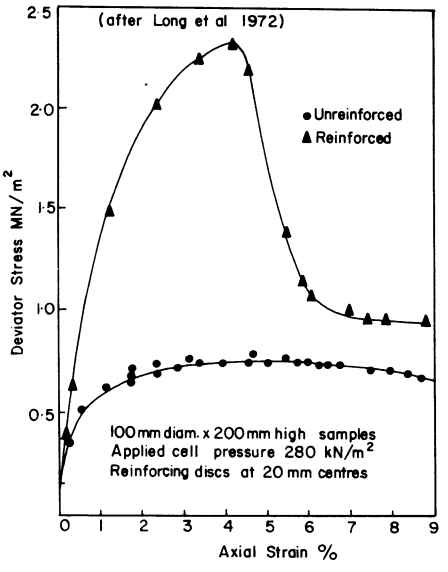

Figure 5 Reinforcement-induced brittleness

applied by compressed air. Samples were generally 200 mm high; however some 300 mm high samples were tested to assess the effects of aspect ratio. The tests were comparative in as much as both reinforced and unreinforced samples were tested. Reinforcement was in the form of 100 mm dia. discs of 18 μm thick aluminium foil, with an ultimate tensile strengh of 1·5 kN/m width, which was placed horizontally at a constant vertical spacing, in any one sample. The effects of reinforcement spacing, h, were investigated, as well as the effects of reinforcement tensile strength, T. Reinforcement tensile strength was varied by varying the number of aluminium foil discs used to form each layer of reinforcement.

Long *et al.* (1972) observed that above a certain threshold value of applied confining pressure there was a constant increase, $\Delta\sigma_1'$, in applied vertical stress at failure in samples with reinforcement at

a given tensile strength and spacing (Fig. 4). Failure of the reinforced samples was very brittle (Fig. 5), with a drastic decrease in strength past the peak. This brittleness was less severe at higher applied confining pressures or in less heavily reinforced samples. Post-failure inspection of dismantled samples consistently showed that the reinforcement had failed in tension. Similar examinations of samples failing below the threshold value of confining pressure showed far less sign of tensile failure in the reinforcement. In general the threshold value of confining pressure was found to be in the range 50–100 kN/m^2. It was concluded that since, for tensile reinforcement failure, the failure envelopes of both the reinforced and unreinforced sand are parallel, and therefore exhibit the same angle of internal shearing resistance, the additional strength imparted by the reinforcement could be represented by an apparent anisotropic cohesion c'.

The LCPC cohesion theory

An authoritative exposition of the LCPC cohesion theory is given by Schlosser & Long (1973). Firstly the failure envelope for the reinforced soil is defined by equation (5), in which the second term relates to the improvement that is caused by the reinforcement:

$$\sigma_1' = K_p\sigma_3' + \Delta\sigma_1' \tag{5}$$

This expression was compared to the Rankine–Bell Equation for a c'–ϕ' soil, equation (6):

$$\sigma_1' = K_p\sigma_3' + 2\sqrt{K_p}c' \tag{6}$$

Equating (5) and (6) leads to equation (7):

$$c' = \Delta\sigma_1'/2\sqrt{K_p} \tag{7}$$

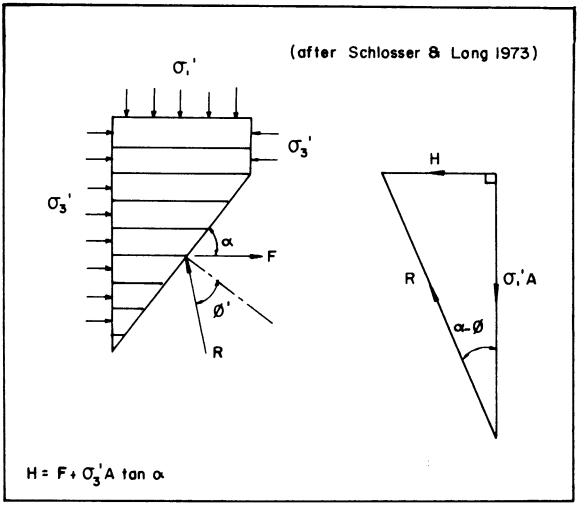

Figure 6 Coulomb analysis

Schlosser & Long (1973) next considered the equilibrium of a reinforced cylinder of soil subjected to axisymmetric loading (Fig. 6), cut by a failure plane inclined at α to the horizontal. In addition to the forces generated by the principal stress σ_3' and σ_1' there is a tensile force F developed by the reinforcements which acts on the failure plane together with a resultant force R. If the cross-sectional area of the cylindrical section is A it follows from the triangle of forces (Fig. 6) that:

$$F + \sigma_3' A \tan\alpha = \sigma_1' A \tan(\alpha - \phi') \tag{8}$$

Taking the sample to fail by breaking of the reinforcements it follows that the tensile force F is equal to the sum of the tensile forces T from each reinforcement cut by the failure plane. This summation is defined by equation (9) assuming the vertical reinforcement spacing h is small compared to the height of the sample.

$$F = \frac{A \tan \alpha}{h} T \tag{9}$$

Combining equations (8) and (9) leads to equation (10):

$$\sigma_1' = (\sigma_3' + T/h) \tan \alpha \cot(\alpha - \phi') \tag{10}$$

On differentiating it is found that the maximum value of σ_1' occurs when $\alpha = 45 + \phi'/2$. For this value of α equation (10) reduces to equation (11):

$$\sigma_1' = K_p \sigma_3' + K_p T/h \tag{11}$$

Comparison of equations (5) and (11) leads to equation (12):

$$\Delta\sigma_1' = K_p T/h \tag{12}$$

This expression is in good agreement with the results of Long *et al.* (1972) which showed $\Delta\sigma_1'$ to vary linearly with T and the inverse of h. Subsequent substitution from equation (12) into equation (7) leads to an expression for the anisotropic cohesion, equation (13):

$$c' = \frac{T}{h} \frac{\sqrt{K_p}}{2} \tag{13}$$

A comparison of this theoretical relationship and the experimental results obtained by Long *et al.* (1972) shows excellent agreement (Fig. 7).

Later tests by Bacot (1974), again using aluminium disc reinforcement, corroborated the results of Long *et al.* (1972) with the experimental results being in good agreement with the predictions from equation (13). The efficacy of this expression was further, and somewhat surprisingly, bolstered by test results published by Saran, Talwar & Vaish (1978) who yet again employed cylindrical sand samples reinforced with foil. However these particular

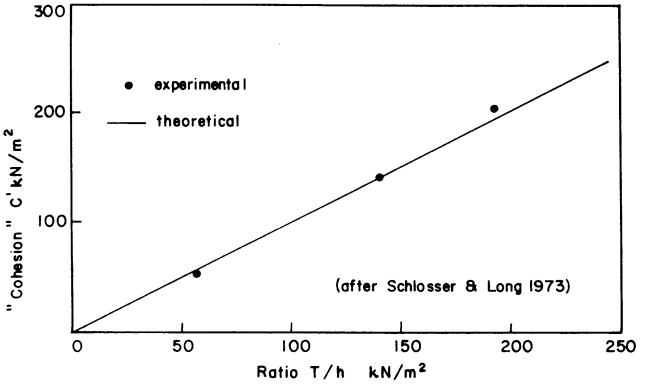

Figure 7 Comparison of theoretical and experimental results

samples, which were 38 mm in diameter, were reinforced with rings of aluminium foil with inner and outer diameters of 10 mm and 37·5 mm respectively, rather than the 'conventional' solid discs. Despite this innovation excellent agreement was found to exist between theoretical and experimental results using a slightly modified version of equation (13) where r is the ratio of the plan area of the reinforcing ring to the cross-sectional area of the sample.

$$c' = \frac{T}{h}\frac{r\sqrt{K_p}}{2} \tag{13a}$$

The NSW Cohesion Theory

Quite independently of the LCPC work on Reinforced Earth a more unified anisotropic cohesion theory was postulated by Hausmann (1976). In fact two models were proposed, the so-called sigma and tau models, both dealing with bond and tensile failure. The sigma model assumes that the reinforcement assists the soil to resist lateral expansion. This effect is interpreted as an intrinsic

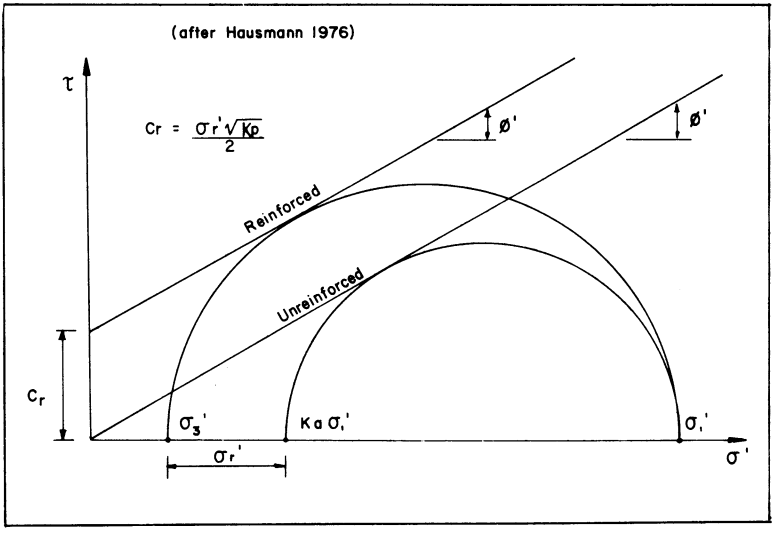

Figure 8 Failure conditions for constant σ_r'

prestress mobilized fully when the soil reaches a state of plastic equilibrium as defined by Rankine theory, that is $\sigma_3' = K_a\sigma_1'$. In the case of a retaining structure the reinforcement is assumed to allow the lateral stress σ_3' to reduce below the active stress by an amount σ_r. In the tau model of the reinforcement is assumed to introduce horizontal and vertical shear stresses, τ_r, into the initially geostatic stress conditions. Since the end-result from the two models is very similar, consideration is limited to the sigma model.

The sigma model

Hausmann (*loc. cit.*) first considered the case of a constant prestress σ_r'. This corresponds to conditions when failure of a reinforced soil mass occurs by rupture of the reinforcement. Lateral expansion of the soil mass creates a prestress statically equivalent to the frictional force developed between the soil and the reinforce-

ment with a maximum value determined by the tensile strength of the reinforcing material. For a constant prestress, σ_r', the increased strength is exhibited by adding a cohesion, c_r, to the soil as shown in Fig. 8. Hausmann proceeds by equating minor principal stresses as shown in equation (14):

$$\sigma_3' + \sigma_r' = K_a\sigma_1' \tag{14a}$$

Whence:

$$\sigma_1' = K_p\sigma_3' + K_p\sigma_r' \tag{14b}$$

Direct comparison between equation (14) and equation (6) yields equation (15):

$$c_r = \sigma_r' \sqrt{K_p}/2 \tag{15}$$

Reference to Fig. 9 shows an element of soil reinforced with a strip of material of cross-sectional area A and ultimate tensile strength σ. At failure the force in the reinforcement is σA; this generates a stress in the soil given by equation (16):

$$\sigma_r' = \sigma A/BH \tag{16}$$

Substitution for σ_r' from equation (16) into equation (15) leads to the expression

$$c_r = \sigma A \sqrt{K_p}/2BH \tag{17}$$

For a multilayered system equation (17) is identical to that derived by Schlosser & Long (1973).

Before considering the sigma model for bond stress failure it is worth comparing the generic equation of Hausmann, equation (15), with that of Schlosser & Long, equation (7). The latter is a statement to the effect that Reinforced Earth is brought to failure by

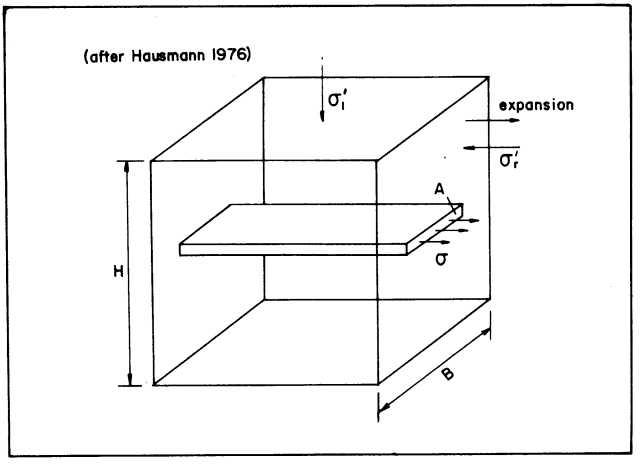

Figure 9 Rupture of reinforcement in unit element

increasing σ_1'. Conversely the former is a statement to the effect that σ_1' is held constant whilst σ_3' is reduced to a value less than the Rankine active pressure, that is $K_a\sigma_1'$. Since both studies used granular soil this argument is fallacious, for if the lateral pressure did in fact drop below the Rankine active pressure there would be failure in the soil itself before the soil could induce a tensile failure in the reinforcement.

For failure by slippage between the soil and reinforcement it is assumed that friction along the reinforcement is proportional to vertical stress. This leads to a variable prestress as defined by:

$$\sigma_r' = F\sigma_1' \tag{18}$$

This has the effect of increasing the friction angle, as shown in Fig. 10. From equations (14a) and (18):

$$\sigma_3'/\sigma_1' + F = K_a \tag{19}$$

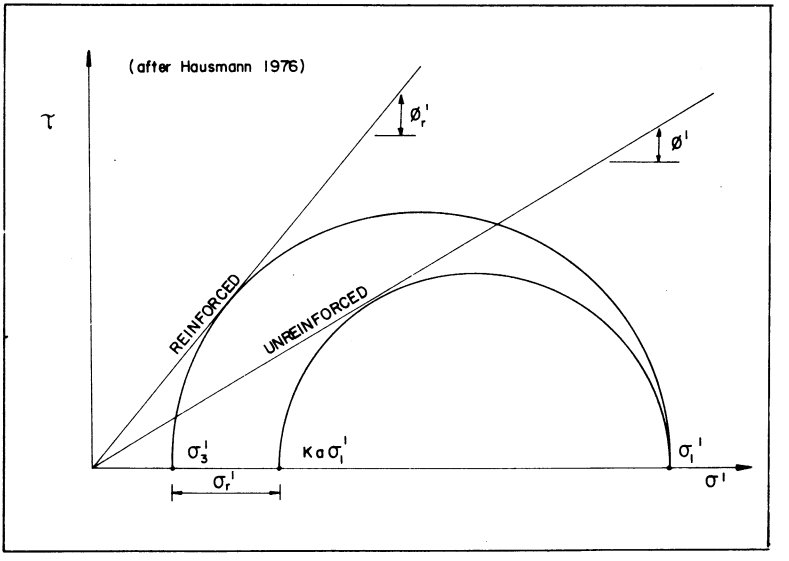

Figure 10 Failure conditions for variable σ_r'

Using the suffix r to denote reinforced, it is convenient to write:

$$\sigma_3'/\sigma_1' = K_{ar} = \frac{1 - \sin\phi_r'}{1 + \sin\phi_r'} \tag{20}$$

Combination of equations (19) and (20) leads to equation (21):

$$\sin\phi'_r = \frac{K_a - F - 1}{F - K_a - 1} \tag{21}$$

Reference to Fig. 11 shows how frictional resistance to lateral expansion is developed by the shear stress τ acting between the soil and the reinforcement. The magnitude of this shear stress will depend on the angle of bond stress, δ, between the soil and the reinforcement as well as the relative movement between the soil

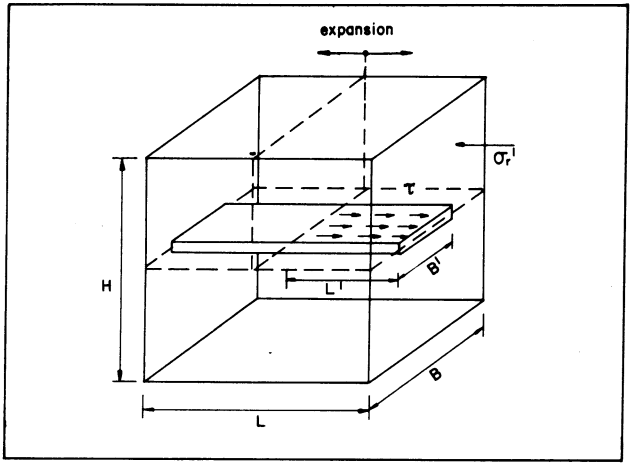

Figure 11 Slippage of reinforcement in unit element

and reinforcement. It might be expected that the shear stress is zero at the midpoint and at the ends of the reinforcing strip, reaching a maximum value of σ_1' tanδ between these two points. The effects of the uneven distribution of shear stress and imperfect transfer could be taken into account by introducing a reinforcement efficiency *e*.

It follows from Fig. 11 that:

$$BH\sigma_r' = 2\tau B'L' \tag{22a}$$

Whence:

$$\sigma_r' = \sigma_1' \tan\delta 2B'L'e/BH \tag{22b}$$

From equations (18) and (22b):

$$F = \tan\delta 2B'L'e/BH \tag{23}$$

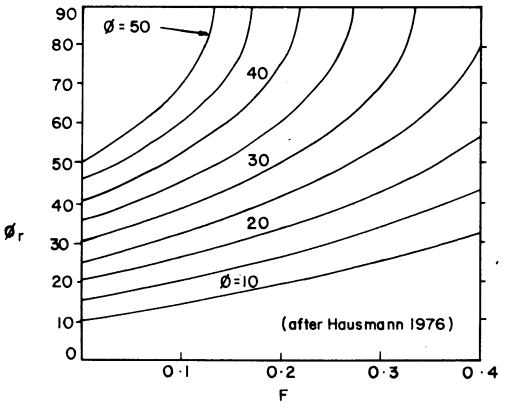

Figure 12 Friction angle ϕ_r as a function of ϕ' and F

The variation of ϕ_r', from equation (21), with F is shown in Fig. 12.

It is apparent that at low stress levels failure in a reinforced earth mass tends to occur by slippage, and at higher stress levels by rupture of the reinforcement. This is depicted in Fig. 13 where circles A and B define failure by slippage and rupture of the reinforcement respectively.

Hausmann tested his theories by conducting a series of tests on 70 mm dia. samples of sand, both reinforced and unreinforced. These tests were interesting in as much as the diameters of the reinforcing discs were varied with the largest disc being 66 mm in diameter. The smallest and intermediate size discs were of 8 mm and 25·4 mm dia. respectively. In using these small reinforcements Hausmann arranged several discs in any one horizontal plane of reinforcement. The results for samples failing by rupture of the reinforcement did not show as good an agreement with the theory as the LCPC results. Conversely samples failing by bond showed quite reasonable agreement with the theory once a 'suitable' value for reinforcement efficiency had been chosen.

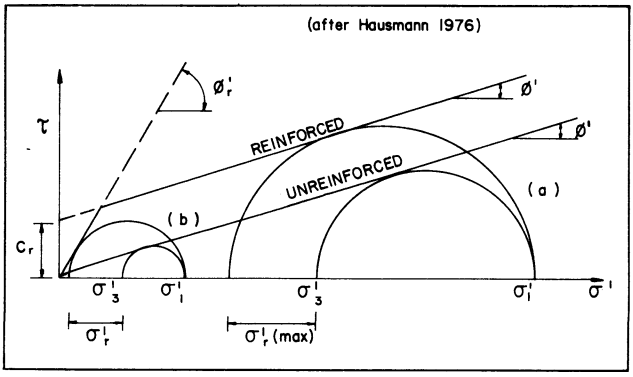

Figure 13 Composite Mohr envelope

THE ENHANCED CONFINING PRESSURE CONCEPT

The experimental work carried out at the LCPC and NSW Institute of Technology used sand. This is by definition a cohesionless soil, yet the theories propounded attributed a cohesion to such soil when combined with reinforcement. One basic assumption made in such an interpretation is that the externally applied stresses are both principal and uniform throughout the sample, yet it was well recognized long before the current spate of research that the internal stress distribution in a cylindrical triaxial sample is far from uniform (Haythornthwaite, 1960).

Analyses based on elastic theory have shown that even for unconfined compression of cylindrical samples with a height to diameter ratio of 2, compressive radial stresses are developed by the frictional effects of the end plattens (Filon, 1902; Pickett, 1944; D'Appolonia & Newmark, 1951; Balla, 1957, 1960). However this effect is most significant in the top and bottom 25% of the sample which are closest to the plattens. A comparison of the distributions obtained from the theories cited is given in Fig. 14. Although these distributions vary from one another the basic theories unanimously

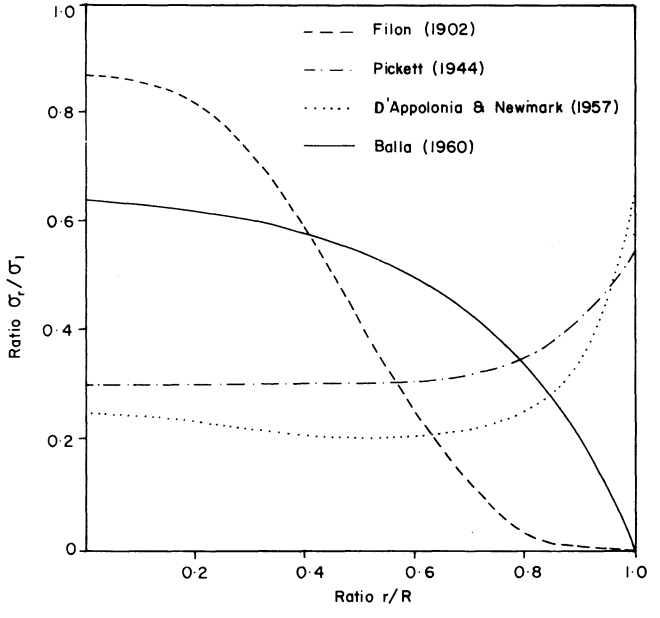

Figure 14 Comparison of induced radial stresses

predict an increase in confining pressure. A particularly interesting analytical method has been presented by Perloff & Pombo (1969) who relate the development of the induced radial stress to axial strain.

Non-uniform stress distributions have been measured directly at the Waterways Experiment Station (Hvorslev, 1957; Shockley & Ahlvin, 1960) as well as indirectly by the measurement of non-uniform porewater pressure distributions (Blight, 1963; Barden, 1963; Crawford, 1963; Barden & McDermott, 1965). The last reference is particularly interesting in as much as high radial gradients were measured from the centre to the periphery of the sample. This tends to confirm the stress distributions determined by Balla (1960) and Filon (*loc. cit.*) (Fig. 14).

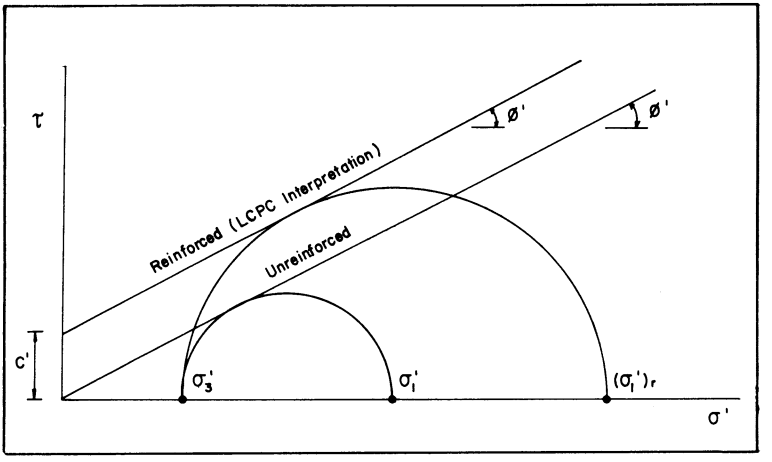

Figure 15 The LCPC interpretation

It follows that the discs of reinforcement used by Long *et al.* (*loc. cit.*) and Hausmann (*loc. cit.*) cause a similar non-uniform stress distribution. The significance of this was first pointed out in a theoretical study carried out at the Institut de Mecanique de Grenôble. A similar conclusion was drawn from contemporary work at the University of California – Los Angeles.

The Grenôble Study

In a general study of walls Chapuis (1972) rejected the assumption that vertical and horizontal stresses were principal stresses within a horizontally reinforced mass of soil. It was argued that since the horizontal reinforcement induced shear stresses in the soil the horizontal plane could not be a principal plane. Similarly, vertical planes within the reinforced mass could not be principal. The consequence of disregarding this fact is shown in Fig. 15 which depicts the Mohr stress circles for a reinforced and unreinforced sample tested at the same applied cell pressure. For the unreinforced

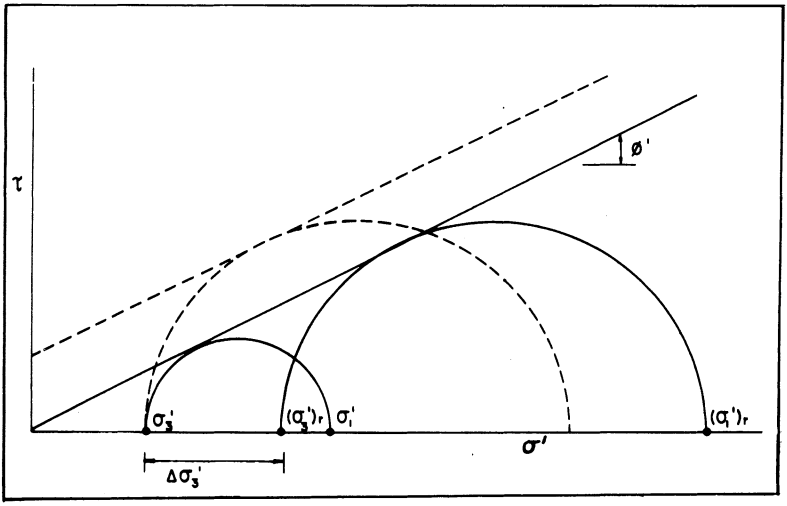

Figure 16 The $\Delta\sigma_3'$ interpretation

sample, with an aspect ratio of 2, the applied cell pressure equals the minor principal stress σ_3' which in this case does act on a vertical plane. The sample fails under a vertical major principal stress σ_1' and the resulting stress circle is tangential to the failure envelope which passes through the origin. When the reinforced sample is tested at the same applied cell pressure it fails at a higher vertical stress level $(\sigma_1')_r$ (Fig. 15); however, the minor principal stress at failure is not equal to the applied cell pressure except at the periphery of the sample. If, however, the applied cell pressure is assumed to equal the minor principal stress the resulting stress circle passes through $(\sigma_3', (\sigma_1')_r)$ (Fig. 15), and consequently falls outside the failure envelope. This was accounted for by the introduction of a pseudo-cohesion intercept c'.

Chapuis (*loc. cit.*) appreciated that within the reinforced sample the minor principal stress $(\sigma_3')_r$ was higher than the applied cell pressure σ_3'. In fact, σ_3' is increased by an amount $\Delta\sigma_3'$ approx-

imated by equation (24) which may be derived by inspection of Fig. 9:

$$\Delta\sigma_3' \simeq A\sigma/BH \simeq T/h \qquad (24)$$

The magnitude of this expression is equal to that derived by Hausmann (*loc. cit.*), equation (16); however $\Delta\sigma_3'$ is a stress increment whereas σ_r' was taken to be a stress decrement. If the stress circle for the reinforced sample is redrawn using the 'true' value of minor principal stress it is found that it becomes tangential to the true failure envelope which passes through the origin (Fig. 16).

Several years later Chapuis (1977) reverted to the use of a pseudo-cohesion, and demonstrated that cohesion would vary according to the distribution of shear stress along the reinforcement. Although there may be substantial rotations of principal stress axes in reinforced samples, the failure surface, for samples failing by rupture of the reinforcement, still obtains the classical shape and inclination (Schlosser & Long, 1973).

The University of California – Los Angeles (UCLA) study

A contemporaneous experimental and analytical study was carried out by Yang (1972), again using triaxial tests on sand. In one series of tests Yang investigated bond failure using 2·7 in. (71 mm) dia. samples with height to diameter ratios, *h/d*, varying between 2·28 and 0·29. The samples were mounted using heavy steel end plattens which in effect acted as infinitely strong rigid reinforcing discs. As before it was found that as the reinforcement spacing decreased, that is as lower *h/d* ratios were used, the compressive strength of the sample increased. Rather than attributing this increase in strength to an enhanced friction angle Yang assumed that the sand failed at constant effective stress ratio, i.e. $\sigma_3' = K_a\sigma_1'$. The value of K_a was deduced from conventional tests. On this basis it was concluded that any increase in σ_1' at failure in the 'reinforced' samples was due to an enhanced confining pressure $\Delta\sigma_3'$, therefore, for an applied confining pressure σ_3'

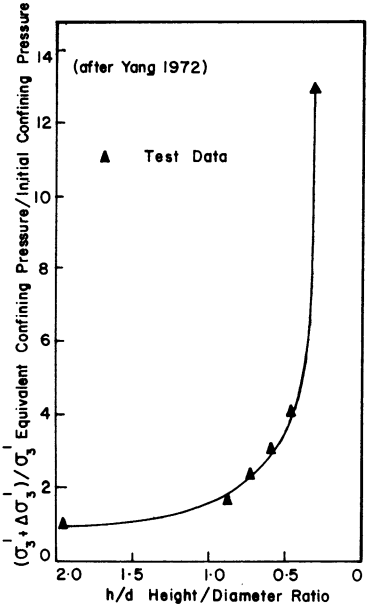

Figure 17 Variation of strength with aspect ratio

$$\sigma_1' = K_p\sigma_3' + K_p\Delta\sigma_3' \tag{25}$$

Thus for a measured value of σ_1' and a known applied value of σ_3' it was possible to evaluate $\Delta\sigma_3'$, equation (26):

$$\Delta\sigma_3' = K_a\sigma_1' - \sigma_3' \tag{26}$$

A normalized plot of equivalent confining pressure $(\sigma_3' + \Delta\sigma_3')/\sigma_3'$ against aspect ratio, *h/d*, is given in Fig. 17. The observed increase in equivalent confining pressure, and hence strength, with decreasing aspect ratio was confirmed by a series of finite element analyses. An initially unexpected result was that $\Delta\sigma_3'$ increased linearly with applied cell pressure σ_3' (Fig. 18). This follows from the fact that σ_1' increases linearly with σ_3' which in turn increases the

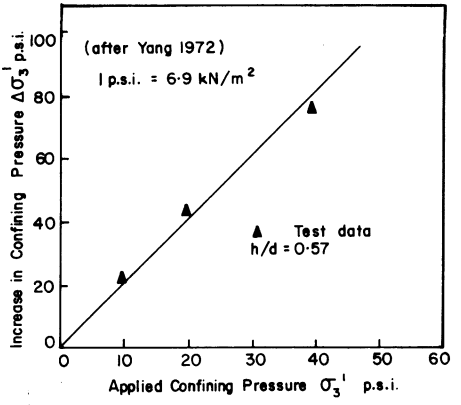

Figure 18 Variation of $\Delta\sigma_3'$ with σ_3'

frictional shear stress σ_1' tanδ and hence $\Delta\sigma_3'$.

In a second series of tests use was made of samples, of the same unit aspect ratio, reinforced with orthogonal fibreglass netting of various tensile strengths. Again equivalent confining pressure was found to increase linearly with applied confining pressure; however, a value of applied confining pressure, termed the critical pressure, was reached above which the net failed in tension. Beyond this critical value the magnitude of $\Delta\sigma_3'$ was found to be constant. This value of $\Delta\sigma_3'$ would be expected to be that predicted by equation (24); however, there was poor agreement between predicted and measured values. This is almost certainly due to the anisotropic tensile strength and frictional properties associated with net structures.

A similar study was presented by Broms (1977) for samples reinforced with fabric. Again the sample strength was found to increase with decreasing reinforcement spacing. A theoretical assessment was made, and this concluded that the strength of the sample is a function of a coefficient K_b relating non-principal horizontal and vertical stresses.

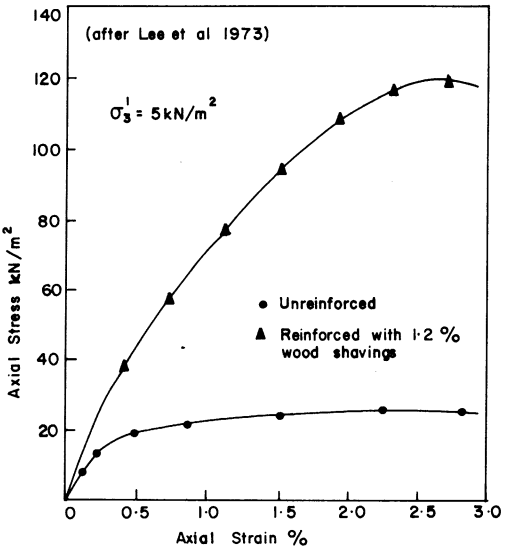

Figure 19 RRE performance

RANDOMLY REINFORCED SOIL (RRS)

In the experimental and analytical investigations previously considered cylinders, or cubes, of soil have been strengthened by the addition of discrete layers of reinforcement. The resulting reinforcement geometry has been simple and therefore amenable to theoretical analysis. If the reinforcement is introduced randomly in the form of discontinuous fibres or short strips the resulting composite defies theoretical analysis. Despite the apparently aloof nature of such material it is worthwhile considering the limited quantity of available experimental data in an attempt to define common mechanisms that relate regular and random reinforcement distributions.

One of the earliest investigations was carried out by Lee (1969) with some of the results being made publicly available several years later (Lee, Adams & Vagneron, 1973). In this investigation Lee

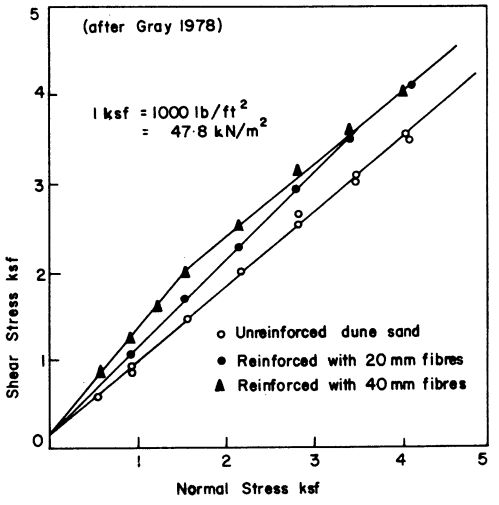

Figure 20 Shear box test results

used, amongst other things, medium sand reinforced with wood shavings 0·2 mm thick by 1·2 mm wide with lengths varying between 25 mm and 75 mm. Figure 19 shows triaxial test results for unreinforced sand and sand reinforced with fir wood shavings constituting 1·2% by weight of the sample. As can be seen the strength is increased by a factor of approximately 6, with a dramatic increase in deformation modulus. However, failure tends to occur at a slightly higher axial strain in the reinforced sample. This tendency towards increased ductility was noticed by Razani & Behpour (1970) who carried out a limited study of the effects of the addition of straw to adobe brick. It was found that the addition of straw actually decreased compressive strength, the strength being halved by the addition of 2½% by weight of straw.

In an outstanding exposition Gray (1978) considered the role of woody vegetation in reinforcing soils and stabilizing slopes. Of particular interest are results of 250 mm dia. direct shear tests carried out on reinforced and unreinforced dune sand (Fig. 20). The rein-

forcement used was broom straw fibre with one sample reinforced with 20 mm long fibres and the other with 40 mm long fibres. As can be seen both failure envelopes show a distinct slackening of slope as the failure mode changes from slippage or bond failure to tensile failure of the reinforcement. At this transition point the ultimate fibre tensile strength, T, must equal the pull-out resistance of the fibre. Considering a fibre of length L and diameter d the limiting pull-out resistance is given by equation (27), assuming a coefficient of soil/fibre friction of f and an ambient normal stress level σ_n.

$$L\pi d\sigma_n f = T \tag{27}$$

Taking all other things as being equal, it follows that the transition from bond to tensile failure is a linear function of normal stress level and fibre length. This is confirmed by Fig. 20 which shows the transition for the 40 mm long fibre occurring at a normal stress level of 1·7 Ksf (91 kN/m^2) with that of the 20 mm long fibre occurring at 3·5 Ksf (187 kN/m^2).

A similar study was reported by Verma & Char (1978) who carried out a series of triaxial tests using fine to medium sand, d_{50} = 0·18 mm, and medium to coarse sand, d_{50} = 0·6 mm, reinforced with mild steel fibres. The fibres were either 1 mm wide by 0·16 mm thick by 2 mm long, or 1 mm wide by 0·16 mm thick by 5 mm long. Although up to 7% by volume of fibre was added there was no measurable increase in strength. Almost certainly this is due to the lack of development of soil/fibre bond stress. This is not surprising since as well as being very short the fibres are also very narrow when compared to the particle size of the sand employed. To some extent this hypothesis is borne out by test results reported by Andersland & Khattak (1979). In this study use was made of pulp fibres with a weighted length of 1·6 mm and a typical diameter of 0·02 mm; however, the soil employed was a kaolin clay with 93% finer than 0·01 mm and 42% finer than 0·001 mm. The fibres and kaolinite were mixed dry with either 16% or 40% of fibre by

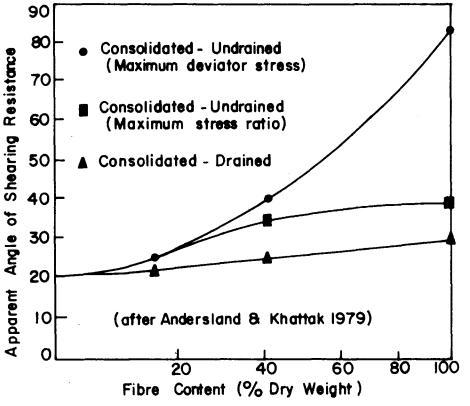

Figure 21 Fibre-reinforced kaolinite

weight. The mixture was subsequently slurried and consolidated to form cylindrical samples suitable for triaxial testing. To enhance the range of the investigation samples of kaolinite and fibre alone were prepared. Two series of tests were carried out, namely consolidated–drained triaxial tests and consolidated–undrained triaxial tests with porewater pressure measurement. In interpreting the results it was assumed that the applied confining pressure reflected the true confining pressure. This led to problems in interpreting the results of the consolidated–undrained tests since the effective minor principal stress σ_3' appeared to closely approach zero. Using the normal failure criterion of maximum stress difference this leads to an apparent angle of internal shearing resistance of 80·4° for the 100% fibre sample. In view of this the results were interpreted using the maximum principal stress ratio failure criterion. This resulted in a maximum apparent internal angle of friction of 39°. The results for the two series of tests are given in Fig. 21. As can be seen, increasing quantities of pulp fibre give rise to increasing strength; however, this is associated with increasing ductility.

A most enlightening investigation was reported by Hoare (1979) who studied the effects of fibre reinforcement on soil 'compactability' as well as strength. The investigation was limited to the use of a sandy gravel, with particle sizes in the range 0·6–5 mm, reinforced either with strips of polypropylene/nylon fabric 7 mm wide by 66 mm long, or with 50 mm long twisted polypropylene staple. Hoare first carried out a series of compaction tests using several different compaction procedures for samples reinforced either with fabric fibre or staple. It was found that increasing quantities of fibre or staple caused a linear increase in porosity for a given compaction method. In other words the addition of random reinforcement inhibits efficient compaction. This increase in porosity was very marked in the fabric fibre-reinforced soil where 0·75% of reinforcement caused porosity to increase from typically 40% to 50%. This tendency was far less severe in the staple-reinforced soil where a similar quantity of reinforcement involved an increase in porosity from approximately 36% to 38%. When samples of the reinforced material were tested in the triaxial apparatus the fabric fibre-reinforced soil showed a distinct decrease in strength with increasing fibre content. This is not surprising since in an unreinforced granular soil the strength, represented by the internal angle of shearing resistance, decreases rapidly with increasing porosity. From this it follows that the high porosity, and hence inherent weakness, imposed by the resistance of the reinforced soil to compaction is not counteracted or surpassed by any strengthening effect of the fabric fibres when subjected to shear in the triaxial test. Conversely the staple-reinforced soil, which was only slightly resistant to compaction, showed a reasonable increase in strength with increasing staple content. The relationship was substantially linear and although the gain in strength was dependent on compaction method there was typically an increase in apparent angle of shearing resistance of 2–3° for the addition of 1% by weight of staple. Again it was found that increasing reinforcement content resulted in increased strain to failure.

THE LIMITATIONS OF LABORATORY STUDIES

With one exception the laboratory and theoretical studies reported have indicated that the addition of reinforcement to soil results in enhanced strength. The mechanism of the strength increase can be expressed either as a pseudo-cohesion, in the case of tensile failure of the reinforcement, or as an apparent increase in the internal angle of shearing resistance when bond failure prevails. More realistically both of these modes of failure can be explained by an enhanced internal confining pressure. What must be borne in mind is that most of the experimental work reported has been carried out under axisymmetric stress conditions with effectively continuous sheet reinforcement, whereas under field conditions most structures, such as walls and embankments, are likely to be stressed under plane strain conditions and be reinforced with much lower percentages of reinforcement – usually in the form of strips rather than sheets. When this divergence from the laboratory investigation conditions is compounded by the effects of the construction process, any resemblance between laboratory and prototype performance is likely to be coincidental rather than mechanistic.

2

Applications

Reinforced Earth exhibits a versatility that is on a par with reinforced concrete. In early publications Vidal (1966, 1969b) advocated the use of Reinforced Earth over a wide spectrum of structures including arches, tunnels and dams as well as in various forms of earth-retaining structures. Before considering such applications in more detail it is necessary to move from the somewhat esoteric models used for mechanistic studies to a more appropriate form of Reinforced Earth. Inspection of Fig. 22 shows the three main component parts of a Reinforced Earth fill – namely earth fill, which is generally a selected granular fill; reinforcement, which is generally in the form of metallic strips; and finally some form of segmental facing unit which is fixed to one end of the reinforcing strips. The facing unit is not a vital component; however, it is necessary to prevent surface erosion and to give an aesthetically acceptable external appearance. These three components may be combined together in many forms; for example, reference to Fig. 23 shows a simple retaining wall in which the Reinforced Earth mass acts as a gravity wall.

Model tests on arches and tunnels have given very encouraging results. Figure 24 shows a plane-strain model of an arch used in an investigation by Behnia (1972, 1973). Each voussoir of the arch is formed by a facing unit, acting as an arch lining, and two strips of reinforcement running back into the fill. The plane-strain effect

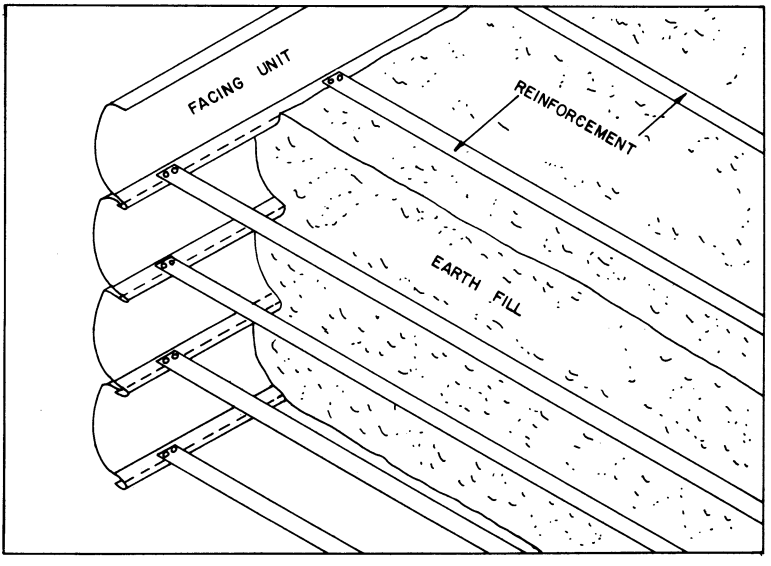

Figure 22 Reinforced Earth

was achieved using small-diameter cylindrical metal rods to model the soil (Schneebeli, 1957). In this manner the 'soil' is restricted to two-dimensional movement with no strain occurring along the length of each cylinder. Successful three-dimensional models of tunnels have been demonstrated by Vidal (*loc. cit.*). In this case the voussoirs form a complete ring around a temporary cylindrical liner. Once sand backfill is placed around the facing units and reinforcing strips the liner is removed, so leaving the facing units supported by the reinforcing strips embedded in the surrounding soil. To date there has been no record of any prototype arches or tunnels; however, it is obvious that such techniques would be limited to 'cut and cover' construction methods.

Another intriguing model was that of a Reinforced Earth beam (Vidal, 1969b); this consisted of a cylinder of cartridge paper, approximately 50 mm in diameter, reinforced with a spiral of ordi-

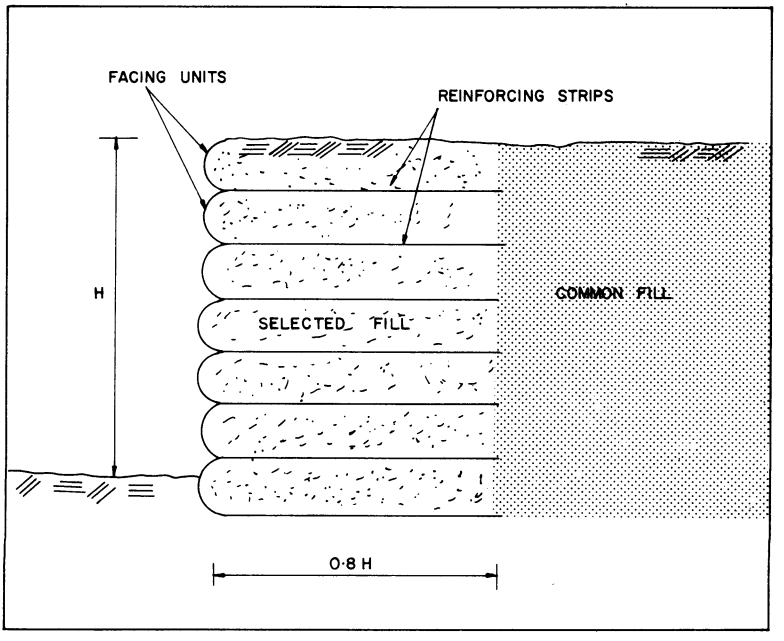

Figure 23 Reinforced Earth wall

nary transparent sealing tape. The paper cylinder was filled with sand and then set upon supports approximately 300 mm apart. Surprisingly this flimsy structure adequately supported the weight of a man. Again there is no record of a prototype construction.

Although the two applications cited above are very embryonic they should not be discounted. Such possibilities have been brought to fruition in the United States of America where reinforced soil bridges, using principles similar to Vidal's, have been constructed with individual spans up to 15 m (Watkins, 1973).

More common applications of Reinforced Earth are in the form of walls. However, before exploring this aspect in detail, it is worthwhile considering other practical uses that have either been applied or are the subject of current research.

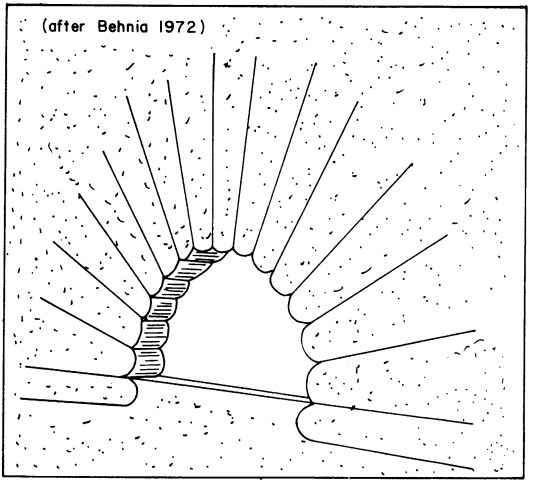

Figure 24 Reinforced Earth arch

GROUND SLABS

A most original application of Reinforced Earth was made on state route SR200 near Norristown, Pennsylvania (Steiner, 1975). A local realignment of SR200 had been planned; however, during very wet weather in January 1970 a hole some 4 m wide and 4 m deep appeared in the existing SR200. Despite the execution of standard remedial works the size of the hole increased during successive rainy periods, until in October 1970 the original hole was some 23 m in diameter and apparently bottomless. Subsequent site investigation revealed that surface and sub-surface water had eroded clay seams supporting the badly weathered dolomitic limestone formation. Similar conditions conducive to sinkhole collapse were found along the route of the proposed realignment. To stabilize the formation it was initially proposed to construct a two-way reinforced concrete slab under the proposed highway embankment. The slab designed was 0.9 m thick, 46 m wide and some

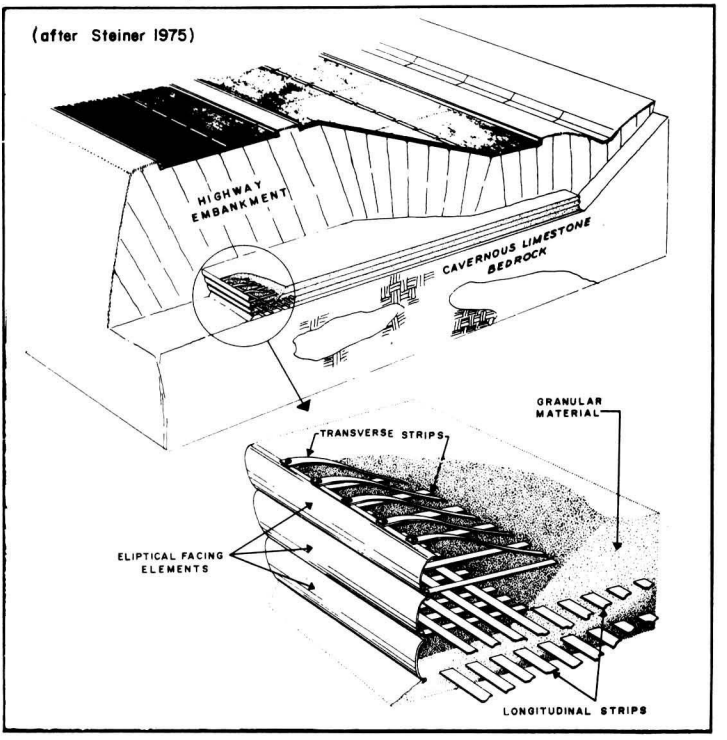

Figure 25 Reinforced Earth slab

336 m long, with a capability of spanning a 15 m dia. cavity without significant deflection. Before finalizing a design the highway authority approached the Reinforced Earth Company who developed a two-way Reinforced Earth slab comparable to the concrete slab yet some 25% cheaper.

The slab was constructed in the form of a low wall approximately 1 m high with semi-elliptical steel facing units forming the perimeter of the slab (Fig. 25). Reinforcing strips were spaced at 127 mm horizontal centres in various lengths and were bolted end-to-end

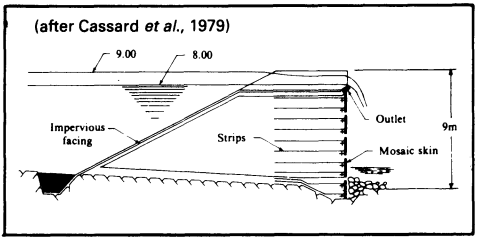

Figure 26 Vallon des Bimes dam

until the width of the slab was covered. A 300 mm layer of selected granular backfill was placed over the strips whence a transverse layer of strips was placed. In all, two transverse and two longitudinal layers of steel were placed (Fig. 25). Although the Reinforced Earth slab was designed to span cavities up to 15 m in diameter it was decided to grout the limestone formation to minimize the possibility of a further occurrence.

DAMS

The first Reinforced Earth dam constructed was a 9 m high prototype in the Bimes Valley which is situated in the south of France (Taylor & Drioux, 1979; Cassard, Kern & Mathieu, 1979). As may be seen from the typical cross-section in Fig. 26 the dam was constructed with a vertical downstream face formed with interlocking precast concrete facing units. Reinforcing strips with a length equal to 80% of the height of the dam were connected to the facing units and ran back into the main earth fill which has an upstream batter of 1 : 2. The upstream slope was sealed with a bitumen impregnated, non-woven fabric. The crest of the dam, which has a width equal to 20% of the dam height, is depressed over the central section of the dam and capped with a concrete sill. By this means the dam functions like a weir with the sill acting both as spillway and overflow channel when overtopping is allowed to occur. Con-

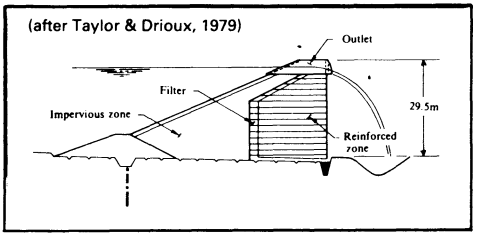

Figure 27 L'Estelle dam

struction of the dam, which contains 2500 m^3 of fill, was completed in 7 weeks. A similar, but slightly smaller, structure has been constructed with non-woven fabric facing units (Kern, 1977).

The success of the Bimes dam has invoked the client to plan the construction of a much larger Reinforced Earth dam at Estelle. This structure will have a maximum height of 29·5 m (Fig. 27), and will be of conventional design in the upstream slope which will incorporate normal impervious and filter zones.

FOUNDATIONS

Foundations have been arbitrarily differentiated from slabs by the fact that they are intended to support loaded areas that are small in comparison to the reinforced plan area. In comparison to walls very little research, and even less construction, has been carried out. This situation may reflect the possibility that foundations using earth reinforcement are not economically viable when compared to other modern processes such as lime piles or vibroflotation. When used in the context of a raft, earth reinforcement may not produce the degree of rigidity required to limit differential settlement.

Several laboratory and analytical investigations have been carried out with possibly the most comprehensive being due to Binquet & Lee (1975a, 1975b). In the first phase of the investigation some 65 model footing tests were executed in a sand-filled

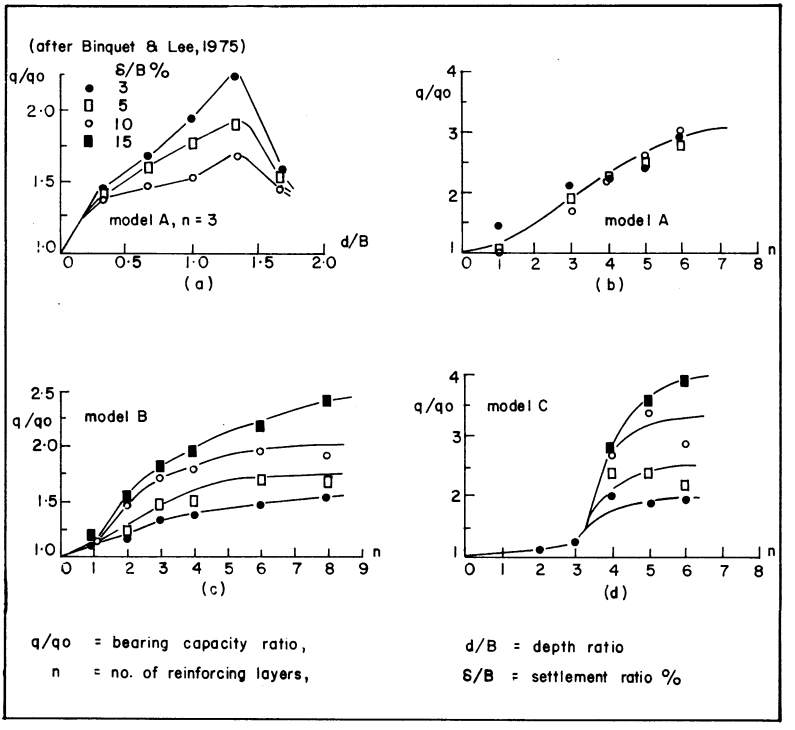

Figure 28 Bearing capacity test results

box 1500 mm long, 510 mm wide and 330 mm deep using a rigid strip footing 76 mm wide placed across the width of the box. The effects of soil reinforcement were investigated using three geological formations modelled in the box.

(a) homogeneous deep sand – model A;
(b) sand above extensive layer of compressible material simulating soft clay or peat – model B;
(c) sand above finite size pocket of very compressible material simulating lens of organic soil or cavernous rock – model C.

The extensive layer of compressible material was modelled with a bed of foam rubber 57 mm thick placed near the bottom of the box. Similarly the lens or cavern was modelled with a piece of foam rubber 150 mm wide and 50 mm thick placed centrally beneath the model footing. The deformation modulus of the compressible and very compressible material was 124 kN/m^2 and 5 kN/m^2 respectively, compared to 2100 kN/m^2 for the sand alone.

Reinforcement was in the form of 13 μm thick aluminium foil strips 13 mm wide placed in layers with a constant vertical spacing of 25 mm. Each layer was reinforced with 17 strips, each 1·5 m long, thus occupying some 42% of the plan area of the box. The variables investigated were the distance d between the bottom of the model footing and the top layer of reinforcement, as well as the number of layers of reinforcement which were installed with a constant vertical spacing. For each of the three basic models datum tests were carried out with no reinforcement to determine the conventional ultimate bearing capacity q_0. By this means the ultimate bearing capacity of the reinforced model, q, could be represented by a bearing capacity ratio factor q/q_0. Similarly the depth to the top layer of reinforcement, d, is expressed as a depth ratio, d/B, where B is the width of the footing. The effects of depth ratio, for model A, are reproduced in Fig. 28a, which shows a maximum bearing capacity ratio occurring at a depth ratio of 1·33 for a range of values of settlement ratio δ/B. As can be seen the reinforcing effect is more pronounced at low settlement ratios. The effect of increasing the number of layers of reinforcement is shown in Fig. 28b where an almost linear increase in bearing capacity ratio occurs for up to six layers of reinforcement. Above this the improvement appears to tail off. It is interesting to note that for model A this relationship seems to be almost independent of the settlement ratio. Conversely the results for model B (Fig. 28c), show a marked dependence on settlement ratio. This tendency is even more pronounced for the model C results (Fig. 28d), where almost no improvement in bearing capacity ratio is measured if less than four layers of reinforcement are used. In the course of an analytical

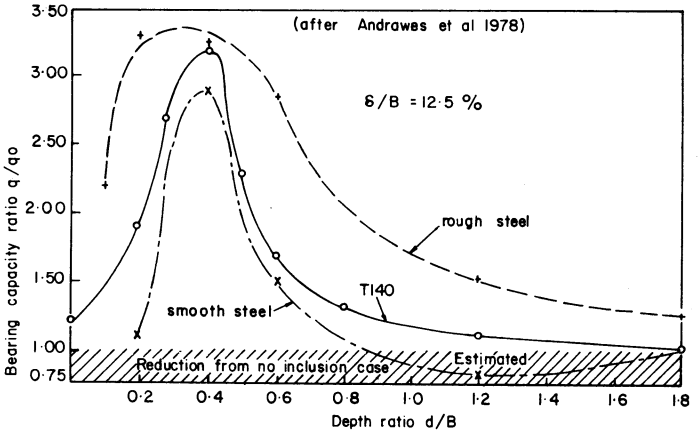

Figure 29 Bearing capacity test results

study Binquet & Lee (1975b) concluded that two distinct zones were formed in the soil beneath the foundation. In the first zone, which exists directly beneath the footing, the loaded soil moves vertically downwards whilst outside the footing there are symmetrical zones which tend to move laterally outwards and upwards, the function of an effective reinforcement being to hold these two zones together. A similar observation was made by Kheang (1972) and reported by Schlosser & Long (1974) with further studies reported by Stefani & Long (1979a, 1979b).

Yamanouchi (1970) and Yang (*loc. cit.*) have also reported enhanced bearing characteristics resulting from the use of reinforcement. Both of these investigators employed a single layer of continuous mesh reinforcement, with Yamanouchi investigating the reinforcing effects on soft clay and Yang the effect on sand. A single layer of reinforcement was also employed in an investigation carried out by Andrawes *et al.* (1978); however, this study investigated the effects of reinforcement stiffness as well as roughness. Typical results are given in Fig. 29 for rough steel, smooth steel and

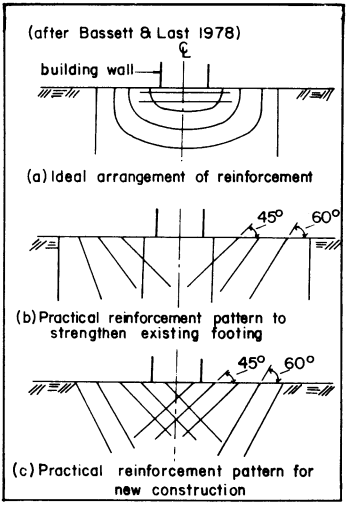

Figure 30 Inclined foundation reinforcement

T140 which is a non-woven fabric. Several interesting features arise from this investigation. Firstly the observed variation between bearing capacity ratio and depth ratio is similar to that reported by Binquet & Lee (1975b); however the maximum bearing capacity ratio occurs at a depth ratio of 0·4 (Fig. 29), as opposed to 1·3 (Fig. 28). This may be due to the use of continuous sheet reinforcement rather than a series of discrete strips. Secondly, at depth ratios between 0·8 and 1·8 the smooth steel is found to give a reduced bearing capacity ratio. This weakening effect is attributed to reinforcement with inadequate interface friction properties having an orientation along, or very close to, the failure lines in the soil. A similar view has been expressed by Bassett & Last (1978) who advocate the use of discrete reinforcements installed at various inclinations (Fig. 30). This system – which is identical to the reticulated root pile, or *pali radice* system pioneered in Italy (Oriani, 1971; Bartos, 1979; Lizzi & Carnevale, 1979) – has the great advan-

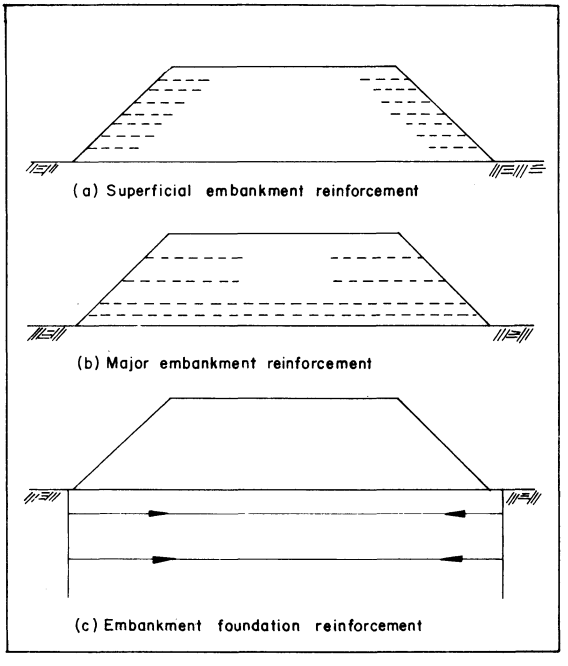

Figure 31 Modes of embankment reinforcing

tage that it can be installed beneath new or existing foundations, without need for excavation.

EMBANKMENTS

The potential saving in the use of reinforcement in embankments is enormous. For example in a 10 m high embankment with side-slopes steepened from 1 : 2 to 1 : 1 a saving of £1000 per metre run has been estimated (Sims & Jones, 1979). Reinforcement may be added to embankments to perform one, or all, of three main functions (Fig. 31):

(a) superficial slope reinforcement and edge stiffening;
(b) major slope reinforcement involving reinforcement of the main body of the embankment;
(c) reinforcement of weak embankment foundations.

The use of superficial slope reinforcement was pioneered by the Japanese (Yamanouchi, 1975), and particularly the Railway Technical Research Institute of Japanese National Railways. Reinforcement used by the Japanese is generally in the form of short lengths of Netlon, a polyolefin net, placed in horizontal layers near the face of the slope (Fig. 31a). Such reinforcement gives resistance to surface erosion and seismic shock as well as permitting heavy compaction plant to operate close to the shoulder of the embankment, so effecting good compaction in this sensitive area (Iwasaki & Watanabe, 1978).

Similar techniques have been employed in the United Kingdom (Dalton, 1977a, 1977b) and the United States of America where redundant car tyres have been used as reinforcement. This is achieved by slicing each tyre, in its plane, to give two rings; these rings are then joined by metal fasteners to give a chain-mail effect (Forsyth, 1978).

Reinforcement of the main body of the embankment (Fig. 31b) has produced mixed results. A reasonable degree of success has been achieved by the Japanese, again using polyolefin net, to improve seismic stability (Uezawa & Nasu, 1973) and static stability (Iwasaki & Watanabe, *loc. cit*). In the latter case the enhanced resistance against lateral spread of the embankment during compaction gave a nearly ten-fold increase in the standard penetration resistance of the material of the embankment.

Reinforcement at the embankment/foundation interface has resulted in minor improvements in stability. Belloni & Sembenelli (1977) monitored the construction of two embankments on deep peat deposits. The first embankment was reinforced with a single layer of non-woven fabric with an ultimate tensile strength of 18·6 kN/m and raised successfully to a height of 1·75 m. An identi-

cal unreinforced embankment failed on reaching 80% of this height. Similar results were obtained by Volman, Krekt & Risseuw (1977), who monitored construction of two identical embankments over a deposit of soft silt and peat. One embankment was reinforced with a single layer of woven nylon fabric with an ultimate tensile strength of 60 kN/m and raised to a height of 4·5 m before instability set in. The unreinforced embankment became unstable at a height of approximately 3·5 m. Somewhat poorer performance was observed by Bell, Greenway & Vischer (1977) during the construction of a 1·5 m high haul road embankment over muskeg, i.e. peat. The fabric was a highly extensible non-woven needle-punched material with an ultimate tensile strength of 13 kN/m attained at an axial strain of 100–200%. Although the fabric acted as a separating layer it had no effect on overall stability but did reduce localized bearing capacity failures in the muskeg. The investigators concluded that the fabric was far too extensible to generate any useful stabilizing force. An analytical study by Maagdenberg (1977) also advocated the use of a stiffer fabric capable of generating its potential restoring force at lower levels of induced deformation.

Published applications of embankment foundation reinforcement generally involve comparatively substantial measures. Both Uesawa & Nasu (*loc. cit.*) and Wager & Holtz (1976) have used shallow continuous-sheet pile walls installed at each toe of the embankment with connecting tie rods running beneath the base of the embankment (Fig. 31c). Holtz & Massarch (1976) have cleverly combined timber piles and geotextile reinforcement to similar effect. An alternative method involving the construction of a Reinforced Earth base slab has already been cited (Steiner, *loc. cit.*).

Various methods of analysis have been proposed; however, these mainly involve an adaptation of slip circle analysis with the reinforcement modelled as a cohesive layer (Volman *et al., loc. cit.*), or an equivalent tensile force developing an additional restoring moment (Phan, Sergrestin, Schlosser & Long, 1979; Christie & El Hadi, 1977). In executing these analyses the reinforcement is in-

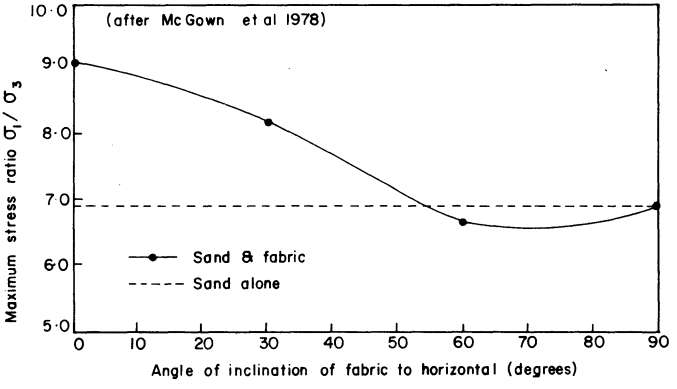

Figure 32 Effects on reinforcement orientation

variably assumed to be arranged in horizontal layers. This configuration is eminently suited to standard embankment construction techniques where the fill is also placed in horizontal layers. However, it must be remembered that the reinforcement should be installed to efficiently resist tension, and as such needs to be oriented along, or close to, the lines of principal tensile strain (Bassett & Last, *loc. cit.*). This assertion has been borne out by laboratory tests reported by Snaith *et al.* (1979) and McGown, Andrawes & Al-Hasani (1978). In the latter investigation plane-strain tests were carried out on cubical samples of Leighton Buzzard sand reinforced with a single sheet either of non-woven fabric or of aluminium foil. Initial tests were carried out with the reinforcement in a horizontal plane and thus along the axis of principal tensile strain. At this orientation the fabric was found to impart a considerable increase in strength as reflected by the maximum principal stress ratio. However as orientation of the fabric was changed in subsequent tests it was found that the fabric actually invoked a decrease in strength (Fig. 32). This decrease was most evident when the reinforcement was close to, or coincided with, the prospective failure plane in the sand. The decrease in strength is largely attributed to

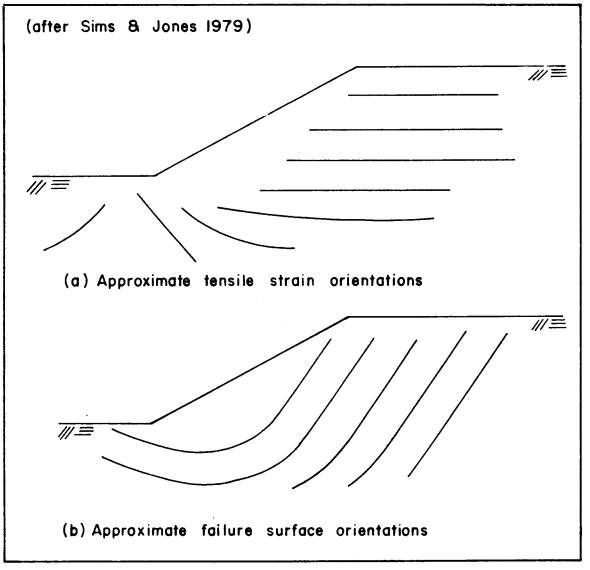

Figure 33 Critical embankment orientations

the angle of bond stress between the reinforcement and the sand being less than the internal angle of shearing resistance of the sand alone, thus creating a plane of weakness.

Studies carried out by Bassett & Horner (1977), Jones & Edwards (1975) and reported by Sims & Jones (*loc. cit.*) show that whilst principal tensile strain directions are substantially horizontal in the main body of an embankment they tend to fan out about the toe of the embankment in the embankment foundation (Fig. 33a). As a corollary to this, potential failure surfaces also exhibit horizontal sections in the embankment foundation (Fig. 33b) where the blind application of continuous horizontal reinforcement could well induce failure. This is not the case for vertical walls: Bassett & Last (*loc. cit.*) confirmed theoretically that a horizontal distribution of reinforcement should be employed.

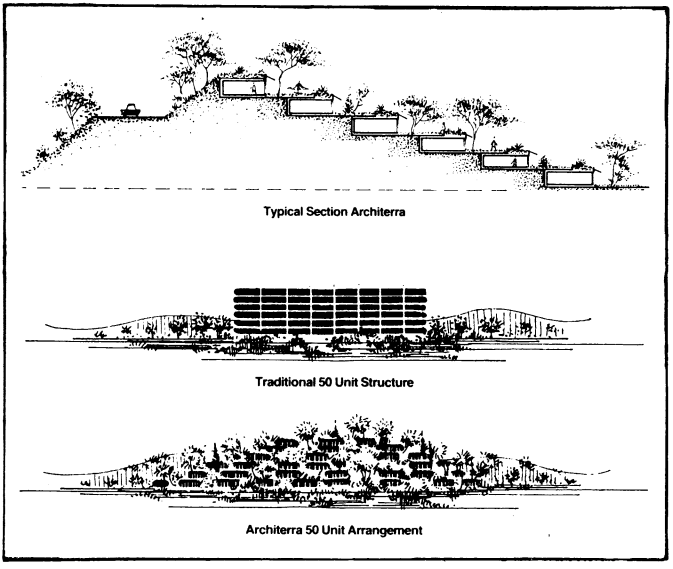

Figure 34 Architerra

REINFORCED EARTH WALLS

Of all the applications of Reinforced Earth considered walls, in one form or another, constitute the largest portion. At the end of 1978 Vidal's licensees had completed in excess of 2000 projects involving 1·3 million m^2 of facing (McKittrick & Darbin, 1979). These applications have been extremely diverse, ranging from earthquake-resistant bund walls at an Alaskan oil terminal (McKittrick & Wojciechowski, 1979) to blast-proof nuclear reactor containments (Reddy *et al.*, 1979). One of the most novel applications is Architerra, or Reinforced Earth houses (Levisalles, 1979). These dwellings are constructed on terraced mounds with a Reinforced Earth wall, forming a quadrant in plan, acting as the backwall of the dwelling as well as a retaining wall for the terrace above it (Fig. 34). The front of each unit is furnished with a patio door

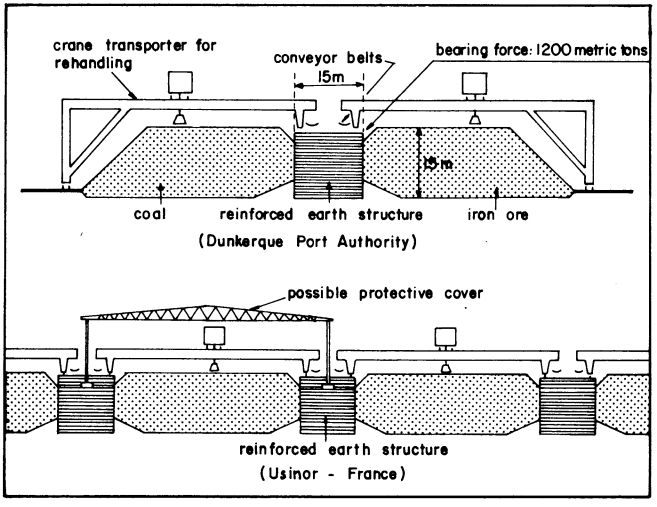

Figure 35 Bulk storage and handling

leading to a garden which is formed by the roof of the unit below.

Other structures erected by Vidal's licensees include crusher unit tip-walls and similar ancillary works involved in the mining industry (Smith, 1979), together with bulk storage and handling units such as those constructed for the Dunkerque Harbour Authority and Usinor of France (Fig. 35). The bulk storage and handling application has been much improved with the gravity-feed slot innovation now used in the United States of America for coal storage (Fig. 36). These structures are formed from long V-shaped trenches having sloping side-walls and a mechanical reclaim system at the base of the slot. The side-walls are formed by newly developed Reinforced Earth facing panels which can be precast at any angle, typically between 45° and 75° (McKittrick & Darbin, *loc. cit.*). Amongst these industrial structures must be counted the Reinforced Earth wall to the rock-crushing plant at Tarbela dam, this structure towering an incredible 26 m high (Price, 1975).

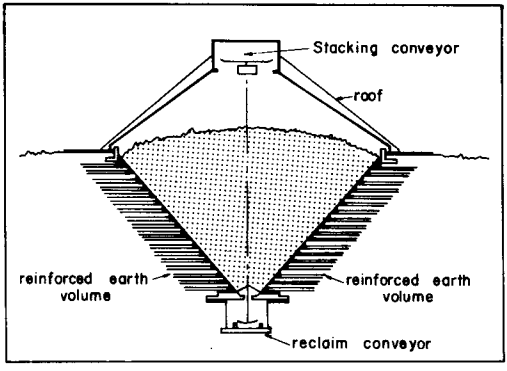

Figure 36 The slot storage system

Reasonable success has been achieved in the construction of marine works; however, construction is hampered if carried out in deep water. In tidal water construction generally follows the sequence of erecting one lift of facing units followed by end-tipping of fill, so forming a causeway for construction plant. With structures in tidal water consideration must be given to the possibility of migration of fines caused by the fluctuating water level. This problem is overcome simply by applying a flexible sealant or a suitable filter fabric to all facing unit joints. Reinforced Earth seems particularly suited to situations subject to wave attack since the comparative flexibility and resilience of the structure permits dissipation of the wave energy without damage. In these circumstances it is not unusual to use a heavier facing unit; indeed this was the case for the Mont St Pierre sea wall where precast concrete units 3·5 m wide, 1·5 m high and 250 mm thick were used (McKittrick & Darbin, *loc. cit.*). For less substantial marine structures it is possible to carry out construction in fairly deep water. This was achieved at the Grande-Mott marina where panels of elliptical cross-section steel facing units were prefabricated in sections approximately 10 m long and 5 m high. These sections, complete

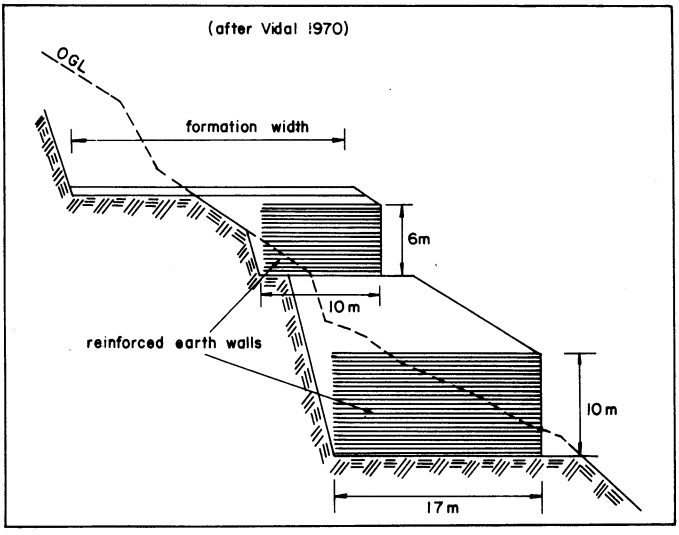

Figure 37 The Vigna wall (French–Italian motorway)

with reinforcement attached and temporarily rolled up, were lowered into position and then backfilled (Schlosser & Vidal, 1969).

By far the largest application of Reinforced Earth, in terms of surface area of facing units, is in the construction of highways and bridges. Reinforced Earth is particularly suited to economical highway construction in steep side-long ground. Some of the early examples of this include the Vigna wall (Fig. 37) on the French–Italian motorway (Vidal, 1970); and the Autoroute de Menton (Darbin, 1970; Marec, Baguelin & Vincentelli, 1971). Extensive use has been made of Reinforced Earth by the US Federal Highway Administration (Walkinshaw, 1975), particularly in construction over steep ground subject to slope instability. A widely documented example of this is the Reinforced Earth wall and stabilizing earthworks (Fig. 38), constructed in 1972 on the California

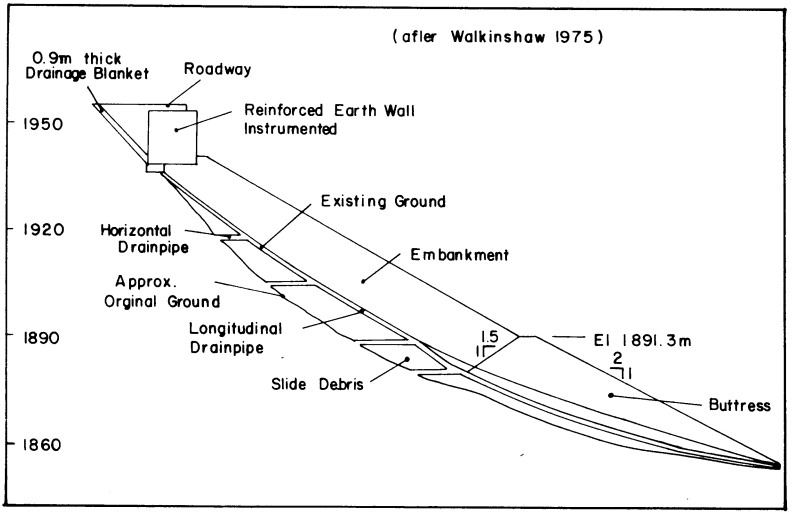

Figure 38 California route 39 – cross-section of remedial scheme

Route 39, this being the first application of Reinforced Earth in the United States (Chang, Forsyth & Smith, 1972; Chang, Hannan & Beaton, 1974; Gedney, 1972; Chang, 1974). Similar treatment was accorded to the slip on Interstate Highway 40 in Tennessee (Royster, 1974; Scott, 1974) and the 'Heart o' the Hills' slide near Washington (Munoz, 1974).

The resilience of Reinforced Earth has made it applicable to constructions of abutments and wingwalls of simply supported or low-tension bridge decks (Sims & Jones, *loc. cit.*). Early examples include quite large structures such as the bridge at Thionville (Price, *loc. cit.*); however, there is more widespread use in motorway bridge construction. Typical of these structures are the abutments constructed on Interstate 80 in Nevada. As may be seen in Fig. 39 these consist of a simple Reinforced Earth wall capped with a reinforced concrete bank seat beam to take the bridge deck. These abutments were founded on deep deposits of soft compress-

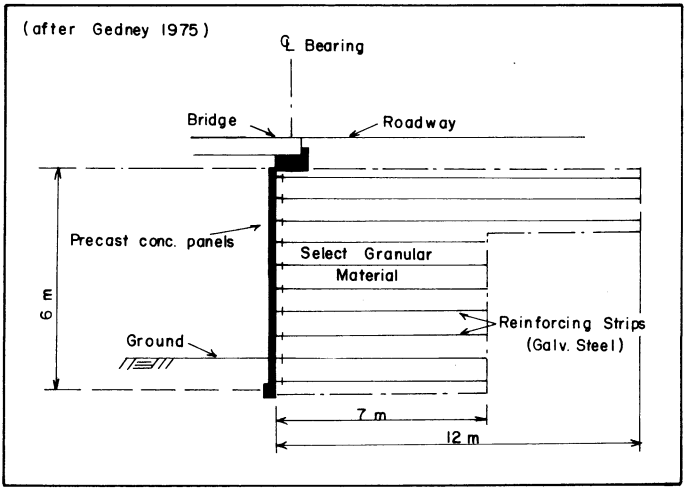

Figure 39 Reinforced earth abutment

ible soil which were predicted to settle approximately 1 m (Gedney, 1975). Under these conditions the alternative of conventional piled foundations would have proven very expensive in view of the large negative skin friction forces generated by the superimposed embankment fill. The resilience of Reinforced Earth was again demonstrated in the Sete Interchange in France where differential rotations of 1:100 were suffered without damage (Schlosser, 1973). In 1975 the LCPC in association with Vidal and his licensees completed a study of reinforced earth abutments which culminated in publication of the then definitive work by the Ministère de L'Equipment (1975).

3

Research and Development

From 1957 to 1962 Henri Vidal carried out a series of experiments and model tests proving that earlier observations on the stabilizing effects of pine needles in beach sand would have practical and significant applications to civil engineering. By 1962 Vidal had completed his preliminary study, which culminated in the production of a thesis, and in due course filed patent applications. In 1966 Reinforced Earth was considered for a major project on the proposed Nice–Menton Autoroute; consequently Vidal entered into discussions with the LCPC who were the authority responsible for assessing and approving such innovations. A programme for verifying Vidal's designs and specifications was mutually agreed and in May 1967 work began at the LCPC using model walls to investigate various failure modes. In 1968 the LCPC completed the work and approved Vidal's designs and specifications for use in major structures on the Nice–Menton Autoroute. Within 5 years similar research had commenced both in the United States of America and the United Kingdom. The end of 1976 heralded a bonanza of research with publication of the proceedings of the international symposium 'New Horizons in Construction Materials' held at Lehigh University, Pennsylvania. This was rapidly followed in 1977 by the international conference 'The Use of Fabrics in Geotechnics', and the TRRL/Heriot–Watt University symposium 'Reinforced Earth and other Composite Soil'. Two international symposia took place

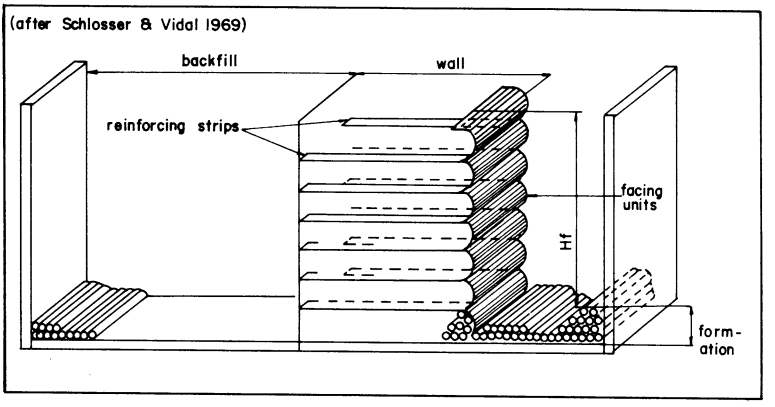

Figure 40 The Schneebeli model wall system

in 1978: the ASCE spring convention symposium 'Earth Reinforcement', held in Pittsburgh, and the New South Wales University/ Institute of Technology symposium 'Soil Reinforcing and Stabilising Techniques', held in Sydney. A further international conference, 'Soil Reinforcement', was held in Paris in 1979. In the same year session eight of the seventh European conference on soil mechanics and foundation engineering was devoted to 'Artificially improved Soils' with a speciality session 'Reinforced Earth' being incorporated in the sixth Panamerican conference. Although these learned gatherings were intended as forums for all applications of soil reinforcing techniques the vast majority of the submissions involved walls.

FRENCH RESEARCH

Most of the research in France was carried out by the LCPC in association with Henri Vidal, their research programme beginning in 1967 with experiments on small-scale plane-strain model walls, using the Schneebeli roller technique (Fig. 40; see Guegan & Legeay, 1969; Long, Schlosser, Guegan & Legeay, 1973). This was followed in 1968 by investigations on full-scale walls built by

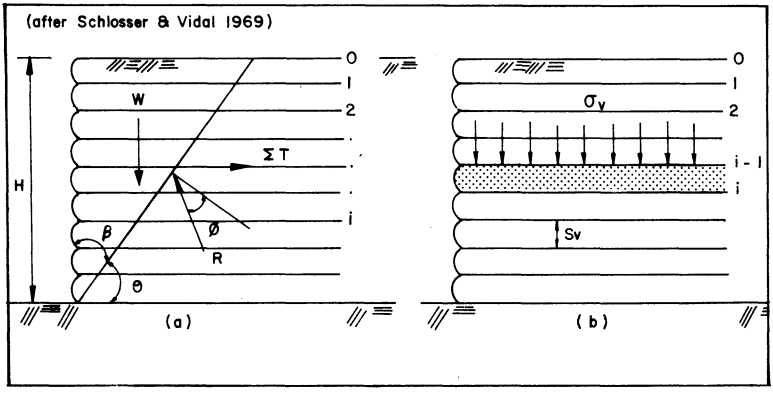

Figure 41 The Coulomb and Rankine methods

Vidal's licensees at Incarville (Schlosser, 1970: Schlosser & Long, 1970), Dunkerque (Hulo, Ramery & Pouilly, 1972) and on the Autoroute de Menton (Baguelin & Bustamante, 1971). Further model studies were carried out at the Institut National de Sciences Appliquées (INSA) at Lyon under the direction of the LCPC (Lareal & Bacot, 1973). Although referred to as 'three-dimensional' as opposed to the 'two-dimensional' Schneebeli model the INSA walls were also plane-strain models employing sand fill placed in rigid-sided tanks. A small amount of model wall work was carried out independently at the University of Lyon (Sanglerat, 1971; Chapuis & Prinquet, 1973; Bacot, 1974).

Analytical studies of Reinforced Earth walls published by Schlosser and Vidal (1969) stated that design considerations fall into two main categories, namely internal and external stability. The problem of internal stability was associated with the reinforced mass proper, in which instability could be invoked either by tensile failure of the reinforcement or bond failure of the reinforcement. The latter mode of failure was not analysed at this stage; it was simply stated that the length of the reinforcement should be 80% of the wall height. In designing against external instability the re-

inforced mass was considered to act as a rigid body, and as such was treated in the same manner as a gravity wall with checks being made on base sliding, overturning and bearing capacity failure as well as the overall stability of the wall and its environs.

Several observations were made concerning internal stability, these being primarily concerned with quantifying the tensile force generated in the reinforcement. The first analytical method presented was the so-called 'Coulomb force method'. Reference to Fig. 41a shows a Reinforced Earth wall of height H with $n + 1$ layers of reinforcement at equal vertical spacings S_v. The lengths of the reinforcement are sufficient to prevent bond failure. If the reinforced mass is assumed to be cut by a failure plane, passing through the toe of the wall and inclined at an angle θ to the horizontal, then the equilibrium of the wedge to the left of the failure plane may be expressed in terms of the weight of the wedge W and the sum of the tensile forces in the reinforcement ΣT per metre run of wall. Taking the unit weight of the soil to be γ, whence $W = \frac{1}{2}\gamma H^2 \cot\theta$, considerations of equilibrium lead to equation (28) where ϕ is the internal angle of shearing resistance of the soil in the wall:

$$\Sigma T = \tfrac{1}{2}\gamma H^2 \cot\theta \tan(\theta - \phi') \tag{28}$$

Differentiation of ΣT with respect of θ leads to a maximum when $\theta = 45 + \phi'/2$. Substitution of this value into equation (28) leads to equation (29):

$$\Sigma T = \tfrac{1}{2}\tan^2(45 - \phi'/2)\gamma H^2 \tag{29a}$$

$$\Sigma T = \tfrac{1}{2}K_a \gamma H^2 \tag{29b}$$

Equation (29b) represents the sum of the reinforcement tensions. To determine the force in each layer of reinforcement Schlosser & Vidal (*loc. cit.*) assumed a triangular distribution with no tension in the top layer, $i = 0$, and the maximum tension in the bottom layer,

$i = n$. This maximum tension, per metre run of wall, is given by equation (30):

$$T_m = \frac{n}{n+1} K_a \gamma H S_v \tag{30a}$$

$$T_m = \frac{n^2}{n+1} K_a \gamma S_v^2 \tag{30b}$$

With the tensile force in the ith layer being given by equation (31):

$$T_i = \frac{i}{n+1} K_a \gamma H S_v \tag{31a}$$

$$T_i = \frac{in}{n+1} K_a \gamma S_v^2 \tag{31b}$$

Thus to ensure internal stability it is necessary to check that the induced tensile force T_i is less than the ultimate tensile strength of the ith layer of reinforcement.

A second analytical method, the 'Rankine force method', was developed to give the tensile force in the ith layer of reinforcement directly. Reference to Fig. 41b shows the ith layer of reinforcement resisting the horizontal thrust on a section of facing unit equal in height to the vertical reinforcement spacing S_v. The $(i-1)$th layer is subjected to a uniform vertical surcharge σ'_v, thus if it is assumed that the ith layer of reinforcement must resist the active thrust imparted to the facing unit between the $(i-1)$th and ith layer then:

$$T_i = K_a \sigma'_v S_v + \tfrac{1}{2} K_a \gamma S_v^2 \tag{32}$$

If the strips are long the vertical stress σ_v may be equated to the overburden pressure $(i-1)\ \gamma S_v$ whence equation (32) becomes:

$$T_i = (i - \tfrac{1}{2}) K_a \gamma S_v^2 \tag{33}$$

The maximum tensile force per metre run of wall again occurs in the bottom layer and is given by equation (34):

$$T_m = (n - \tfrac{1}{2}) K_a \gamma S_v^2 \tag{34}$$

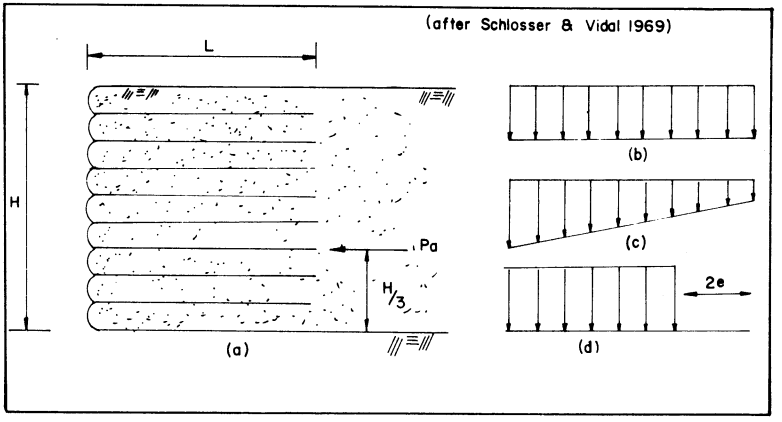

Figure 42 The trapezoidal and Meyerhof distributions

When n is large equations (30) and (34) yield approximately the same result – equation (35):

$$T_m = nK_a\gamma S_v^2 \tag{35a}$$

$$T_m = K_a\gamma HS_v \tag{35b}$$

Equation (35) may be expressed in the more general term given by equation (36):

$$T_m = K_a\sigma'_v S_v \tag{36}$$

In concluding their analysis Schlosser and Vidal considered the effects of the horizontal thrust generated by the fill on the back of the reinforced earth mass. Inspection of Fig. 42a shows a wall of height H with reinforcement of length L. The backfill may be considered to impose an active thrust P_a, acting at a height $H/3$ above the base of the wall, thus generating a bending moment of $K_a\gamma H^3/6$ about the centre of the base. At the toe of the wall the vertical stress σ'_v assumes a maximum value which may be evaluated using a trapezoidal stress distribution (Fig. 42c); equation (37):

$$\sigma'_v = \gamma H + K_a\gamma H^3/L^2 \tag{37a}$$

$$\sigma'_v = \gamma H(1 + K_a H^2/L^2) \tag{37b}$$

Three years later Schlosser (1972) proposed a further analytical method based on the Meyerhof distribution (Fig. 42d); equation (38):

$$\sigma'_v = \frac{\gamma H}{1 - K_a H^2/3L^2} \tag{38}$$

Equations (37) and (38) give the vertical stress at the base of a wall of height H which may be substituted into equation (36) to calculate the tensile force per metre width at that level. For intermediate reinforcement layers σ'_v may be calculated by replacing H by the depth of fill above the particular layer under consideration. For walls where the height approximately equals the length of the reinforcement and good-quality backfill is used equations (37) and (38) predict a maximum vertical stress that is some 25% and 10%, respectively, greater than the simple overburden pressure. Where the reinforcement is long, as in the case of the model tests, then the vertical stress approximates to the overburden pressure (Fig. 42b), whence equation (35) applies.

Comparison of the theory and results obtained both from model and full-scale walls showed poor agreement. Interpretation of the model test results was made from equation (35b) which gives the maximum tensile force per metre run at the base of a wall of height H. For a model of width B equation (35b) becomes:

$$T_m = K_a \gamma H B S_v \tag{39}$$

The model walls were reinforced with aluminium foil of known equivalent tensile strength T_u*. Since the height of each wall was increased until it failed it was known that $T_m = T_u$ thus equation (39) was rearranged to give the theoretical failure height H_f, equation (40), which could be compared with the measured failure height H_m.

* T_u = ultimate tensile strength per reinforcement × number of reinforcements per layer per metre run of wall.

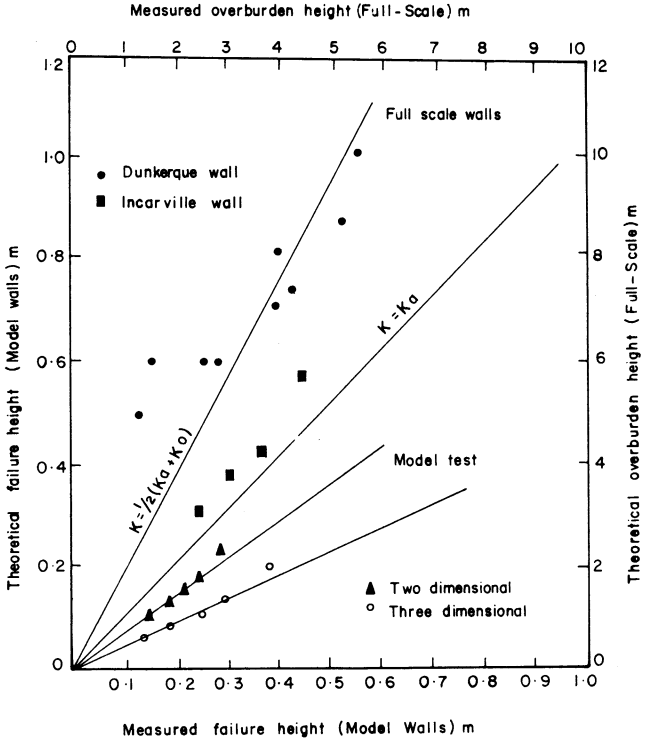

Figure 43 Comparison of theoretical and experimental results

$$H_f = T_u/K_a\gamma BS_v \tag{40}$$

The full-scale walls were not loaded to failure; however, the maximum tensile force generated in the reinforcements was measured as was the height of overburden above each reinforcement. Thus the measured tension could be used as a pseudo-ultimate tensile strength from which a pseudo-failure height could be calculated. This is then compared to the 'actual failure height' which is simply the measured height of overburden.

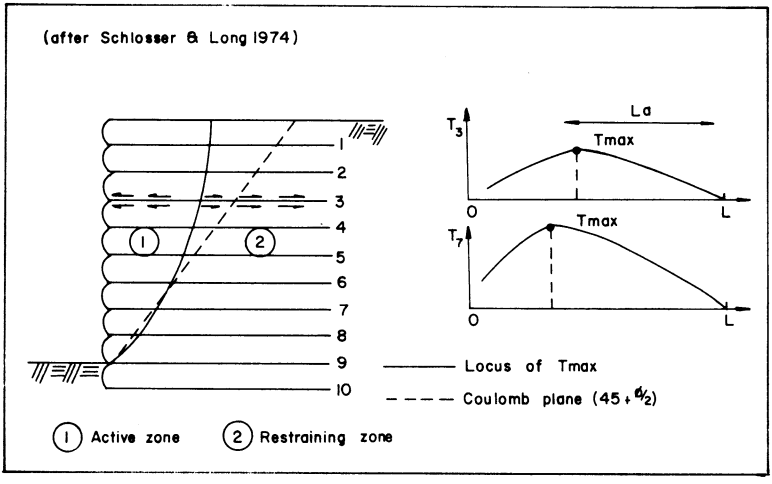

Figure 44 Distribution of reinforcement tensions

Figure 43 shows a comparison between theoretical and experimental results. As can be seen the model walls failed at heights considerably greater than those predicted, with this tendency being much more pronounced in the 'three-dimensional' models. This poor agreement is thought to be due to a combination of factors. Firstly the models are operated at very low stress levels with maximum wall heights less than 400 mm. Consequently if the soil has even the slightest tendency to dilate the internal angle of shearing resistance would increase, hence decreasing K_a and increasing H_f. Since it appears that no appropriate low stress level testing of the soil was carried out this effect might pass unnoticed. Next there is the effect of the rigidity of the model facing units. Even with no internal reinforcement the facing units would be capable of supporting some finite height of fill which should be added to the theoretical height given by equation (40). There is also the problem of base friction in the model which tends to reduce the tensile force otherwise generated in the bottom layer of reinforcement. Finally there is the problem of side friction which is

peculiar to the 'three-dimensional' tests which were carried out in glass-sided tanks with a width to height ratio of approximately 0·5. Obviously for such narrow models the soil would tend to arch across the tank and therefore fail at heights significantly greater than those predicted. This influence possibly accounts for the significant difference in the results of the 'two' and 'three' dimensional models.

Quite reasonable agreement between theoretical and experimental results was found for the Incarville wall; however, poor agreement was observed for the Dunkerque wall results. Reference to Fig. 43 shows that the theoretical overburden heights/pseudo-failure heights were approximately 100% higher than the measured values. This is almost certainly due to additional earth pressure, and therefore reinforcement tension, induced by compaction plant.

Analysis of the reinforcement tension measurements from the full-scale walls showed some very interesting results. As is shown in Fig. 44 the reinforcing strip tensions did increase with depth but the distribution of tension along each strip was such that the maximum tension occurred some distance back from the facing unit. This distribution is very significant, as can be seen from equation (4):

$$\mathrm{d}T/2\sigma' b\mathrm{d}l = f \tag{4a}$$

Since $\sigma' f = \tau$:

$$2b\tau = \mathrm{d}T/\mathrm{d}l \tag{4b}$$

As the tension reaches a maximum the slope of the tension *vs.* length curve changes from positive to negative, implying a change in the sign of the shear stress acting on the reinforcement (Fig. 44). This leads to the conclusion that there are two well-defined zones within the reinforced mass: the active zone, adjacent to the facing units, and the restraining zone. The dividing line between these two zones is the locus of the points of maximum reinforcement tensions where the shear stress on the reinforcement is zero. As can be seen from Fig. 44 this locus is quite different from

the Coulomb failure plane. Later analytical work based on the finite element method (Corte, 1977) and photoelastic models, (Santini & Long, 1978) endorsed these observations.

These results instigated further thought on the problem of bond failure. One basic conclusion was that the bond length of the reinforcement, that is the length of reinforcement embedded in the restraining zone (Fig. 44), must be long enough to resist the maximum tensile force, T_m, generated in the reinforcement. A simple analytical method was proposed by Schlosser (1972). First consideration was given to one layer of reinforcement containing N strips of width b per metre length of wall. Taking the vertical stress on the reinforcement to be σ'_v and the coefficient of soil/reinforcement friction to be f the limiting condition is defined by equation (41):

$$T_m = \int_0^{L_a} 2Nbf\sigma'_v dL \tag{41}$$

If the vertical stress is taken equal to the overburden pressure γH equation (42) results:

$$L_a = T_m/2Nbf\gamma H \tag{42}$$

If T_m is evaluated from equation (35) the limiting bond length becomes:

$$L_a = K_a S_v/2Nbf \tag{43}$$

This shows that to a first approximation the bond length is independent of the level of the reinforcing layer. A more meaningful calculation would involve consideration of the distribution of vertical stress along the length of the reinforcement. Somewhat simply the Meyerhof distribution was applied to give the expression:

$$L_a = \frac{K_a S_v}{2Nbf\,[1 - (K_a H^2/3L^2)]} \tag{44}$$

It was pointed out that the limiting bond length L_a must be increased by an amount equal to the width of the active zone to arrive at the total length of reinforcement at any given level. Having made this statement the LCPC then advocated the use of equation (43) to evaluate the *total* reinforcement length on the basis that dilation occurs in the vicinity of the reinforcement causing the vertical stress level to rise locally above the ambient overburden pressure, thus compensating to some extent for the use of such a simple expression.

THE UCLA STUDY

The earliest comprehensive study of walls in the United States of America was carried out at the UCLA under the direction of the late Professor Lee. The initial research was limited to model walls which were used to investigate static behaviour (Lee *et al.*, 1972, 1973; Vagneron, 1972), as well as behaviour under seismic loading (Richardson & Lee, 1974). Later research involved the construction of a 7 m high prototype wall again used to investigate both static and dynamic behaviour (Richardson, 1976).

The study commenced by making the same initial assumptions as the LCPC; namely that active conditions would prevail giving rise to maximum tensile forces in the reinforcement occurring at the facing unit. Expressions were again derived for the maximum tensile force based on the Rankine method (R) and the Coulomb force method (CF). Additionally an expression was derived using the Coulomb moment method (CM) in which the sum of the moments of the reinforcement tensile forces about the toe of the wall are equated to the active earth pressure moment, also about the toe of the wall; equation (45):

$$T_m = [n^2/(n^2 - 1)]\, K_a \gamma H S_v \tag{45}$$

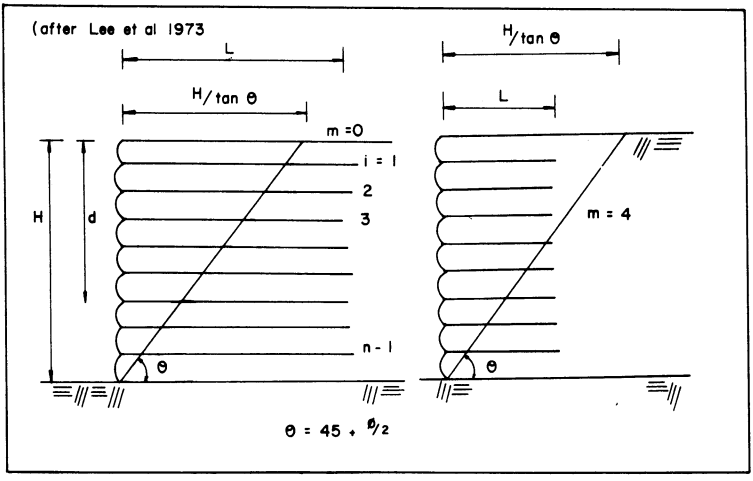

Figure 45 Key factors used in UCLA design

Analytical investigations of pull-out, or bond failure, again considered the Rankine approach which results in a constant bond length L_a projecting from the potential failure plane into the restraining zone. For this case the total length of each reinforcement would increase linearly from a minimum at the bottom of the wall to a maximum at the top. It was pointed out that if the wall was to be constructed with reinforcements all of the same length then the minimum length would be dictated by conditions at the top of the wall (Fig. 45), where for a factor of safety F_b against bond failure:

$$L = \frac{H}{\tan\theta} + F_b L_a \tag{46a}$$

$$L = \frac{H}{\tan\theta} + \frac{K_a S_v F_b}{2Nbf} \tag{46b}$$

The study continued by drawing attention to the fact that the

Coulomb methods consider overall stability rather than local stability, as in the case of the Rankine method, and thus it is not necessary that all the reinforcements extend beyond the potential failure plane. To some extent this vindicated the assumption of the LCPC that the total reinforcement length could be expressed by equation (43). On this basis then the total maximum pull-out resistance, for the case in which all the reinforcements have a constant length L with only some of them extending into the restraining zone, was defined by equation (47) where P is the pull-out resistance per unit length of wall and m is the value of i for the first reinforcement from the top to extend into the restraining zone:

$$P = 2\gamma bfNS_v \sum_{i=m}^{n} i[L - (n - i)S_v\tan(45 - \phi'/2)] \qquad (47)$$

The factor of safety against bond failure was obtained using the Coulomb force method by dividing equation (47) by total active thrust; equation (48):

$$F_b = \frac{4bfNS_v}{K_aH^2} \sum_{i=m}^{n} i[L - (n - i)S_v\tan(45 - \phi'/2)] \qquad (48)$$

A corresponding expression was obtained using the Coulomb moment method; however, in this case the sum of the moments about the toe of each reinforcement pull-out resistance is divided by the total moment about the toe of the active thrust; equation (49):

$$F_b = \frac{12bfNS_v^2}{K_aH^3} \sum_{i=m}^{n} (n - i)i[L - (n - i)S_v\tan(45 - \phi'/2)] \qquad (49)$$

The required constant length of reinforcement, L, for a given wall height H was determined from equation (48) or equation (49) by a quick trial-and-error procedure. To facilitate comparison of the results for the three different methods calculations were carried out

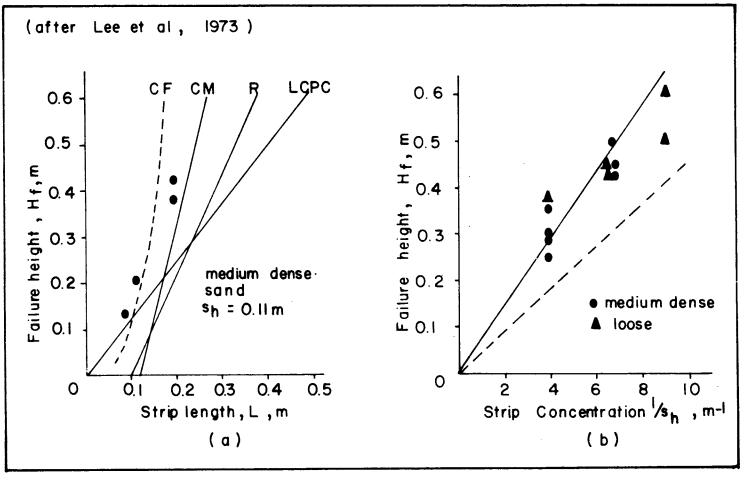

Figure 46 Comparison of theoretical and experimental results

using the dimensions and properties of one of the series of model tests. These results are shown graphically in Fig. 46a. The Coulomb force method computes the shortest length of reinforcement, whereas the Rankine method leads to the longest reinforcement and therefore is the most conservative.

Following the analytical assessment model tests were carried out to investigate both tensile and bond failures. The apparatus comprised a wooden box 1220 mm long, 760 mm wide and 610 mm high, in which the model walls were constructed. Facing units were constructed of 0·3 mm thick aluminium foil formed to give a semicircular cross-section. The reinforcing strips, which were 3·9 mm wide, were made of 0·013 mm thick aluminium foil giving an ultimate strength of 4·9 N per strip. A limited number of strips were instrumented with electrical resistance strain gauges. Although the length and horizontal spacing of the strips were varied from test to test the vertical spacing was maintained constant at 25 mm. The model walls were constructed in the same

manner as a full-scale wall with one facing unit and its attending strips being positioned and filled before placing of the subsequent facing unit. The fill, which was a fine uniform sand, was rained from a hopper to ensure a uniform density. During placement of the sand a thin layer of coloured sand was installed at alternate layers to act as a marker bed. To investigate the effects of density, tests were carried out with the sand at a relative density of 63%, i.e. medium-dense, or 20%, i.e. loose. The corresponding angles of internal shearing resistance which were measured using the triaxial apparatus, operating at appropriately low stress levels, were found to be 44° and 31°. Pull-out tests on the reinforcing strips indicated an angle of bond stress of 31° corresponding to $f = 0{\cdot}6$. The heights of the model walls were increased until failure was induced, when the models were dismantled to allow location of the failure plane, as indicated by the marker beds, and any tensile fractures.

Typical results for walls failing by strip breakage are shown in Fig. 46b. As can be seen the test results for medium-dense sand are in reasonable agreement with the simple Rankine theory. Conversely the test results for the loose sand show greater failure heights than those predicted by theory; in fact these results were found to be very close to those for the medium-dense sand. This result may reflect the fact that no allowance was made for the effect of the backfill thrust on the distribution of vertical stress within the reinforced mass. Measurement of the distribution of tension along the reinforcing strips gave slightly ambiguous results. These indicated that the highest stress level occurs close to the facing unit; however, the overall stress levels seemed to be low suggesting that some of the stress was being taken by the strain gauge lead wires. In view of this, later models were fitted with strain gauges close to the face to minimize such interference.

Typical results showing the variation of tensile stress with depth are given in Fig. 47a. As can be seen there is a trend involving the anticipated increase of tensile stress with depth; however, this trend is curtailed towards the base of the wall. This effect is almost certainly induced by base friction. On inspection after failure of the

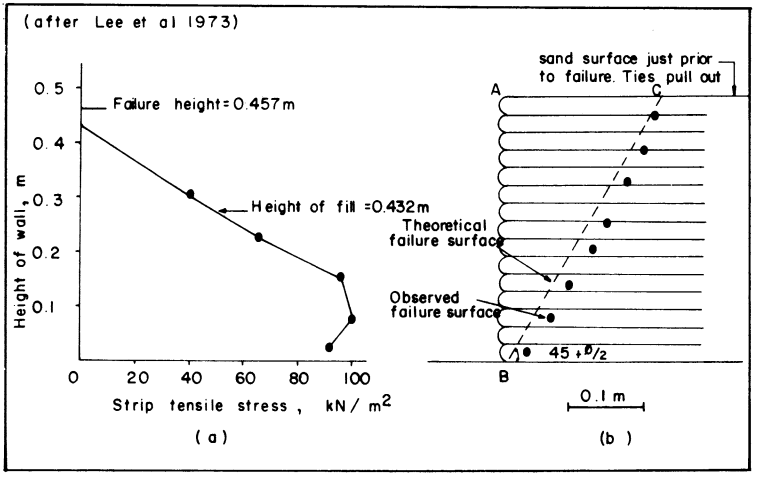

Figure 47 Observed tensile stress and failure plane

wall the ties were found to have fractured at the facing unit, as predicted by the strain gauge measurements. These findings were contrary to those of the LCPC. However, later and more reliable measurements on the full-scale wall confirmed that maximum strip tensions occurred some distance back from the facing.

Results for walls failing by pull-out of the reinforcement (Fig. 46a), show fairly close agreement with the theoretical results from the Coulomb methods. As expected the Rankine theory was found to be conservative. For comparison Fig. 46a shows the LCPC rule-of-thumb design which takes $L = 0{\cdot}8H$.

An extremely interesting result was obtained for the shape and location of the failure surface. Figure 47b shows a typical series of test results compared with the classical Coulomb failure plane inclined at $(45 + \phi'/2)$ to the horizontal. As can be seen the observed failure plane is slightly curved but emanates from the toe of the wall and finally converges with the Coulomb plane at the top of the wall. The original references did not make clear whether the

observed plane was associated with a tensile or bond failure mode. However, later work (Lee, 1976), states that in model walls loaded to failure, either in bond or tension, the outer boundary of the failure zone always approximates to the theoretical failure plane.

This observation was found to be at variance with the subsequent full-scale wall investigation where the locus of the points of maximum strip tension fell along a curve very similar to that observed by the LCPC (Fig. 44). Further variance between model and full-scale applications was found in the magnitude of strip tensions with the field results being quite close to the 'at rest' distribution in the upper sections of the wall. A similar observation was made by Chang (*loc. cit.*) during his investigation of a full-scale wall on Highway 39. This result is not entirely unexpected since as explained by Schlosser & Vidal (1969) if the same distribution of reinforcement is used in each layer the reinforcement in the upper layers will be understressed and therefore suffer negligible strains thus giving rise to a K_0 pressure regime. At depth the same reinforcement would be exposed to higher lateral pressures inducing higher tensile stresses and strains. If the strain is large enough there would be a corresponding lateral yield in the adjacent fill, ultimately leading to the development of an active pressure regime.

THE DoE/TRRL STUDY

The first Reinforced Earth wall constructed in the United Kingdom is situated on the Leith to Granton bypass near Edinburgh. This wall, which was constructed in 1972, is some 106 m long and up to 7 m high with construction being completed in 5 weeks (Finlay & Sutherland, 1977; Finlay, 1978). This success was repeated on the Huntingdon–Godmanchester bypass and the Runcorn–Widnes bridge. In all three cases the Vidal concrete panel system was used. At about this time the Department of the Environment (DoE) started its own research and development programme with Banerjee of the DoE, assisted by Bolton at University of Man-

chester Institute of Science and Technology (UMIST), appointed to carry out a theoretical study. Jones, of the West Yorkshire Metropolitan County Council was responsible for devising a practical construction system (Reina, 1975). These studies culminated in the production of two reports: Banerjee (1973) and Bolton (1972), together with the construction of a 100 m long prototype wall on the M62 in Yorkshire using the so-called 'York Method' of construction (Jones, 1978). The first technical publication on this subject was by Symons (1973) of the DoE/TRRL, who briefly reviewed the LCPC and UCLA studies. This was followed by a state-of-the-art study sponsored by the then West Riding County Council (Mamujee, 1974).

One year later Banerjee (1975) published a paper presenting principles of analysis and design. This extremely abstruse dissertation, which is based on the Coulomb force method, presents a general analysis involving a $c'-\phi'$ soil and a uniform surcharge at the top of the wall. For simplicity the presentation here is confined to a purely frictional soil with no surcharge. Consideration was given to a wall of height H where the reinforced mass is cut by a plane inclined at β to the vertical (Fig. 41a). It follows that the sliding and restoring forces along the plane are given by equation (50):

$$\text{Sliding force} = \tfrac{1}{2}\gamma H^2 \sin\beta \tag{50a}$$

$$\text{Resisting force} = \tfrac{1}{2}\gamma H^2 \sin\beta \tan\beta \tan\phi' + \Sigma T(\cos\beta \tan\phi' + \sin\beta) \tag{50b}$$

Introducing a factor of safety, F, defined as the ratio of resisting force to sliding force, equation (51) is derived where $X = 2\Sigma T/\gamma H^2$:

$$F = \tan\beta \tan\phi' + X(1 + \cot\beta \tan\phi') \tag{51}$$

On the assumption that ΣT and hence X is not very sensitive to changes in β Banerjee obtained a value of β for the minimum factor of safety, equation (52):

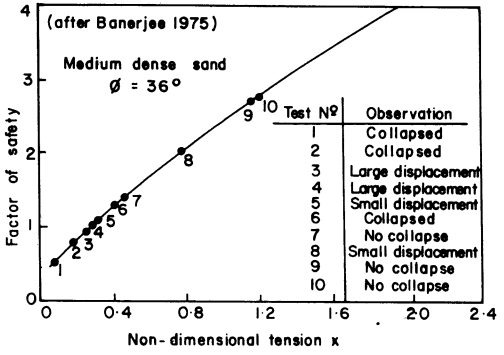

Figure 48 Comparison of theoretical and experimental centrifuge results

$$\tan\beta = \sqrt{X} \tag{52}$$

The value of ΣT will depend on whether all the bars fail in tension or bond. Thus if all the bars fail in tension:

$$\Sigma T = nT_u \tag{53}$$

Conversely for bond failure Banerjee derived an equation identical to equation (47); however it was assumed that $m = 0$ whence the expression was summed over n terms to give equation (54):

$$\Sigma T = \gamma bfNS_v[(n^2 + n)(L - H\tan\beta) + \tfrac{1}{3}(n^2 + n)(2n + 1)S_v\tan\beta] \tag{54}$$

It was then argued that the value of β could only be determined if ΣT were known. The statement was then made that ΣT is not very sensitive to the value of β, whence β was put equal to $(45 - \phi'/2)$. This assumed value was then substituted into equation (54) to give a value of ΣT. This value of ΣT was then substituted into equation (52), in the form of X, to give a 'more accurate value of β' which in

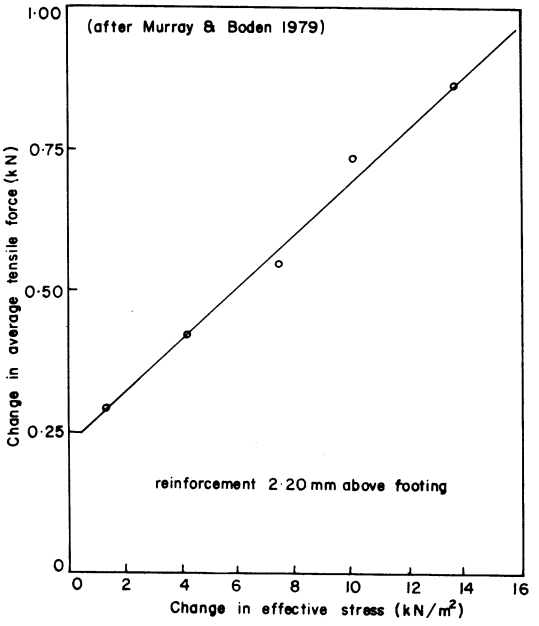

Figure 49 Relationship between change in average tensile force and change in effective stress

turn was substituted, with ΣT, into equation (51) to finally give a factor of safety against bond failure. Although not stated, it follows that to derive a factor of safety against tensile failure equation (53), in the form of X, is substituted into equation (52) to give β which is in turn substituted into equation (51), with ΣT from equation (53).

To assess the veracity of this approach the theoretical results were compared with those obtained from a series of centrifugal tests on models, constructed using dry sand, with reinforcement lengths and spacings which were varied from test to test. The comparison is shown in Fig. 48 in for form of a plot of factor of safety against non-dimensional tension $X = 2\Sigma T/\gamma H^2$. As can be seen

there is reasonable agreement between theoretical and experimental results with all models having a theoretical factor of safety of unity or less, either collapsing or suffering large displacements. There is only one anomaly, concerning test No. 6, in which the model wall collapsed at a theoretical factor of safety of approximately 1·3. It is interesting to reflect on the theoretical value of the non-dimensional tension, equation (55), at failure. Assuming that active thrust is developed then $\Sigma T = \frac{1}{2}K_a\gamma H^2$ whence $X = K_a$:

$$X = 2\Sigma T/\gamma H^2 \tag{55}$$

This is borne out by Fig. 49 where, for a factor of safety of unity, $X = 0{\cdot}26$ which exactly equals the value of K_a for $\phi' = 36°$.

To make some assessment of the likely reinforcement tensions under service conditions Banerjee (1973) carried out a finite element analysis in which the soil and reinforcement were assumed to exhibit linear–elastic behaviour. For vertical and horizontal reinforcement spacing S_v and S_h the strip tension T_s at any depth d was defined by a further dimensionless parameter $T/\gamma d S_v S_h$. It was found over a wide range of relative soil/reinforcement stiffness that the maximum value of this parameter was sensibly constant at 0·35. This value was subsequently recommended for design in association with a factor of safety of 3.

The initial centrifuge work was extended under the auspices of the TRRL to include comparatively sophisticated models with instrumentation for measuring the distribution of tension in the reinforcing strips as well as the distribution of vertical stress across the wall base (Bolton, Choudhury & Pang, 1978a, 1978b). One of the main findings from these series of tests was that the vertical pressure distribution across the width of the models was not uniform with the stress at the toe of the wall being up to 25% above the theoretical overburden pressure (Choudhury, 1977). It was concluded that this variation of vertical stress could be quite safely modelled using the trapezoidal stress distribution advocated by

Schlosser & Vidal (1969). The sand used in the construction of the model walls proved to be strongly dilatant with the angle of internal shearing resistance varying from 50° to 42° over the normal stress range 0–100 kN/m^2. This led to problems in correlating theoretical and experimental data, since for the range of ϕ' the value of K_a increased some 50% from 0·13 to 0·20.

The TRRL investigation which is concurrent with that at UMIST commenced with an analytical and model wall study. The model walls, which were 1 m high, showed a well-defined Coulomb wedge at failure as observed by Lee *et al.* (*loc. cit.*). Also there was a tendency for the lateral pressures, as backfigured from measured strip tensions, to be closer to the 'at rest' distribution in the upper reaches of the structure. Murray (1977) argued that this phenomenon could be induced by the mode of wall deformation; for example if the wall translates, as certain of the model walls did, then the resulting pressure distribution is not the familiar linear distribution associated with walls rotating about their toes. Simple Dubrova (1963) theory was applied to show that translation results in a parabolic pressure distribution with $K \geqslant K_o$ at the top of the wall and $K < K_a$ at the base of the wall. A further, and most revealing, result obtained from the model wall tests concerned the effect of factor of safety on the distribution of strip tension. For a comparatively high factor of safety of 2·5 the maximum tension occurred some distance back from the face of the wall; however, at a factor of safety of 1·1 the maximum tension occurred at the face of the wall as found by Lee *et al.* (*loc. cit.*).

One of the prime objectives of the TRRL research was to investigate the use of cohesive backfill. This was achieved through the study of small scale models followed by the construction of pilot and full-scale walls. After successful construction of a 3 m high pilot-scale wall backfilled with clay full-scale field trials were started in the summer of 1977 (Boden, Irwin & Pocock, 1978). The full-scale structure comprised a 6 m high embankment retained on three sides by vertical facing units (Murray & Boden, 1979). The main body of the embankment was 14 m wide and some 25 m long

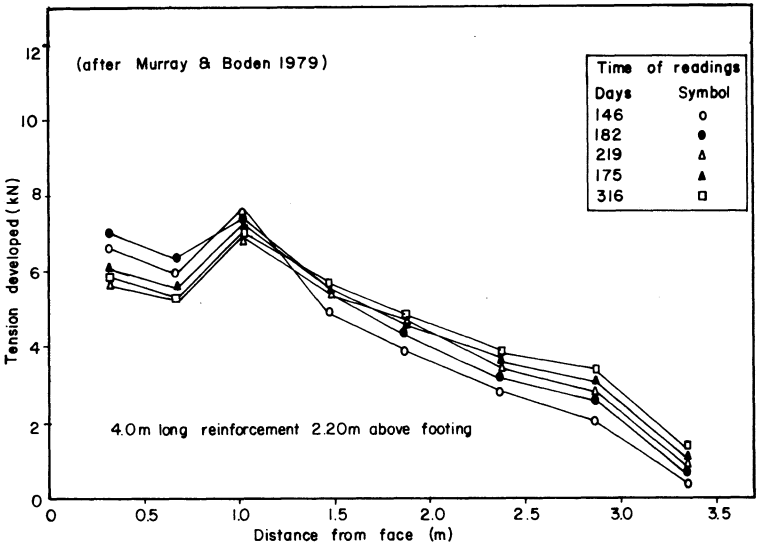

Figure 50 Distribution of tension in reinforcement

with a construction ramp approximately 20 m long. The backfill was made up of three main layers, each layer occupying approximately one-third of the height. At the lowest level was a sandy silty clay with liquid and plastic limits of 30% and 17% respectively. This fill was placed as wet as possible consistent with trafficability by the construction plant. The middle layer was a granular fill installed to give a comparison between the performance of conventional and cohesive fills. The upper layer of fill, which was a silty clay – liquid limit 42%, plastic limit 21% – was placed at a moisture content of 18%.

A range of different types of reinforcing strips were installed, including stainless steel, mild steel either galvanized or with plastic or aluminium coating, prestressed concrete planks, fibre-reinforced plastic, and non-woven fabric. Several types of facing

unit were employed to assess the relative performance of large and small units, as well as to study the influence of the flexibility of the jointing between the units (Boden *et. al., loc. cit.*).

During construction alarmingly high excess porewater pressures amounting to 90% of the overburden pressure were developed in the lower layer of cohesive fill; however, there was no sign of bond failure of the reinforcing strips. Very small or zero excess porewater pressures were recorded at all times for locations less than 1 m distant from the facing. Contrary to what was originally anticipated the horizontal pressures acting on the wall did not reduce significantly as porewater pressure dissipated, but remained fairly constant. This behaviour was attributed to differential settlements caused by consolidation occurring more rapidly at the facing units which were backed with a drainage layer as well as to changes in mobilized interface friction between the soil and the reinforcement (Murray & Boden, *loc. cit.*). Although some evidence was put forward to substantiate the assertion that the mobilized friction and the tension which developed in the reinforcement was controlled by effective stress (Fig. 49) this appears to be at variance with the published tension distribution, for the same reinforcement, given in Fig. 50. One unequivocal observation was that compaction plant has a very significant effect on lateral pressures generated at shallow depths of fill. Figure 51 shows lateral pressures recorded by a pressure cell located 1·125 m above the footing of the wall. As can be seen, until the depth of fill exceeded approximately 2·5 m the lateral earth pressures were dominated by the effects of compaction plant. The results of a finite element analysis incorporating such effects are also given in Fig. 51. Above a depth of fill affected by compaction plant the measured lateral pressures were in reasonable agreement with those obtained using a Meyerhof distribution associated with K_o, the coefficient of lateral earth pressure at rest, rather than K_a, the coefficient of active earth pressure. The DoE study extended to the development of several construction systems, an investigation of reinforcement corrosion, as well as the publication of a formal

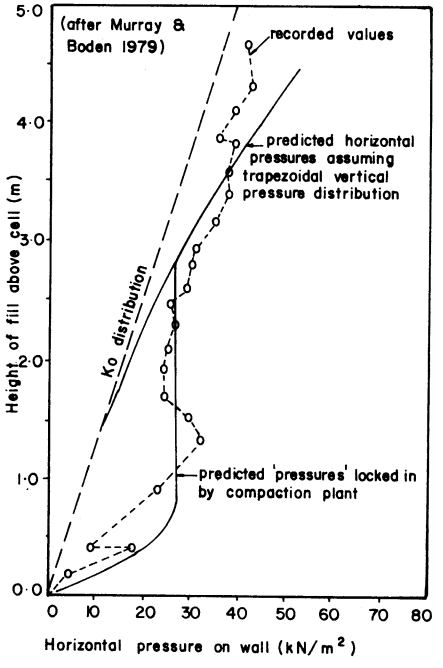

Figure 51 Relation between height of fill and horizontal pressure on wall for a cell installed 1·125 m above footing

design manual. These developments will be considered in later sections.

RECENT RESEARCH

The years 1976–79 witnessed a mass onslaught of research with six major conferences and symposia being held during this short period. To review every contribution in detail is beyond the scope of this short text and would only result in a mere catalogue; therefore consideration will be limited to the major innovations. With

few exceptions these fall into two main categories: namely investigations of failure modes and investigations of soil-reinforcement bond.

Investigations of failure modes

It has long been recognized that walls might fail through external instability, as might be suffered by a conventional gravity wall, or by internal instability invoked by either tensile or bond failure of the reinforcement (Schlosser & Vidal, *loc. cit.*). However, what was not recognized was that the density, distribution and in-service stress levels of the reinforcement might affect the location and form of failure surfaces within and adjacent to the reinforced mass. The formation of a failure surface other than that assumed in design could have catastrophic consequences. For example to guard against bond failure all design methods rely on the existence of a calculated bond length extending beyond an assumed failure surface into stable backfill. If the true failure surface deviates from that assumed the result is either an uneconomical design, or, even worse, an unsafe design.

A most enlightening investigation of such possible deviations was carried out at Cambridge University using small-scale model walls constructed of sand and aluminium foil reinforcement (Smith, 1977). By using well-established radiographic techniques (James, 1973), it was possible to define rupture surfaces where the sand had dilated and thus become less opaque to X-rays. Three different reinforcement arrangements were investigated: (a) dense reinforcement; (b) short wide reinforcement; (c) long thin reinforcement (Smith & Wroth, 1977). The dense reinforcement was modelled by sheets of aluminium foil placed in such a concentration that the reinforced zone acted as a rigid body. Radiographs revealed what appeared to be a well-defined active zone developed at the back of the wall. A simple analysis revealed that the stability of the wall was governed by the H/L ratio and its effects on overturning (Smith & Bransby, 1976). This result would

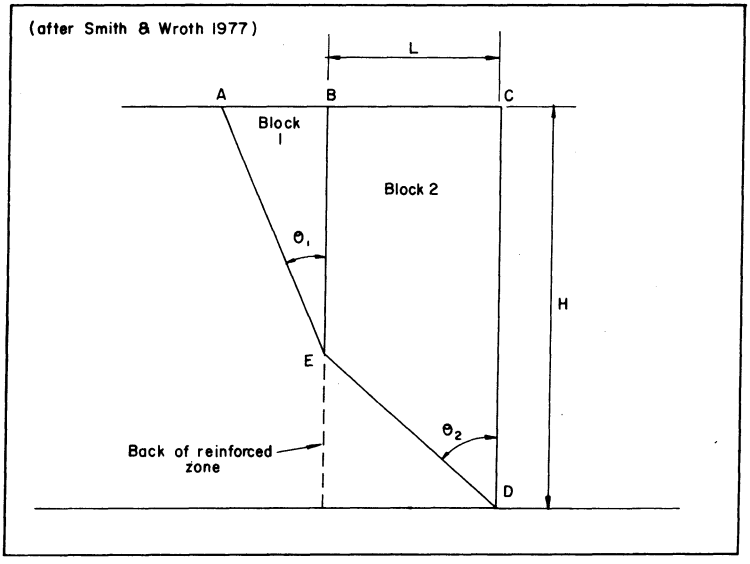

Figure 52 Geometry of failure surfaces

not be entirely unexpected since the walls had very high H/L ratios in the range 5–10 compared with the more normally adopted in-service ratio of approximately unity. The next reinforcement configuration investigated involved walls with short wide reinforcement where the ratio of the length to the total width of the reinforcement across the model wall was less than 10. In this case a substantially planar failure surface was found to pass through the toe of the wall within the reinforced earth mass. However, there was a distinct increase in the slope of the failure surface as it emerged from the back of the reinforced zone (Fig. 52). This was associated with a zone of high strain running up the back of the wall above the point of emergence of the failure surface. The final case considered long thin reinforcement where the ratio of reinforcement length to total width was greater than 10. For this

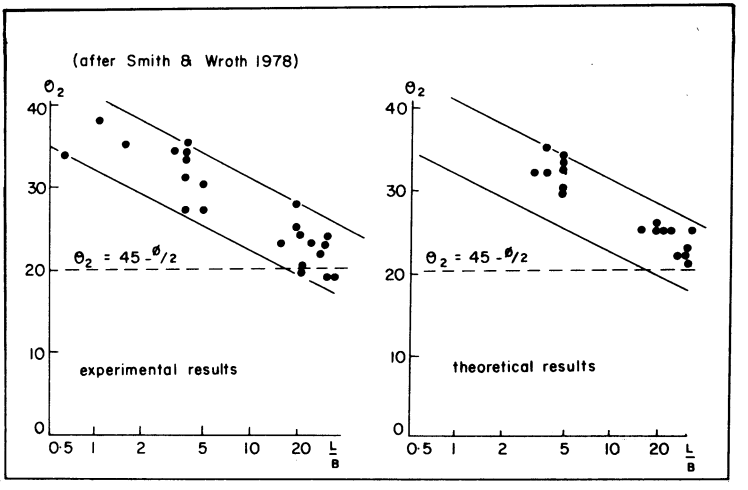

Figure 53 Inclination of failure surface to the vertical

configuration the rupture surface again passed through the toe of the wall; however, the surface was substantially planar and steeper than those observed in the models with short wide reinforcement. From consideration of the equilibrium of the two blocks of soil shown in Fig. 52 a simple analysis was carried out to determine the value of θ_2 to give the minimum failure height for reinforcement of a known width B and length L. The experimental and theoretical results are shown in Fig. 53: as can be seen, as L/B increases the value of θ_2 decreases. The significance of the change in θ_2 can be seen by reference to Fig. 52. As θ_2 becomes smaller the failure surface ED becomes steeper; the kink at the back of the reinforced zone becomes less pronounced and disappears completely if the failure surface is entirely within the reinforced zone. If θ_2 becomes larger it eventually approaches 90°; the failure mechanism is then that of the reinforced zone overturning under the action of a Coulomb wedge behind it. It is interesting to reflect that in the model tests carried out to failure by Lee *et al.* (*loc. cit.*) the

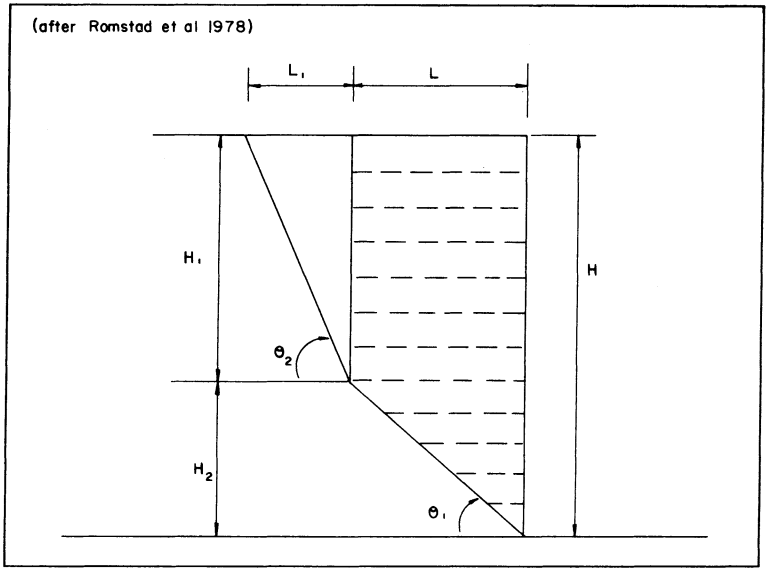

Figure 54 Geometry of failure surfaces

observed value of θ_2 of $(45 - \phi'/2)$ was associated with reinforcing strips generally having $L/B>20$.

A very similar result was obtained by Romstad, Al Yassin, Herrmann & Shen (1978) who developed a very simple analysis to determine the effects of reinforcement spacing and failure mode on the geometry of the rupture surface. This analytical investigation was limited to granular soils where failure is defined by equation (56):

$$\sigma_1 - \sigma_3 = \frac{2\sigma_3' \sin\phi'}{1 - \sin\phi'} \tag{56}$$

The analysis assumed a failure surface made up of two straight lines. The lower line, inclined at θ_1 to the horizontal, passes

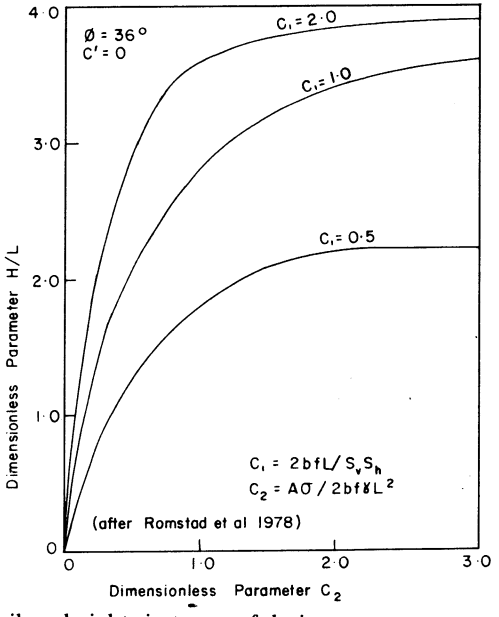

Figure 55 Failure heights in terms of design parameters

through the reinforced zone cutting the back of the wall at a height H_2 above the base (Fig. 54). A second line extends from this point, inclined at θ_2 to the horizontal, up to the level of the top of the wall. By considering the equilibrium of the mass contained between the failure surface and the front of the wall a quadratic equation was derived in terms od $H/L - \tan\theta_1$ having coefficients that include the variables θ_1, θ_2, $\Sigma T/\gamma L^2$ and an assumed lateral earth pressure coefficient K. For given values of θ_1, θ_2 and assumed value of $\Sigma T/\gamma L^2$ and K, the equation became a simple quadratic in H/L. By fixing values of θ_1 and varying θ_2 it was possible to find a critical value of θ_2 corresponding to a minimum value of H/L. The effects of the mode of reinforcement failure and spacing were modelled by two dimensionless parameters where A and σ are

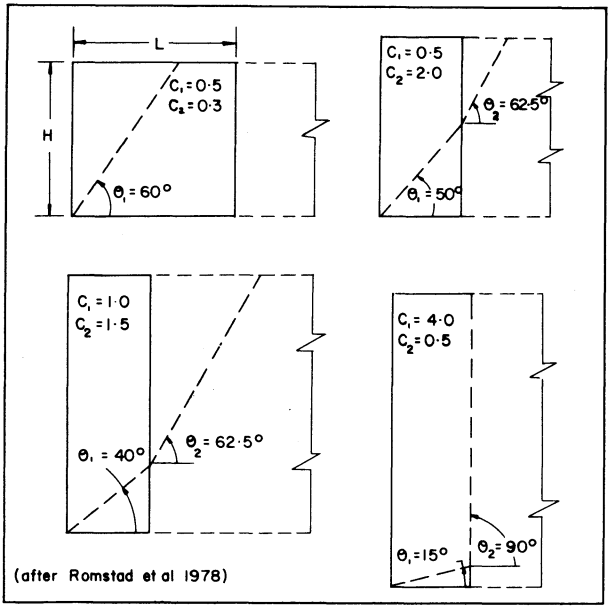

Figure 56 Typical failure surfaces in terms of design parameters

respectively the cross-sectional area and yield stress of a reinforcement:

$$C_1 = 2bfL/S_vS_h$$
$$C_2 = A\sigma/2bf\gamma L^2$$

Solutions were developed for a range of the design parameters C_1 and C_2 to study failure heights and the geometry of the failure surfaces. In Fig. 55 the solution for H/L may be viewed by taking a given value of C_2 and noting the increase in failure height as C_1 is increased. This is equivalent to holding all reinforcement parameters constant and simply decreasing their horizontal and vertical spacing. Alternatively it is possible to hold C_1 constant and

consider H/L as a function of increasing C_2. This is equivalent to holding all parameters constant except increasing the yield force capacity of the strips. As expected, the failure height increases with decreasing spacing or increasing yield capacity unless no strips reach yield at failure. The solution for any given value of C_1 with increasing C_2 becomes horizontal when pull-out becomes the mechanism of failure for all strips.

Typical failure surfaces for combinations of C_1 and C_2 are illustrated in Fig. 56. Generally, increasing the values of C_1 and C_2 decreases the value of θ_1. For all values of $C_1 = 1{\cdot}0$ and $C_2 > 1{\cdot}5$ the θ_2 value was 90° and the same observation was noted for $C_2 = 1{\cdot}0$ and $C_1 > 1{\cdot}5$. In general, the larger values of C_1 and C_2 represent greater percentages of reinforcement relative to the contributing area of soil and the failures begin to represent merely a sliding of the entire reinforced earth mass as a monolithic unit. As pointed out by Romstad *et al.* (*loc. cit.*), laboratory tests would normally be designed for small values of C_1 and/or C_2 because of low overburden stress levels; hence they fail with the classical Coulomb failure plane while prototype walls are designed with larger values for C_1 and C_2 resulting in much different failure surfaces.

Unfortunately Romstad *et al.* (*loc. cit.*) did not appear to investigate the effects of factor of safety on the geometry of potential failure surfaces. From results of the DoE study it would appear that this has considerable effect. For example Bolton *et al.* (*loc. cit.*) found that at high factors of safety the locus of the maximum reinforcement tensions was substantially a vertical line $0{\cdot}4H$ back from the face of the wall; however, in models taken to failure by tensile fracture of the reinforcement the fractures were found to occur along a classical Coulomb plane (Murray, *loc. cit.*). Similarly the TRRL model wall tests showed that for a factor of safety of 2·5 maximum tensions occurred well back from the facing, whilst for a factor of safety of 1·1 the maximum tensions occurred at, or very close to, the facing.

The LCPC have long been aware that the locus for maximum reinforcement tensions does not coincide with the Coulomb plane.

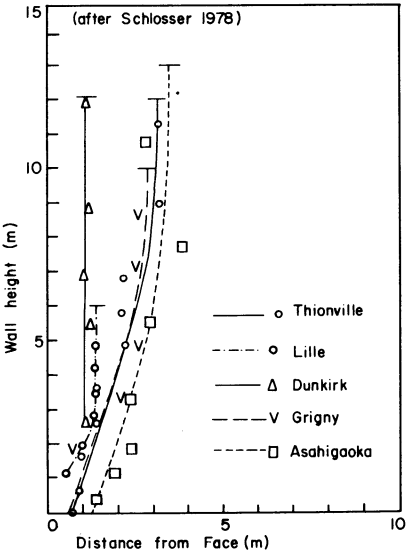

Figure 57 Loci of points of maximum tension

Figure 57 shows the results for six full-scale walls presented by Schlosser (1978). As can be seen the loci are substantially vertical in the upper sections of the walls with a gentle curve in the lower sections bringing the loci through or close to the toes of the walls. However, it must be remembered that these results come from walls operating at their in-service stress levels at which there would be a factor of safety of at least 2 against failure. In the light of this LCPC embarked upon a theoretical analysis assuming a log-spiral failure surface which in the upper half of the wall is a substantially vertical line $0{\cdot}3H$ back from the face of the wall (Juran, 1977). The analysis further assumes that the toe of the wall rotates about the top of the wall (Juran & Schlosser, 1978). This assertion warrants additional investigation since many researchers have observed that walls consistently rotate actively about their toes (Lee *et al.*, *loc.*

cit.; Finlay, *loc. cit.*; Al Hussaini & Johnson, 1978; Magyarne, Radnoti, Scharle & Szalatay, 1979).

A possible explanation for the geometry of the in-service 'failure surface' was given by Bassett & Last (*loc. cit.*). It was argued that potential slip or rupture planes are coincident with so-called 'zero extension lines'. In the case of a rigid smooth wall rotating actively about its toe one family of zero extension lines coincide with the familiar planar failure surface inclined at $45 + \phi'/2$ to the horizontal. However when horizontal reinforcement is introduced the comparative rigidity of such inclusions induces a family of horizontal zero extension lines. The conjugate family of zero extension lines are vertical and as such constitute the observed vertical section of the 'failure plane'. Bassett and Last suggested that the curved lower section of the failure plane might be caused by yielding of the reinforcement. Such yielding would, of course, no longer qualify the plane of the reinforcement as a zero extension plane which on such yielding would rotate back to an inclination near to $45 + \phi'/2$ to the horizontal.

Investigations of soil-reinforcement bond

In designing a Reinforced Earth wall it is necessary to make an assessment of the likely bond stress and hence effective length of the reinforcement consistent with adequate pull-out resistance. Since the fill generally used in Reinforced Earth is of a granular nature the bond between soil and reinforcement is frictional and as such depends on the ambient normal stress level, σ_v', and the coefficient of soil-reinforcement friction, f. Early investigations by Vidal and his licensees made use of the conventional shear box with a sample of the reinforcement mounted flush with the shearing surface of one box and soil filling the other half of the box (Schlosser & Vidal, *loc. cit.*). Figure 58 shows results that are typical of this type of test. As can be seen there is a linear relationship between the maximum mobilized bond stress and normal stress, giving rise to a constant angle of bond stress δ where $\tan \delta = f$. Results for the smooth reinforcing strip tested in a sand with $\phi = 43°$ show a quite

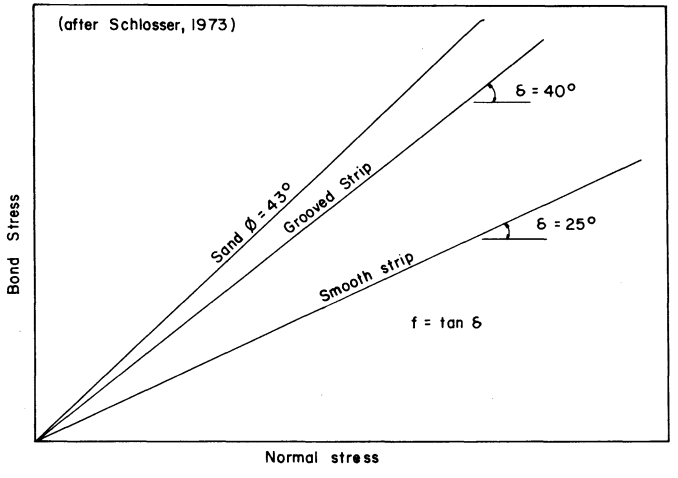

Figure 58 Shear box test results for bond stress

modest angle of bond stress of 25°, $f = 0{\cdot}47$. Conversely with the reinforcement machined with transverse grooves, approximately 0·5 mm deep, there is a radical increase in δ to 40°, $f = 0{\cdot}84$. As a consequence of this the early Reinforced Earth design methods assumed that $f = 0{\cdot}4$ for fill with less than 15% finer than 80μm. A higher coefficient could only be used if substantiated by testing (Schlosser, 1973). On this basis the bond stress acting on a reinforcement at a depth z was taken to be $0{\cdot}4\ \gamma z$.

It was apparent that the simple shear box test did not model the behaviour of a strip subjected to a tensile load; thus a more realistic investigation was conducted through Vidal's licensees (Mevellec, 1977). This involved pull-out tests on strips of reinforcement from a model embankment 600 mm high (Fig. 59). All of the reinforcing strips were led out through the shoulder of the embankment by way of a smooth plastic tube so that the gauge length of each reinforcement was acted upon by a constant overburden depth generated in the main body of the model embankment. Some of the strips had

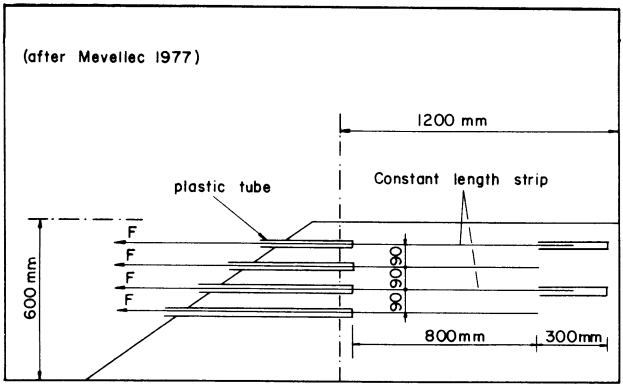

Figure 59 Small-scale pull-out tests

their free ends encased in a further smooth plastic tube embedded in the body of the fill; this ensured a constant exposed gauge length. The reinforcing strips, which were made of smooth bronze, were 0·2 mm thick, 150 mm wide and either 800 mm or 1000 mm long. Prior to conducting the pull-out tests the bond stress characteristics were measured in the shear box. Using a Fontainebleau sand at a dry unit weight of 17·3 kN/m^3 the angle of bond stress was found to be 27°, tan $\delta = 0{\cdot}51$, compared with $\phi^1 = 47°$ for the sand alone, (Alimi, Bacot, Lareal, Long & Schlosser, 1977). The first series of pull-out tests was used to investigate the effects of soil density. In interpreting the pull-out test results the LCPC introduced an apparent coefficient of friction f^*, equation (57), derived from knowledge of the pull-out force, F, the embedded length L, over-burden γh and reinforcement width b:

$$f^* = F/\gamma h\, 2bL \tag{57}$$

The results of these tests are summarized in Table 1 for a reinforcement length 1000 mm under an overburden height, h, of 150 mm.

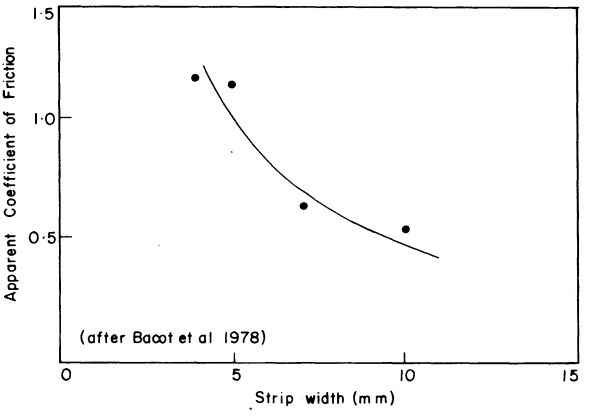

Figure 60 Variation of f^* with strip width

It was observed that at low density the peak value of f^* was obtained at small displacements of typically 2 mm, whereas at high density the peak was obtained after much greater displacement, typically 160 mm. The most striking effect of high density was the greatly enhanced value of f^* which rose from 0·30 at a dry density of 1·56 Mg/m^3 to 2·50 at a density of 1·76Mg/m^3. This was attributed to dilatancy effects.

A further series of tests was carried out to determine the effects of strip width. The results were somewhat inconclusive since,

Table 1 Results of pull-out tests

Dry density (Mg/m^3)	tan ϕ	f (shear box)	f^* (peak)	ε% (peak)	f^* (residual)	ε% (residual)
1·56	0·50	0·34	0·30	0·2	0·17	10·0
1·66	0·70	0·38	0·54	0·6	0·30	11·0
1·76	1·07	0·51	2·50	18·0	2·36	24·0

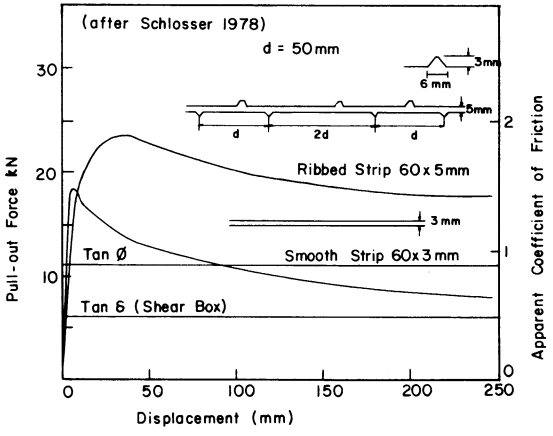

Figure 61 Full-scale pull-out test results

although for overburden heights less than 180 mm there was a well-defined decrease in f^* with increasing width, there was no discernible relationship for overburden heights above 180 mm. This tendency for f^* to decrease with width was later confirmed by Bacot *et al.* (1978); see Fig. 60.

Vidal's licensees also carried out full-scale pull-out tests (Alimi *et al.*, *loc. cit.*) to investigate the effects of embedded length, overburden and strip roughness. The influence of strip roughness has been studied in some 500 pull-out tests conducted by the Reinforced Earth Companies in France and Spain. Two types of reinforcement have been used in these tests (Fig. 61):

(a) plain galvanized steel strips;
(b) ribbed galvanized steel strips.

Typical load–displacement curves are shown in Fig. 61. As can be seen the peak resistance for the ribbed strip is higher than that for the smooth strip; however, this higher peak occurs at a displacement of approximately 50 mm compared to 5 mm for the

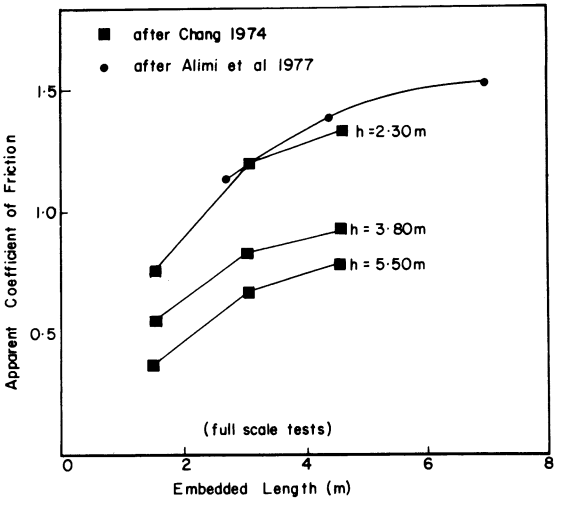

Figure 62 Variation of f^* with length

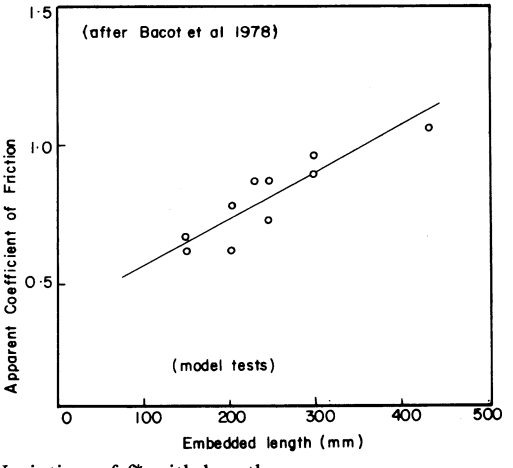

Figure 63 Variation of f^* with length

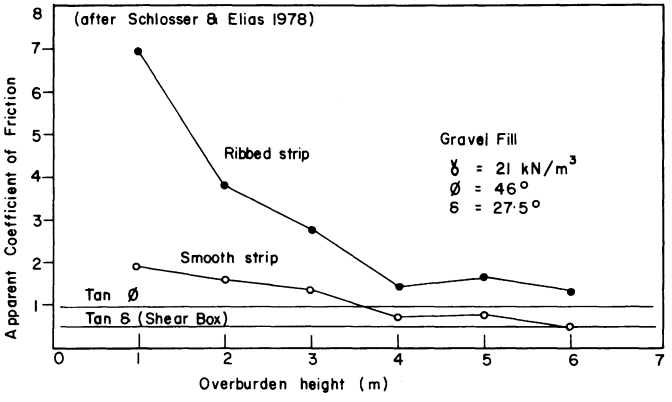

Figure 64 Variation of f^* with overburden

smooth strip. For both types of reinforcement the value of f^* was greater than tan ϕ' measured using a shear box.

The effects of reinforcement length have been reported by several investigators (Alimi, 1978; Bacot *et al., loc. cit.*; Schlosser & Elias, 1978).

Reference to Fig. 62 shows the results of full-scale pull-out tests on Highway 39 (Chang, *loc.cit.*) and the Satolas wall (Alimi *et al.*, *loc. cit.*). As can be seen f^* shows a well-defined increase with increasing embedded length. This relationship was corroborated in model tests carried out by Bacot *et al.* (1978); Fig. 63. No satisfactory explanation of this phenomenon was advanced by the reporters; however, an analysis presented by Naylor & Richards (1977), suggests that a considerable amount of slip occurs at the end of the strip subjected to the pull-out load. If this length is sensibly constant for a given set of soil and reinforcement parameters it follows that the apparent coefficient of friction, which is calculated from the total embedded length, would appear to increase for longer embedded lengths. It appears from the results for the Satolas wall that for embedded lengths greater than

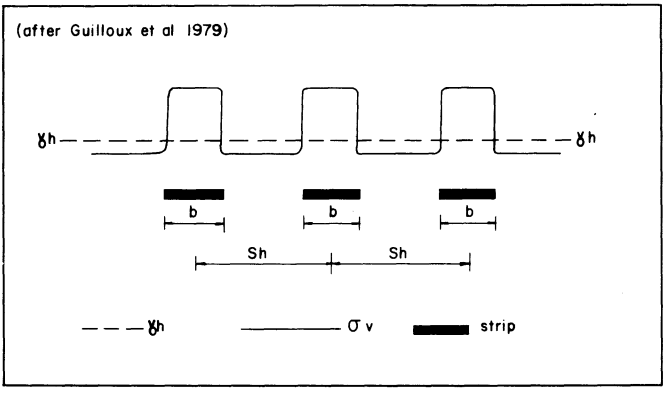

Figure 65 Arching over reinforcing strips

6 m the value of f^* levels off. This is almost certainly due to local yielding in the reinforcement.

Results from full-scale tests carried out by the Reinforced Earth Company to determine the effects of overburden pressure show staggering values of f^* for ribbed reinforcement (Schlosser & Elias, *loc. cit.*). A comparison of typical results for ribbed and smooth reinforcement is given in Fig. 64. It can be seen that for an overburden depth of 1 m $\sigma_v' = 21\text{kN/m}^2$, the value of f^* rises to approximately 2 for smooth reinforcement and 7 for ribbed reinforcement. McKittrick (1978) has attributed this to dilatancy. This is possible in the case of the smooth reinforcement where δ is some 17° greater than ϕ' for an overburden of 1 m. However, it seems highly unlikely that dilatancy would account directly for the 36° enhancement recorded for the ribbed reinforcement. This hypothesis is borne out by Cornforth (1973) and Ponce & Bell (1971) who attributed an increase in ϕ_{cv} of 17°, or less (Cornforth, 1961), as due to dilatancy. Following further studies by the Reinforced Earth Company, a more feasible explanation of this behaviour was later offered by Guilloux, Schlosser & Long (1979) who suggested that dilatancy occurs in a comparatively small zone in the immediate vicinity of

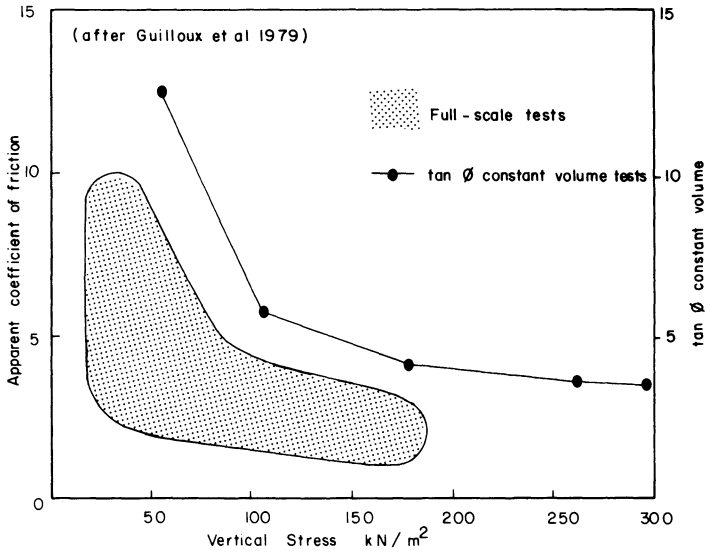

Figure 66 Comparison of full-scale and laboratory test results

the reinforcing strip. Arching occurs across the strip by which the ambient backfill suppresses the volumetric expansion normally associated with dilatancy. This suppressed dilatancy results in a locally enhanced vertical stress (Fig. 65), which gives rise to an increased pull-out resistance and hence an enhanced apparent coefficient of soil-reinforcement friction. This hypothesis was confirmed by the results from a series of constant-volume shear box tests on sand. The loading platten of the shear box was controlled by a servomechanism which automatically increased the vertical stress level to prevent volumetric contraction. The results of these tests are shown in Fig. 66 together with the envelope of full-scale pull-out test results. As can be seen the constant-volume shear box tests corroborate the field test results.

The vast majority of studies of soil-reinforcement bond have

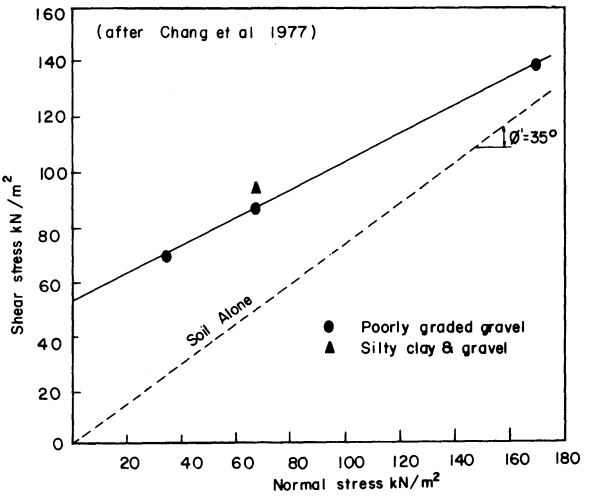

Figure 67 Pull-out test results for steel mesh

been rather staid in so far as they have been limited to horizontal layers of strip reinforcement. Some refreshing and promising deviations from this path have been made by Chang *et al.* (1977a, 1977b), Birgisson (1978), and Smith & Birgisson (1979). The former investigated the pull-out characteristics of steel mesh reinforcement obtaining the typical results shown in Fig. 67. Despite the fact that the tests were carried out in a granular soil a bond adhesion has been attributed to the reinforcement at low stress levels. This is obviously erroneous; however the tests do serve to illustrate that meshes are potentially much more efficient than strips in developing bond stress. Birgisson has carried out some very simple yet very informative model wall tests in which inclined reinforcement has been used. The observed variation in failure height with reinforcement inclination is reproduced in Fig. 68. As can be seen the observed failure height obtained maxima for reinforcements sloping at 10° from the facing to the back of the reinforced zone. This simple amendment appears to give a 10–15%

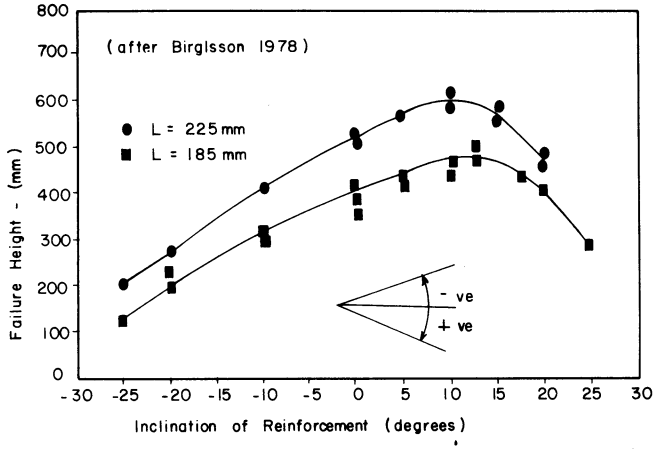

Figure 68 Variation of failure height with reinforcement inclination

increase in failure height, compared to horizontal reinforcement, as well as easing the problem of installing underground services at the back of the wall.

CURRENT DESIGN AND CONSTRUCTION SYSTEMS

Three proprietary systems are currently used in the UK: Reinforced Earth, due to Vidal, the DoE or York system, due to Jones, and the Websol system, due to Price. The Reinforced Earth system is used universally: over 4000 structures have been erected by Vidal's licensees. The other two systems account for only a small number of structures with their use in the UK restricted to certain public sector applications, pursuant to a lump sum being paid under the licence agreement concluded between M. Vidal and the DTp in January 1980. The basic requirements are the same in all three systems with the need for a facing unit, to prevent surface erosion, a series of reinforcing strips or sheets, and suitable backfill. Additionally, it is necessary to incorporate a mechanism which

permits the fill and associated reinforcing strips to settle without inducing unacceptable stresses in the facing units and the reinforcing strips. With the advent of the Department of Transport technical memorandum a number of *ad hoc* systems have appeared; however, these tend to lack the finesse of the proprietary systems.

Reinforced Earth

Vidal developed two systems for constructing Reinforced Earth walls and has been granted patents for both which when contested were held to be valid in the English courts. The first, shown in Fig. 22, comprises semi-elliptical cross-section facing units, typically 250 mm high, which have a locating slot formed along the bottom edge. Reinforcing strips are connected to the units by bolts passing through the strip and the interlocking edges of the facing units. The standard units are straight, measure up to 10 m long, and weigh 115 kg. Shorter units and specials are supplied to form corners. Mild steel and galvanized mild steel are standard construction materials, these being typically 1·5–3·0 mm thick. These thicknesses are consistent with a vertical unit stiffness that allows flexure under vertical load. If the backfill and reinforcing strips suffer internal settlement this vertical movement is reflected in the facing units which compress like a bellows. This obviates high stresses at the reinforcement connections that would otherwise be induced by differential settlement between the fill and the facing units.

The metal facing unit has now been largely superseded by a more substantial precast concrete unit (Fig. 69) which is cruciform-shaped in front elevation. Standard units weigh approximately 1 tonne and are 1·5 m by 1·5 m with a total thickness of 180 mm. All edges of the unit are rebated to obviate any straight-through joints with the rebates doubling as guide-rails to facilitate alignment of the units during construction. A further aid to alignment is in the form of a dowel bar extending from the upper and lower edge of one arm of the cruciform. These dowels are also used as pivot points for the construction of curved walls. Each unit is furnished

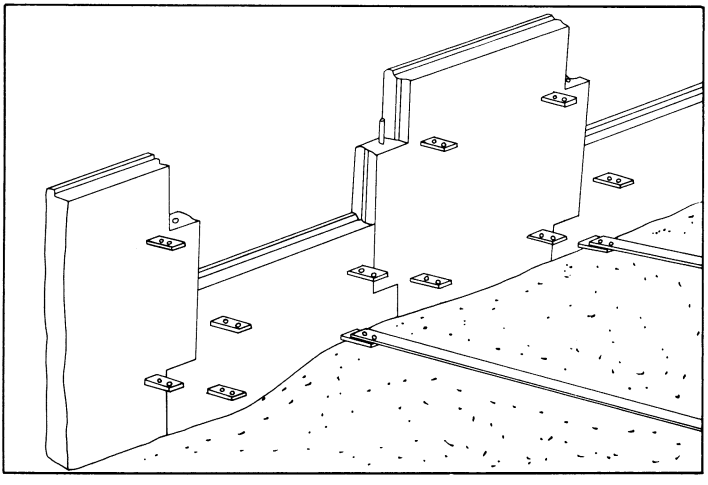

Figure 69 Precast concrete facing units (Reinforced Earth)

with four steel lugs, cast in situ during manufacture. These lugs, which are usually at 1 m horizontal and 0·75 m vertical centres, are drilled to take the reinforcing strip connecting bolts. During construction a strip of compressible filler, such as cork board, is laid on the back edge of the horizontal joints before the next unit is placed. Frequent use is made of temporary wedges to form an open joint and aid vertical alignment. These construction techniques allow the facing unit to compress vertically in sympathy with any internal settlement of the fill.

The reinforcing strips are almost exclusively metal, usually galvanized steel. Up until 1975 plain strips 60 mm or 80 mm wide and 3 mm thick were in common use. These were subsequently superseded by ribbed strips 40 mm or 60 mm wide and 5 mm thick (Schlosser & Elias, *loc. cit.*). In extremely corrosive fill environments stainless steel may be used. The effect and rates of corrosion are still not totally predictable; however, recent research work suggests that the 5 mm thick galvanized steel strips offer a service life in excess of 100 years in all but the most aggressive

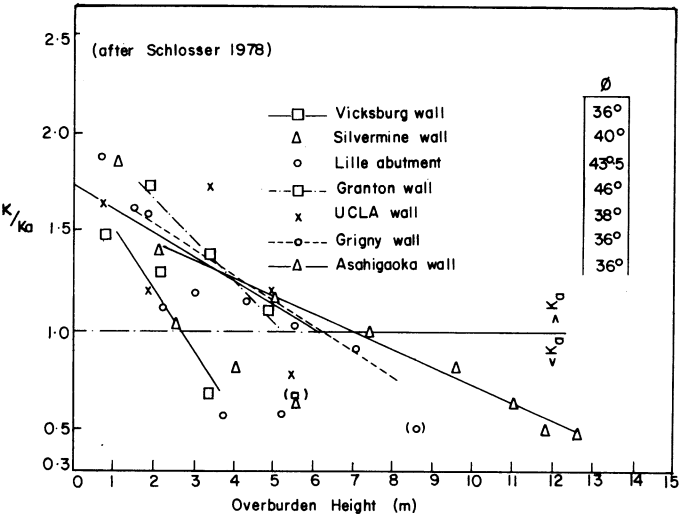

Figure 70 Variation of K with overburden height

environments (Darbin, Jailloux & Montuelle, 1978). Suitable fill material is generally of a granular nature with a limit of no more than 15% finer than 80 μm. The maximum particle size is restricted to 350 mm with no more than 25% of the fill being coarser than 150 mm (Long, 1977).

The current design methods adopted by the Reinforced Earth Company have been set out in the papers presented at the 1978 Sydney Conference by both Schlosser and McKittrick and are presented formally in a design directive issued by the Ministere des Transports (1979) through the LCPC.

For horizontal and vertical strip spacings S_h and S_v the strip tension at any depth z is given by equation (58) where σ_v is the vertical stress calculated using Meyerhof's distribution and K is an earth pressure coefficient given by equation (59):

$$T_s = K\sigma'_v S_h S_v \tag{58}$$

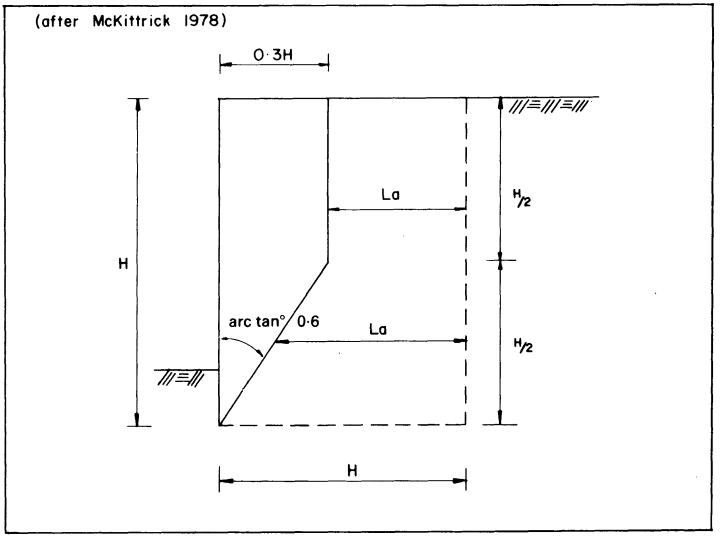

Figure 71 Idealized failure surface

For $z < 6\,\text{m}$:

$$K = K_0 + z(K_a - K_0)/6 \tag{59a}$$

For $z > 6\,\text{m}$:

$$K = K_a \tag{59b}$$

This variation of K with depth was derived empirically from observation of several full-scale walls (Fig. 70). No indication was given as to appropriate factors of safety against tensile failure. However, in earlier work (Schlosser, 1976), a factor of safety of 3 was applied to ultimate tensile strength for galvanized steel.

In designing against bond failure the effective bond length is that projecting beyond the idealized 'failure surface' shown in Fig. 71. The coefficient of friction is taken to be 0·4 for plain strips and $\tan\phi'$

for ribbed strips (Schlosser and Elias, *loc. cit.*). For overburden heights less than 6 m f^* is assumed to reduce linearly from unity at the free surface to $\tan\phi'$ at a depth of 6 m. Taking a factor of safety of 1·5 against bond failure the required bond length, L_a, at depth z is calculated from equation (60) (Schlosser & Elias, *loc. cit.*):

$$L_a = 1{\cdot}5T_s/2bf^*\gamma z \qquad (60)$$

Having designed for internal stability the structure must be checked for external stability. Reinforced Earth may be designed to comply with DTp requirements set out in DTp Technical Memorandum (Bridges) BE 3/78.

The York system – DoE

This system, which was largely developed by Jones (1978) most commonly uses lightweight glass-reinforced cement facing units weighing 18 kg. The units take the form of a hexagon-based pyramid 225 mm deep and 600 mm across the flats. One pair of diametrically opposite flanges on each unit is drilled with large-diameter holes which allow the unit to be threaded onto vertical guide poles (Fig. 72). The vertical poles, which serve as face reinforcement, are made up of short lengths of 35 mm diameter PVC tubing with spigot and socket connections. In the finished wall these poles are reinforced with mild steel bars grouted in situ to render the vertical pole rigid. The reinforcement, which is again in the form of strips, is drilled with one hole at one end which allows the reinforcement to be threaded onto the vertical pole at the required vertical spacing. When any settlement occurs in the fill and associated reinforcing strips the 'attached' end of the reinforcement simply slides down its vertical pole, thus obviating any settlement-induced stresses at this connection.

All aspects of the design and specifications for the component parts are clearly set out in BE 3/78. Permitted reinforcing materials include aluminium alloy, galvanized carbon steel, copper, and pro-

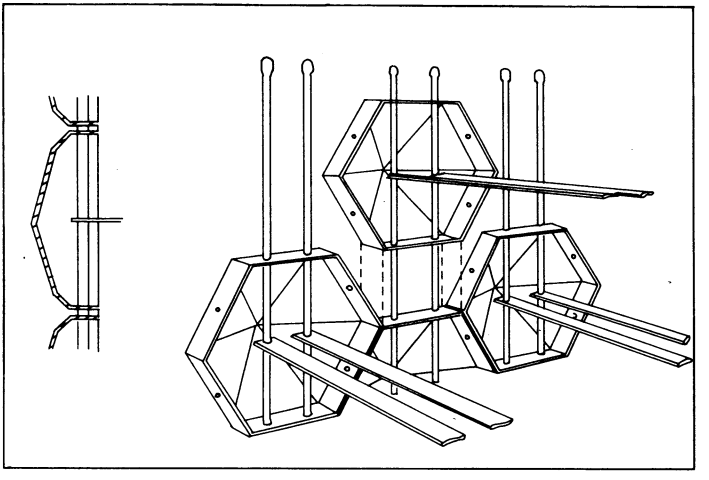

Figure 72 The DoE York system

prietary material, awarded an Agrement Board Certificate. Three reinforcing strips falling into this latter category are Fibretain, a glass-fibre-reinforced plastic, Paraweb, a linear composite of Terylene fibre cores in an Alkathene sheath and the high adherence Reinforced Earth galvanized steel strip. The allowance made for corrosion of the metallic reinforcement during the specified 120-year design life is dependent on the class of backfill used (Table 2).

Table 2 Corrosion allowances

Material	Thickness to be allowed for on each surface exposed to corrosion (mm)	
	Frictional fill	Cohesive frictional fill
Aluminium alloy	0·15	0·30
Copper	0·15	0·30
Galvanized steel	0·75	1·25
Stainless steel	0·10	0·20

Both frictional and cohesive frictional fill are limited to a maximum particle size of 125 mm; however it is specified that frictional fill shall not contain more than 10% passing the 63 μm sieve. Conversely the so-called cohesive-frictional fill may contain more than 10% finer than this size provided that the liquid limit and plasticity index do not exceed 45% and 20% respectively. However the clay fraction, i.e. 2 μm and finer, is limited to a maximum of 10%. The coefficient of friction between the soil and the reinforcement may either be measured directly using the shear box or taken from the expression $\mu = \alpha \tan \phi'$ where α is in the range 0·46–0·50 for plain strip. For the more efficient Reinforced Earth ribbed strip, the Agrement Board recommend a value of 0·9. The lengths of the various reinforcements are determined by calculation; however, in no circumstance is the reinforcement length to be less than the greater of $0{\cdot}8H$ or 5 m.

The design method for checking internal stability is a very conservative composite involving both the Rankine and Coulomb methods. First a check is made on the stability of each layer by calculating the maximum tensile force, T_i, per metre run of wall, to be resisted in the ith layer. This force is taken to be the sum of the tensions created by five possible loadings, equation (61):

$$T_i = T_1 + T_2 + T_3 + T_4 + T_5 \tag{61}$$

where:

T_1: due to overburden equals $K_a \gamma z_i$
T_2: due to uniform surcharge q at top of wall
T_3: due to strip loading at top of wall
T_4: due to horizontal loading at top of wall
T_5: due to bending moment caused by external loading on wall.

It is apparent from the expression given for T_5 that the bending moment referred to is that generated by lateral thrust at the back of the reinforced earth wall. Having evaluated T_i a check is made to ensure against tensile failure and pull-out failure. The required reinforcement perimeter p per metre run of wall is calculated from

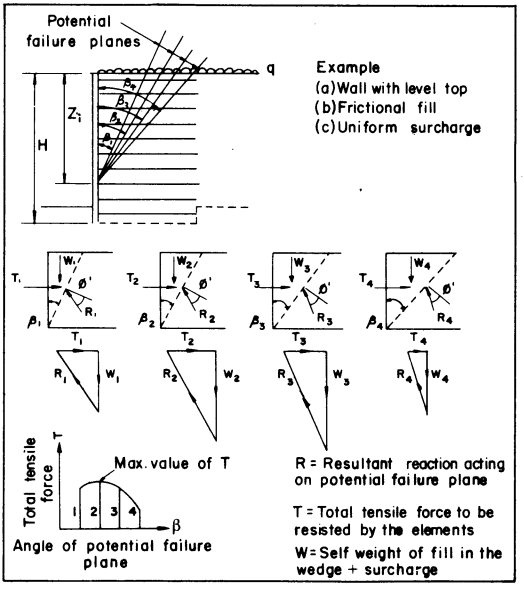

Figure 73 Wedge stability check calculation – Tech. Memo. BE3/78

equation (62) which, somewhat oddly, incorporates the total length, L_i, of each reinforcement in the ith layer. The factor of 2 is a factor of safety on $\mu = \alpha\tan\phi'$:

$$p_i = \frac{2T_i}{\mu L_i(\gamma z_i + q)} \qquad (62)$$

Once the stability of each and every layer of reinforcement has been checked the overall stability of several trial wedges is checked using a graphical method. The proposed technique is illustrated in Fig. 73 for a simple wall loaded by a uniform surcharge q and the self weight of the backfill. As can be seen a family of potential failure surfaces are assumed to originate from the face of the wall at a depth z_i. Several inclinations are assumed for the failure surface, i.e. β_1, β_2 etc. For each value of β a triangle of forces is drawn to

determine T the total tensile force to be resisted by the reinforcements cut by the failure plane under consideration. By evaluating T for several trial values of β it is possible to determine a critical value of β associated with a maximum value of T. This maximum value of T is compared with both the allowable tensile and pull-out resistance of the reinforcing strips within the depth z_i. In this case the length of each reinforcement considered is the effective bond length L_{ai} extending beyond the potential failure plane under consideration, equation (63):

$$T \leqslant \sum_{i=1}^{m} \tfrac{1}{2}\mu p_i L_{ai}(\gamma z_i + q) \tag{63}$$

Satisfied that stability is ensured at depth z_i a further family of potential failure planes is investigated for another value of z_i. In fact the memorandum implies that up to five locations be checked down the face of the wall.

The Websol system

This system differs from the two previously described in as much as it incorporates non-metallic reinforcement. However, since this system was judged in December 1981 to infringe Vidal's UK patents its use in the UK is limited to certain public sector applications falling within the licence agreement previously concluded between Vidal and the Department of Transport. In this system the reinforcing strips are made from Paraweb, a material made by ICI, which comprises synthetic fibres encased in a polythene sheath, the strength of the strip being developed in the fibres whilst the sheath gives the strip its required form and shape. The strips are placed doubled so as to form a loop at the wall end with the loop secured by a short toggle bar passing through a pair of metal eyes cast into the back of the facing unit. The facing panels are of precast concrete, 120 mm thick, and are T-shaped in front elevation with a face

area of 3·2 m^2. Settlement-induced stresses between the facing panel and the reinforcement, are relieved partly by local rotation between the Paraweb and its toggle bar fixing and partly by the provision of compressible packing along the joints. It is understood that modifications to this system are currently under consideration by its proprietors, Soil Structures Limited.

COHESIVE FILL

In comparison to a great deal of on-site fill available in the United Kingdom the fill specified by the Reinforced Earth Company is of high quality and therefore likely to be expensive. To a lesser degree this is true of the fill material specified by the DoE. This may have a very significant effect on overall economy. A cost analysis carried out by Mamujee (1974) based on current prices for the third quarter of 1973, showed that walls employing the York system excluding backfill, were very approximately half the cost of conventional reinforced concrete cantilever walls, excluding backfill (Fig. 74). However when some allowance is made for the cost of fill a quite different result may emerge. Suppose for example that the on-site fill is a clay costing £1/m^3 to excavate, place and compact. This material may well be suitable only as backfill to a conventional cantilever wall in which case the York system may require a much higher grade of imported material. Again using very approximate prices for 1973 this fill would cost in the order of £4/m^3 to transport, place and compact. The effect on the overall costs for the two types of construction and backfill are shown in Fig. 74. As can be seen, under these circumstances neither form of construction shows a clear economic advantage. Thus it would appear that to show consistent savings in the United Kingdom any system should be amenable to construction using as-found cohesive backfill.

Research carried out at the LCPC does not bode well for the use of cohesive fill. Schlosser & Vidal (1969) argued that there would

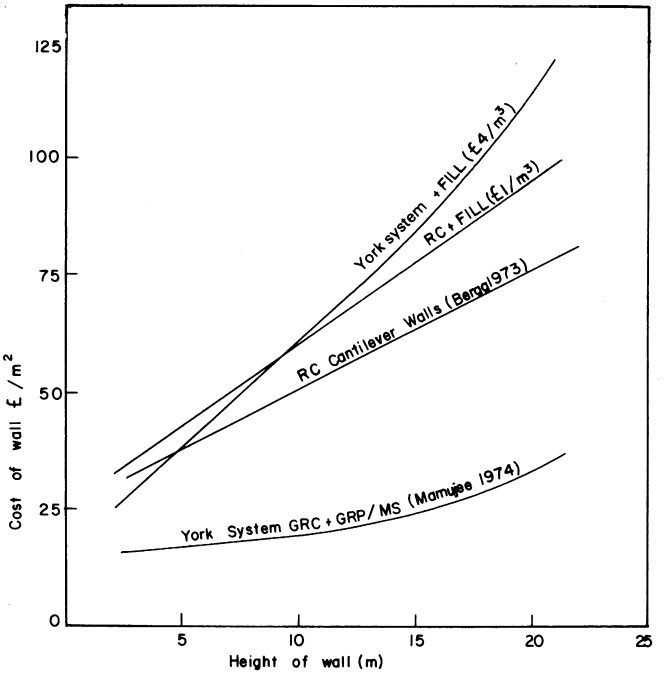

Figure 74 Comparative wall costs

be problems in developing the necessary reinforcement pull-out resistance. It was pointed out that when using granular backfill the bond stress is proportional to $\gamma z \tan$ and therefore increases with depth. For clay, however, it was argued that the short-term strength, C_u, is independent of stress level, thus at very best the maximum bond stress would be C_u. It was thought that this maximum bond stress would be insufficient to ensure stability using established techniques. This judgement seems very harsh since even very simple calculations indicate that if C_u is fully mobilized in bond stress quite reasonable bond lengths result; equation (64):

$$L = \frac{(\gamma H - 2C_u)S_h S_v F}{2bC_u} \tag{64}$$

For:

$\gamma = 20\,\text{kN/m}^3$, $C_u = 40\,\text{kN/m}^2$
$H = 10\,\text{m}$, $S_h = S_v = 0{\cdot}5\,\text{m}$
$b = 0{\cdot}06\,\text{m}$, $F = 1{\cdot}5$
$L = 9{\cdot}4\,\text{m}$.

Consistent with the notion that cohesive fill should not be used the LCPC carried out a series of shear box tests on fully saturated mixtures of granular soil and clay to demonstrate the detrimental effects of high clay content (Schlosser, Mandagaran & Ricard, 1971; Schlosser & Long, 1974). The tests involved the use of a standard 60 mm shear box with drainage top and bottom. In the first stage of the investigation a purely granular soil was tested at various normal stress levels to determine the effective angle of internal shearing resistance ϕ'. Although a rapid rate of shear of 2% per minute was used the purely granular soil was sufficiently permeable to permit complete dissipation of porewater pressure, thus ensuring drained shear. This procedure was repeated; however, progressively increasing quantities of clay were added to the granular soil. The effect of this was progressively to decrease the permeability of the mixture and so, at this high rate of shear, progessively change the shearing conditions from drained to undrained. Of course, in the extreme case when the mixture was pure clay, the angle of shearing resistance was zero. Results for intermediate clay contents are shown in Fig. 75 for mixtures of Loire sand and Provins clay, and glass ballotini and Provins clay. Since the results were interpreted in terms of total stress the intermediate angles of shearing resistance are denoted ϕ_u. As can be seen, the Loire sand substantially performed as a saturated clay at clay contents above 50%; similarly the performance of the ballotini was transformed at a clay content of 70%. Commenting

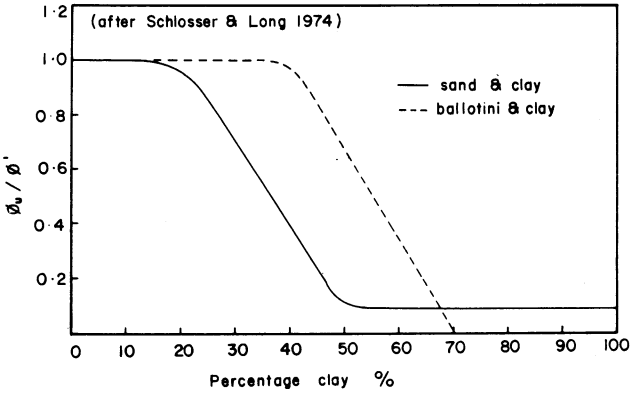

Figure 75 Effect of clay content on angle of shearing resistance

on these results Simons (1975) pointed out that the tests were conducted at a very high rate of shear with failure resulting in less than 10 min under undrained conditions at the higher clay contents. It was argued that in the field the generation of porewater pressures could be controlled by construction rate and provision of suitable drainage layers. Combining this with an effective stress analysis, rather than the somewhat conservative total stress analysis, Simons saw no reason why cohesive fill should not be used successfully.

This assessment was borne out by subsequent research work (Ingold, 1979a, 1980a), involving triaxial testing of both reinforced and unreinforced clay samples. It was found that the addition of reinforcement gave considerable improvement in strength provided that no excess porewater pressure was allowed to develop. This was achieved either by shearing the samples slowly, or by using permeable reinforcement which permitted rapid shearing with the reinforcement acting as a drainage layer allowing rapid dissipation of excess porewater pressure. If rapid loading was attempted with impermeable reinforcement it was found that the reinforcement actually caused a decrease in strength. This was

caused by the radial migration of high induced porewater pressures causing a reduction in lateral effective stress leading to premature failure (Ingold, 1979b). The TRRL have successfully constructed a 6 m high experimental wall using alternate layers of cohesive and non-cohesive fill (Murray & Boden, *loc. cit.*; Boden *et al.*, *loc. cit.*). To minimize porewater pressures induced during construction the base of the fill was furnished with a granular drainage blanket. The backfill was made up of three main layers, each layer occupying approximately one-third of the wall height. At the lowest level was a sandy silty clay with liquid and plastic limits of 30% and 17% respectively. Above this was a layer of granular fill which acted as a further drainage layer. The uppermost layer of fill was a more plastic silty clay with liquid and plastic limits of 42% and 21% respectively. To further aid drainage and dissipation of excess porewater pressures a vertical granular drainage blanket was constructed at the back of the wall during placement of the main body of fill. Despite these precautions very high excess porewater pressures were developed in the cohesive fill, especially in the lower layer which had been placed at a high moisture content. Although the wall proved quite stable certain of the facing panels suffered substantial movement. This is thought to be due to the excessively high lateral earth pressures induced by compaction plant (Fig. 51). Subsequent investigations of compaction effects have shown that they can be taken into account using simple analytical method (Ingold, 1979c).

ECONOMICS

At present there are insufficient data published to make a meaningful comparison between the relative costs of Reinforced Earth and conventional structures in the United Kingdom; however, wide application in France, the USA and Australia has indicated that Reinforced Earth structures can show a substantial saving in cost over traditional structures. Schlosser (1976) has cited savings in the range 25–65%, with the larger savings being made on

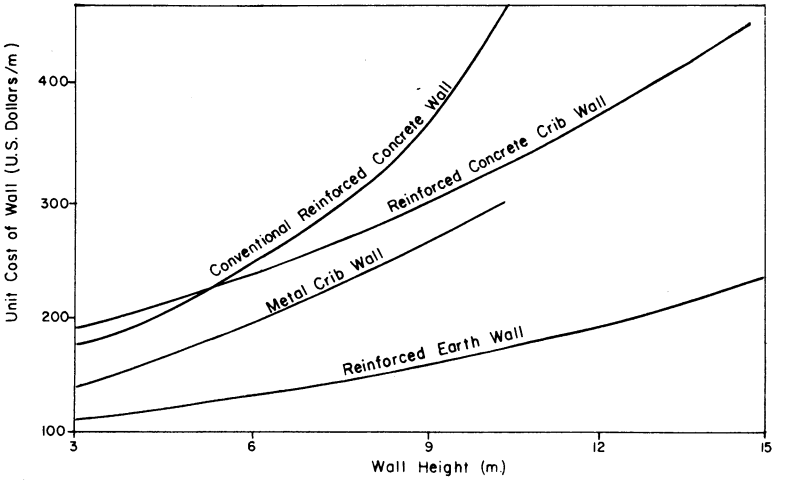

Figure 76 Comparative wall costs

sites where conventional structures would require expensive piled foundations. It was found that the inherent resistance of Reinforced Earth to damage by large total and differential settlements obviated the need for piled foundations in the corresponding Reinforced Earth structures. This is substantiated by experience in the USA where comparative tenders to the Georgia Department of Transport for Reinforced Earth and convential reinforced concrete walls showed a saving of 27%. Substantial savings were also reported by the California Department of Transport (Fig. 76). Over a wide range of soil types in Australia savings varied between 20% and 50% with an overall average saving in walls and abutments of 32%.

POLYMER REINFORCEMENT

To date the vast majority of earth structures erected have been walls in one form or another. In this application almost exclusive

use has been made of metallic reinforcement by virtue of its strength, stiffness, cheapness and resistance to creep deformation. The one outstanding difficulty in designing such structures is the accurate prediction of rates of reinforcement corrosion likely to occur during the design life of the structure. Despite these difficulties the technical memorandum issued by the Department of Transport (1978), gives guidance as to the sacrificial thickness to be allowed for on each surface of the reinforcement exposed to corrosion. For a 120-year design life this thickness is typically 0·75–1·25 mm for galvanized steel and 0·1–0·2 mm for stainless steel, depending on the nature of the backfill.

Non-metallic reinforcements are almost exclusively made of one, or a combination, of the many polymers available with the strength and deformation properties of the resulting reinforcement being largely governed by the specific polymer and the manufacturing process used to form the end-product. However, in general non-metallics are less strong and more extensible than their metallic counterparts. One considerable advantage of polymers is that they do not suffer from corrosion as such; however, they are susceptible to attack by various other agencies. The degradation resistance of some of the more commonly used polymers is qualified in Table 3 (after Cannon, 1976).

A less desirable property of polymers is the tendency to creep. Creep, which is a time-dependent phenomenon, is manifested by strain, at constant load, in excess of that caused by initial loading. The significance of creep in earth structures depends upon the design life of the system and the particular application. Obviously in temporary structures creep would cause little problem. In permanent structures consideration must be given to the particular application; for example, in the case of embankments it is the relative rates of consolidation and plastic yielding of the subsoil measured against the rates of creep in the reinforcement that determine the reinforcing effect. Many unstable soil deposits, such as silts and peats, consolidate relatively rapidly and it is conceivable that materials exhibiting high creep would prove satisfactory under

Table 3 Degradation resistance of various synthetic fibres

Resistance to attack by	Types of synthetic fibres				
	Polyester	Polyamide	Poly-ethylene	Polypro-pylene	PVC
Fungus	Poor	Good	Excellent	Good	Good
Insects	Fair	Fair	Excellent	Fair	Good
Vermin	Fair	Fair	Excellent	Fair	Good
Mineral acids	Good	Fair	Excellent	Excellent	Good
Alkalis	Fair	Good	Excellent	Excellent	Good
Dry heat	Good	Fair	Fair	Fair	Fair
Moist heat	Fair	Good	Fair	Fair	Fair
Oxidizing agents	Good	Fair	Poor	Good	–
Abrasion	Excellent	Excellent	Good	Good	Excellent
Ultraviolet light	Excellent	Good	Poor	Good	Excellent

such conditions (Holtz, 1977). Alternatively for more rigid structures, such as reinforced earth walls, long-term creep could have serious effects. Promising results have been published by Holtz & Broms (1977), who carried out tests on model walls reinforced with a woven polyester fabric. The creep coefficient of this material was found to be in the range 0·14–0·18.

Creep is a function of stress level, temperature, and obviously material type. In general the total strain, $\varepsilon_t\%$, at some time, t minutes, can be defined from knowledge of the initial strain $\varepsilon_0\%$ and the creep coefficient b which is defined in units of per cent per log $(10t)$ cycle (Finnigan, 1977); equation (65):

$$\varepsilon_t = \varepsilon_0 + b \log(10t) \tag{65}$$

Tests reported by both Finnigan and Van Leeuwan (1977) confirm that creep coefficients for polyester at approximately 50% of ultimate load are in the range quoted by Holtz and Broms. Further

Table 4 Basic forms of common synthetic polymers

Composition	Form	
	Fabric manufacture	Non-fabric manufacture
Polyamide: nylon	Staple or tape	–
Polyester: Terylene	Staple or tape	Resin
Polyolefin: polypropylene, polyethylene	Staple or tape	Plastic sheet or granules
Polyvinyl: acrylic, PVC	Staple or tape	–

results published by both Finnigan and Van Leeuwan indicate that the creep coefficients for polyamide are in the range 0·22–0·36, whilst for polypropylene Van Leeuwan indicates a creep coefficient of 1·44. From this it is apparent that polypropylene would be unsuitable for use in reinforced earth walls where, based on a 50-year design life, creep strain would theoretically amount to some 12%. There is need for further investigation into creep; particularly creep in the soil reinforcement environment.

The structure of polymer soil reinforcements

On first encountering the world of polymer materials the civil engineer finds himself in a morass of unfamiliar terminology. To combat the resulting confusion it is useful to attempt an ordered classification of some of the more commonly used polymers and forms of polymer soil reinforcement. One basic division may be made between fabrics and non-fabrics. As the name implies, fabrics are textiles which are manufactured by weaving, knitting or bonding polymer fibre or yarn. The non-fabrics are generally in the form of polymer plastic nets, meshes or strips, the latter being reinforced with fibreglass or polymer yarn. Table 4, which is based on work by McKeand & Sissons (1978), lists commonly used synthetic polymers and their respective basic forms for subsequent use in the manufacture of fabrics and non-fabrics.

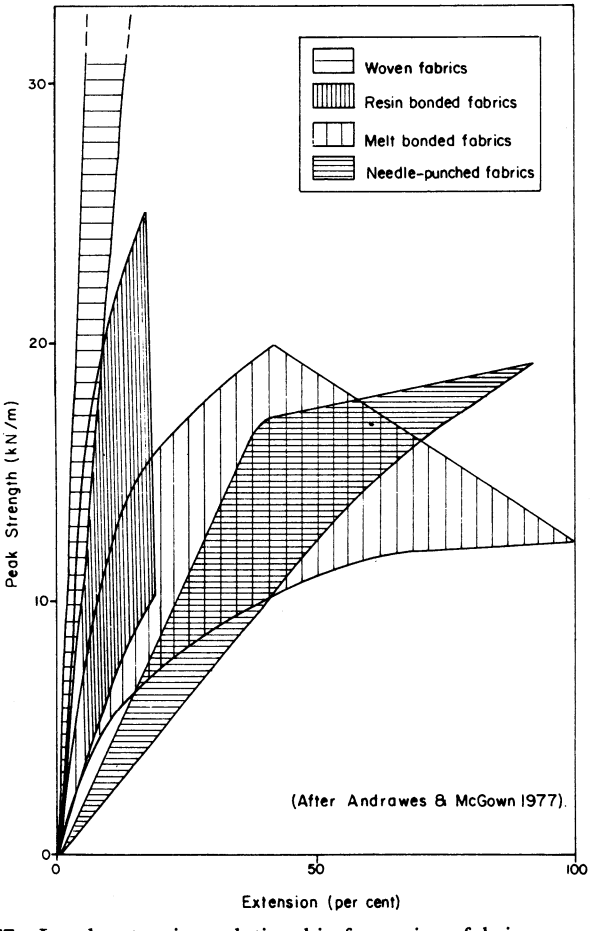

Figure 77 Load–extension relationship for various fabrics

Fabrics

Polymer fibres are the basic constituent in the manufacture of fabrics. These are either manufactured as staple, which are fibres between 20 mm and 200 mm in length, or as continuous filaments (McKeand & Sissons, *loc. cit.*). The actual manufacturing process falls into two main categories; namely woven and non-woven. The woven fabrics are generally manufactured using yarn which in turn has been spun from the basic fibre. Alternatively the fabric may be woven from polymer tape. Knitting is a further, but less common, process which tends to be grouped under the general heading of woven fabric. This classification is useful since it embraces the intermediate process whereby a comparatively weak knitted base fabric can be used as a support for a stronger warp which is woven into the base to give a strong unidirectional fabric. The majority of the non-wovens for use in civil engineering are produced either by felting or bonding. The most common form of felting is needle-punching. In this process a series of rapidly reciprocating barbed needles is inserted into a web of loose fibre. The action of the needles is to cause the fibres to tangle and ensnare one other, so forming a dense coherent web. On the application of heat this web contracts to give a dense needle-punched felt. The process of bonding can be divided into three sub-categories: resin-bonding, melt-bonding, or stitch-bonding. In these processes a mass of staple or continuous filaments is made coherent by the respective actions of heat and a chemical bonding agent or heat alone which fuses the fibres at their contact points or by literally sewing the mass together.

As might be expected, the manufacturing process has a very pronounced effect on the strength and deformation properties of the resulting fabric. These variations are reflected in the force extension curves reproduced in Fig. 77 (after Andrawes & McGown, 1977). As can be seen, the melt-bonded and needle-punched fabrics tend to be very extensible with failure strains up to 100%. These structures are also associated with relatively low

strengths. Resin-bonding appears to give a marginal increase in strength and a significant improvement in deformation modulus. By far the best performance is manifested by the woven fabrics, including unidirectional knitted/woven composites, which give much higher strengths and higher deformation moduli. The best of these fabrics mobilize ultimate strengths in the order of 100 kN/m at strains of approximately 10%.

Non-fabrics

This somewhat negative term applies to some of the more promising wall reinforcements. Since so few reinforcing materials fall into this category there is at present no real need for the classification into sub-categories. Two strip reinforcements which have been used in full-scale walls are Paraweb and Fibretain. Paraweb is a composite formed from continuous aligned high-tenacity polyester yarns enclosed in a sheath of durable black polyethylene. This reinforcing material is formed in strips 75–100 mm wide taking minimum loads in the range 10–100 kN per strip. Design loads vary between 3 and 33 kN. Fibretain, which is a fibreglass-reinforced plastic (FRP), is a composite of chemically resistant thermosetting resins and unidirectionally aligned glass fibres. The high strength and long-term stability of the glass fibres render this material less susceptible to creep. Again this material is manufactured in strips, with widths in the range 40–160 mm. Long-term ultimate strengths per strip fall in the range 16–80 kN. Both of these materials are currently under test in the full-scale experimental wall construction at the Transport and Road Research Laboratory (Boden. *et al., loc. cit.*; Murray & Boden, *loc. cit.*). Additionally Paraweb has been used very successfully in association with the Websol system on several major projects. Another promising non-fabric is Netlon's Tensar, a high density polyethylene geogrid, which has recently been used in the construction of several large earth structures.

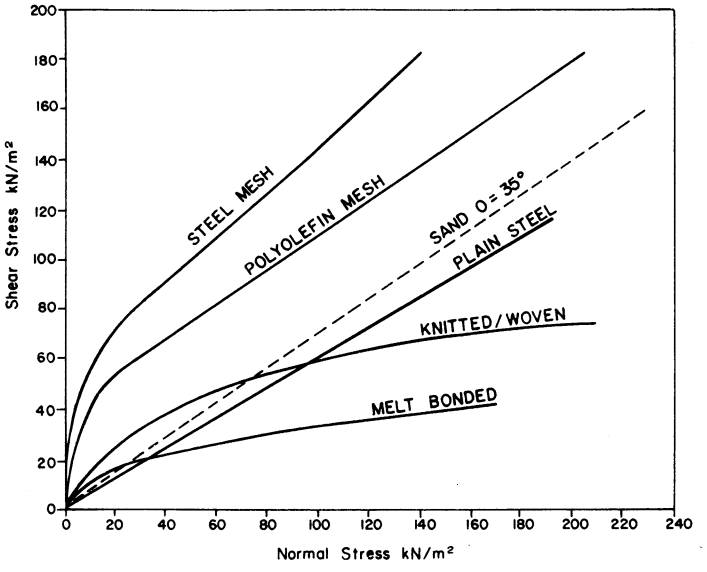

Figure 78 Comparison of pull-out test results

Bond stress

As well as requiring sufficient tensile strength an acceptable reinforcement must be capable of mobilizing sufficient soil reinforcement friction to render economic bond lengths.

Shear box tests carried out at the TRRL (Boden *et al., loc. cit.*) indicated angles of bond stress for Paraweb and Fibretain of 22° and 28° respectively when tested in a soil with an angle of internal shearing resistance of 37°. Pull-out tests carried out by Ground Engineering Limited (Ingold & Templeman, 1979; Ingold, 1980a) have shown a wide range of values of angle of bond stress for various fabrics and non-fabrics tested, in sand (Fig. 78). Reference to Fig. 79 shows the angle of bond stress to be dependent on normal

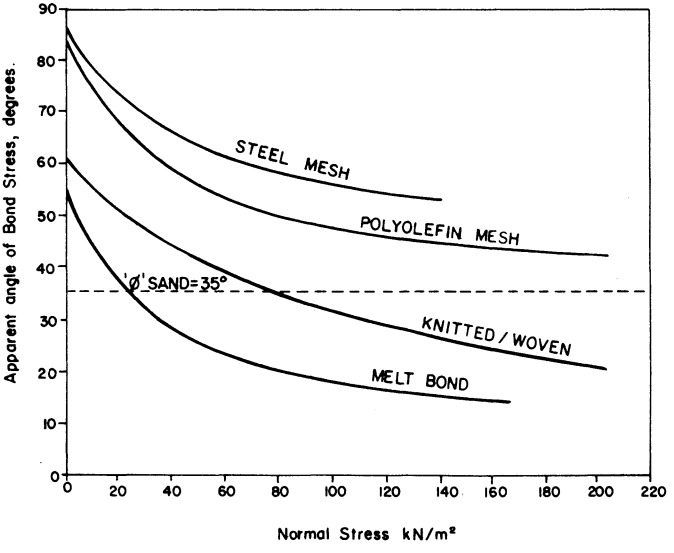

Figure 79 Comparison of bond stress characteristics

stress level. Meshes appear to give excellent performance with the shear strength of the sand being fully mobilized; however, the fabrics tested showed a marked deterioration of mobilized bond stress with increasing normal stress level.

4

Future trends

At the time of writing there is active research being undertaken in numerous universities and research establishments throughout the world; thus it would be presumptuous to attempt to draw any firm conclusions. The foregoing chapters have given a necessarily limited account of the current state of the art which, in brief, centres largely upon the empirical design of walls using earth reinforcement. Later research has broadened significantly to encompass several well-defined trends. The first and possibly the most important of these involves more profound investigations of the underlying mechanisms of Reinforced Earth with a view to promoting a much wider spectrum of application. One example of this is the use of reinforcement in embankments where it has been shown that the consistent use of horizontal reinforcement can lead to a local weakening of the embankment rather than strengthening. Similarly loss of strength can be induced when reinforcement is associated with saturated clay subject to undrained loading. Other basic studies have introduced the notion that earth reinforcement operates through a strain-, rather than stress-, controlled mechanism. This approach is of special significance in designing structures such as reinforced embankments where large movements such as settlements may make it appropriate to use more extensible reinforcement. Conversely in more rigid structures, for example retaining walls, the use of more extensible reinforcement would be

precluded on the grounds that unacceptably large movements would be necessary to mobilize the required reinforcing effect.

Another well-defined trend is the search for alternatives to the now widespread use of reinforced concrete for facing units, and metal – generally steel – for the reinforcement. In particular there has been much debate on the validity of methods of predicting rates of corrosion, especially pitting of metallic reinforcement. This has led to extensive research and development of 'non-corrodable' synthetic reinforcing materials including resin-bonded glass fibres, encapsulated polyester yarn, plastic meshes and a wide range of fabrics or so-called geotextiles.

With the exception of the first two materials the desirous quality of high resistance to degradation is often associated with high creep coefficients. Although creep deformation may be tolerated, account must be taken of long-term strength. This caution is reflected by results from an experimental Reinforced Earth wall at Poitiers where Tergal, a woven polyester reinforcing strip, suffered a 50% loss in strength over 11 years. It is almost certain that synthetics will play an important role in certain aspects of soil reinforcing, especially now that manufacturers are producing reinforcements to specifications that are becoming progressively better defined. Geotextiles in particular are expected to play a major role in the future, since as well as their potential as reinforcement they have added applications including separation, filtration and drainage.

It is thought that now adequate empirical design rules have been established for Reinforced Earth walls there may be development of other applications. Several of these, including Reinforced Earth arches, beams and foundations, have been the subject of initial research. Others such as Reinforced Earth slabs and soil bridges have already been been constructed as full-scale prototypes. There has to date been great flair shown in the application of walls to structures that could not be economically constructed using reinforced concrete. These include the construction of Reinforced Earth dwellings which have very useful applications to steep sites that can

be terraced, and slot storage systems. The latter is encouraging in as much as the provision of bulk storage facilities has been successfully translated from one form and medium, namely reinforced concrete silos, to another mutually compatible form and medium with the added bonus of more economic construction.

References

Alimi, I. (1978). Critère de choix des matériaux de la terre armée – étude de l'adhérence terre-armature. Thesis, LCPC.

Alimi, I., Bacot, J., Lareal, P., Long, N. T. & Schlosser, F. (1977). Adherence between soil and reinforcement insitu and in the laboratory. *Proc. IXth ICSMFE*, vol. 1, pp. 11–14.

Al-Hussaini, M. M. & Johnson, L. D. (1978). Numerical analysis of reinforced earth wall. *Proc. ASCE Symp. Earth Reinforcement*, Pittsburgh, pp. 98–126.

Andersland, O. B. & Khattak, A. S. (1979). Shear strength of kaolinite/fibre soil mixtures. *Proc. Int. Conf. Reinforced Earth*, Paris, vol. 1, pp. 11–16.

Andrawes, K. Z. & McGown, A. (1977). Alteration of soil behaviour by the inclusion of materials with different properties. *Proc. Symp. Reinforced Earth & Other Compos. Soil Techqs*, TRRL/Heriot–Watt Univ., pp. 88–108. (Published as TRRL Supp. Rept. 457–1979).

Andrawes, K. Z., McGown, A. & Al-Hasani, M. M. (1978). Alteration of soil behaviour by the inclusion of materials with different properties. *Ground Engng.*, vol 11, no. 6, pp. 35–42.

Bacot, J. (1974). *Étude théorique et expérimentale de soutenement realisé en terre armée*. Lyon: Claude Bernard Univ.

Bacot, J., Iltis, M., Lareal, P., Paumier, T. & Sanglerat, G. (1978). Study of the soil reinforcement friction coefficient. *Proc. ASCE Symp. Earth Reinforcement*, Pittsburgh, pp. 157–185.

Baguelin, F. & Bustamante, M. (1971). Conception et étude de la stabilité des ouvrages en terre armée. *Bull. de Liais. LCPC* (Spec. edn, *Autoroute de Menton*).

Balla, A. (1957). Stress conditions in the triaxial compression test. *Proc. 4th ICSMFE*, vol. 1, pp. 140–143.

REFERENCES

Balla, A. (1960). Stress conditions in triaxial compression *J. Soil Mech. Fdns Div. Am. Soc. Civ. Engrs.*, vol. 86, no. SM6, pp. 57–84.

Banerjee, P. K. (1973). Principles of analysis, design and construction of reinforced earth retaining walls. DoE Rpt. no. HECB/B1/4.

Banerjee, P. K. (1975). Principles of analysis and design of reinforced earth retaining walls. *J. Instn. Highw. Engrs.*, **22,** No. 1, 13–18.

Barden, L. (1963). *Discussion – lab. shear test. of soils.* ASTM Pub. no. 361, p. 184.

Barden, L. & McDermott, R. J. W. (1965). Use of free ends in triaxial testing of clay, *J. Soil Mech. Fdns. Div. Am. Soc. civ. Engrs.*, vol. 91, no. SM6, pp. 1–23.

Bartos, M. J. (1979). One-hundred-and-one uses for earth reinforcement. *Civ. Engng ASCE*, January, pp. 51–57.

Bassett, R. H. & Horner, J. N. (1977). Centrifugal model testing of the approach embankment to the M180 Trent crossing. NERCU Rep., Univ. of London.

Bassett, R. H. & Last, N. C. (1978). Reinforcing earth below footings and embankments. *Proc. ASCE Symp. Earth Reinforcement*, Pittsburgh, pp. 202–231.

Behnia, C. (1972). Étude des routes en terre armée. Ing. Thesis – Paris University.

Behnia, C. (1973). Étude des routes en terre armée. *Rapp. de Rech.*, no. 26. LCPC.

Bell, J. R., Greenway, D. R. & Vischer, W. (1977). Construction and analysis of a fabric reinforced low embankment. *Proc. Int. Conf. Fabrics in Geot.*, Paris, vol. 1, pp. 71–75.

Belloni, L. & Sembenelli, P. (1977). Remblais routiers sur terrains compressibles executé a l'aide de textiles synthétiques. *Proc. Int. Conf. Fabrics in Geot.*, Paris, vol. 1, pp. 49–54.

Bergg, J. A. (1973). Eighty highway bridges in Kent. *Proc. ICE,* Part 1, vol. 54.

Binquet, J. & Lee, K. L. (1975a). Bearing capacity tests on reinforced earth slabs. *J. Geot. Engng. Div. Proc. ASCE*, **101,** GT12, 1241–1255.

Binquet, J. & Lee, K. L. (1975b). Bearing capacity analysis of reinforced earth slabs. *J. Geot. Engng. Div. Proc. ASCE*, **101,** GT12, 1257–1276.

Birgisson, G. I. (1978). Horizontally and inclined reinforced earth structures. M.Sc. Thesis, Heriot–Watt Univ.

Blight, G. E. (1963). The effect of non-uniform pore pressures on laboratory measurements of the shear strength of soils. *Lab. Shear Testing of Soils.* ASTM Pub. No. 361, pp. 173–184 (see discussion also).

Boden, J. B., Irwin, M. J. & Pocock, R. G. (1978). Construction of experimental reinforced earth walls at the TRRL. *Ground Engng*, **11,** no 7, 28–37.

Bolton, M. D. (1972). *Reinforced earth – a centrifugal study*. UMIST.

Bolton, M. D., Choudhury, S. P. & Pang, P. L. R. (1978a). Reinforced earth walls – a centrifugal model study. *Proc. ASCE Symp. Earth Reinforcement*, Pittsburgh, pp. 252–281.

Bolton M. D., Choudhury, S. P. & Pang, P. L. R. (1978b). Modelling reinforced earth. *Ground Engng*, **11,** no. 6, 19–24.

Broms, B. B. (1977). Triaxial tests with fabric reinforced soil. *Proc. Int. Conf. Fabrics in Geot.*, Paris, vol, 3, pp. 129–134.

Cannon, E. W. (1976). Fabrics in civil engineering. *Civil Engng.*, March, pp. 39–42.

Cassard, G., Kern, F. & Mathieu, G. (1979). Utilisation des techniques de renforcement dans les barrages en terre. *Proc. Int. Conf. Soil Reinforcement*, Paris, vol. I, pp. 229–233.

Chang, J. C. (1974) Earth reinforcement techniques. Final Rept. CA–DOT–TL–2115–9–74–37, Dept. of Transport, California.

Chang, J. C., Forsyth, R. A. & Beaton, J. L. (1974). Performance of a reinforced earth fill. *Transp. Res. Bull.*, **510,** 56–67.

Chang, J. C., Forsyth, R. G. & Smith, T. (1972). Reinforced earth highway embankment – Road 39. *Highw. Focus*, **4,** 15–35.

Chang, J. C., Hannon, J. B. & Forsyth, R. A. (1977a). Pull resistance and interaction of earthwork reinforcement and soil. Presentation to the 56th Annual Meeting, TRB.

Chang, J. C., Hannon, J. B. & Forsyth, R. A. (1977b). Pull resistance and interaction of earthwork reinforcement and soil. Transp. Res. Rec., vol. 64.

Chapuis, R. (1972). Rapport de recherche de DEA. Institut de Mécanique de Grenôble (unpublished internal report).

Chapuis, R. (1977). Stabilité interne des murs en terre armée. *Can. Geot. J.*, **14,** No. 3, 389–398.

Chapuis, R. & Prinquet, P. (1973). Terre armée – étude sur modèles réduits. Internal report, Ecole Central de Lyon.

Choudhury S. P. (1977). A study of reinforced earth retaining walls with sand backfill by centrifugal modelling. Ph.D. Thesis, UMIST.

Christie, I. F. & El Hadi, K. M. (1977). Some aspects of the design of earth dams reinforced with fabric. *Proc. Int. Conf. Fabrics in Geot.*, Paris, vol. 1, pp. 99–103.

Cornforth, D. H. (1961). Plane strain failure characteristics of a saturated sand. Ph.D. Thesis, Univ. of Lond.

REFERENCES

Cornforth, D. H. (1973). *Prediction of drained strength of sands from relative density measurements*. ASTM. Spec. Tech. Pub. No. 523, pp. 281–303.

Corte, J. (1977). La méthode des éléments finis appliquée au ouvrages en terre armée. *Bull. de Liais. LCPC*, No. 90, pp. 37–47.

Crawford, C. B. (1963). Pore pressures within soil specimens in triaxial compression. *Lab. Shear Testing of Soils*. ASTM Pub. No. 361, pp. 192–199 (see discussion also).

Dalton, D. C. (1977a). Written contribution *Proc. Symp. Reinforced Earth & Other Compos. Soil Techqs*. TRRL/Heriot–Watt Univ, pp. 320–324. (Published as TRRL Suppl. Rep. 457–1979.)

Dalton, D. C. (1977b). Use of waste tyres in highway construction. Internal report Yorkshire MCC.

D'Appolonia, E. & Newmark, N. M. (1951). A method for solution of the restrained cylinder under axial compression. *Proc. 1st US Nat. Conf. Appl. Mechs*. ASME, pp. 217–226.

Darbin, M. (1970). La terre armée dans la construction des routes et autoroutes. *Revue gen. Routes et des Aerodr.*, No. 457, Sept.

Darbin, M., Jailloux, J. & Montuelle, J. (1978). Performance and research on the durability of reinforced earth reinforcing strips. *Proc. ASCE Symp. Earth Reinforcement*, Pittsburgh, pp. 305–333.

Department of Transport (1978). Reinforced earth retaining walls and bridge abutments for embankments. Tech. Memo (Bridges), BE3/78.

Envo Publishing Co. Inc. (1976). *New horiz. in constr. mater.*, Pennsylvania: Envo. Pub. Co. Inc.

Filon, L. N. G. (1902). The elastic equilibrium of circular cylinders under certain practical systems of load. *Phil. Trans. Roy. Soc.*, Series A, **198,** 147.

Finlay, T. W. (1978). Performance of a reinforced earth structure at Granton. *Ground Engng*, **11,** No. 7, 42–44.

Finlay, T. W. & Sutherland, H. B. (1977). Field measurements on a reinforced earth wall at Granton. *Proc. 9th ICSMFE*, vol. 2, pp. 511–516.

Finnigan, J. A. (1977). The creep behaviour of high tenacity yarns and fabrics used in civil engineering. *Proc. Int. Conf. Fabrics in Geot.*, Paris, Vol. 1, pp. 305–309.

Forsyth, R. A. (1978). Alternative earth reinforcements. *Proc. ASCE Symp. Earth Reinforcement*, Pittsburgh, pp. 358–370.

Gedney, D. S. (1972). Reinforced earth as a highway structure. *Proc. 10th Ann. Engng Geol. & Soils Engng Symp.*, Univ. Idaho, pp. 165–172.

Gedney, D. S. (1975). *Reinforced earth – U.S. experience*. Federal Highway Authority.

Gray, D. H. (1978). Role of woody vegetation in reinforcing soils and stabilising slopes. *Proc. Symp. Soil Reinforcing and Stabilising Techniques.* NSWIT/NSW Univ., pp. 253–306.

Guegan, Y. & Legeay, G. (1969). Étude en laboratoire de la terre armée en modèles reduits bidimensionnels. Internal report, LCPC.

Guilloux, A., Schlosser, F & Long, N. T. (1979). Étude du frottement sable – armature en laboratoire. *Proc. Int. Conf. Soil Reinforcement*, Paris, vol. 1, pp. 35–40.

Harrison, W. J. & Gerrard, C. M. (1972). Elastic theory applied to reinforced earth. *J. SMF Div. Proc. ASCE*, vol. 98, no. SM12, pp. 1325–1345.

Hausmann, M. R. (1976). Strength of reinforced soil. *Proc. 8th Aust. Road Resh. Conf.*, vol. 8, sect. 13, pp. 1–8.

Haythornthwaite, R. M. (1960). Mechanics of the triaxial test for soils. *J. SMF Div. Proc. ASCE*, vol. 86, no. SM5, pp. 35–62.

Hoare, D. J. (1979). Laboratory study of granular soils reinforced with randomly oriented discrete fibres. *Proc. Int. Conf. Reinforced Earth*, Paris, vol. 1, pp. 47–52.

Holtz, R. D. (1977). Laboratory studies of reinforced earth using a woven polyester fabric. *Proc. Int. Conf. Fabrics in Geot.*, Paris, vol. 3, pp. 149–154.

Holtz, R. D. & Broms, B. B. (1977). Walls reinforced by fabrics – results of model tests. *Proc. Int. Conf. Fabrics in Geot.*, Paris, vol. 1, pp. 113–117.

Holtz, R. D. & Massarsch, K. R. (1976). Improvement of the stability of an embankment by piling and reinforced earth. *Proc. 6th Euro. Conf. SMFE*, vol, 1.2, pp. 473–478.

Hulo, Y., Ramery, J. & Pouilly, F. (1972). Les résultats de l'expérimentation sur les murs en terre armée de Dunkerque. Internal report LRPC, Lille.

Hvorslev, M. J. (1957). Discussion. *Proc. 4th ICSMFE*, vol. 3, pp. 105–107.

Ingold, T. S. (1979). Discussion session 8. *Proc Euro. Conf. SMFE*, vol. 4, pp. 294–297.

Ingold, T. S. (1979a). Reinforced clay – a preliminary study using the triaxial apparatus. *Proc. Int. Conf. Soil Reinforcement,* Paris, vol. 1, pp. 59–64.

Ingold, T. S. (1979b). Some observations on failure mechanisms in reinforced clay. Speciality session. *Proc. VIth Panamerican Conf. Soil Mech. and Found. Engng,* Peru.

Ingold, T. S. (1979c). ICE Discussion 'Reinforced Earth', see 'Reinforced Earth–Research and Practice'. *Ground Engng,* **13,** no. 4, 17–27.

REFERENCES

Ingold, T. S. (1980a), Reinforced clay. Ph.D. Thesis, Univ. of Surrey.
Ingold, T. S. (1980b). Reinforced earth. *Int. J. Cem. Composites*, **2,** No. 3 (October).
Ingold, T. S. (1980c). Reinforced earth related to the geological environment. Regional Meeting, Eng. Group Geological Society.
Ingold, T. S. (1981). Reinforced earth – theory and design. *Proc. Inst. Highw. Engrs.* **28,** No. 7.
Ingold, T. S. & Templeman, J. E. (1979). The comparative performance of polymer net reinforcement. *Proc. Int. Conf. Soil Reinforcement*, Paris, vol. 7, pp. 65–70.
Iwasaki, K. & Watanabe, S. (1978). Reinforcement of railway embankments in Japan. *Proc. ASCE Symp. Earth Reinforcement*, Pittsburgh, pp. 473–500.
James, R. G. (1973). The determination of strains from the radiographic technique. Cambridge Univ. Rep. CUED/C–SOILS/LN3.
Jewell, R. A. (1979). Discussion session 8. *Proc. European Conf. SMFE*, vol. 14, pp. 286–289.
Jones, C. J. F. P. (1978). The York method of reinforced earth construction. *Proc. ASCE Symp. Earth Reinforcement*, Pittsburgh, pp. 501–527.
Jones, C. J. F. P. & Edwards, L. W. (1975). Finite element analysis of M180 Trent embankment. NERCU Rep., Yorkshire MCC.
Juran, I. (1977). Dimensionnement interne des ouvrages en terre armée. Doc. Ing. Thesis, LCPC.
Juran, I. & Schlosser, F. (1978). Theoretical analysis of failure in reinforced earth structures. *Proc. ASCE Symp. Earth Reinforcement*, Pittsburgh, pp. 528–555.
Kern, F. (1977). Réalisation d'un barrage en terre avec parement aval vertical au moyen de poches en textile. *Proc. Int. Conf. Fabrics in Geot.*, Paris, vol. 1, pp. 91–94.
Kheang, L. P. (1972). Murs en terre armée sous des surcharges verticales. Internal report., LCPC.
Laing, B. & McDermott, R. J. W. (1965). Use of free ends in triaxial testing of clay. *J. Soil Mech. Fdns Div. Proc. ASCE*, **91,** No. SM6, 1–23.
Lareal, P & Bacot, J. (1973). Étude sur modèles réduits tridimensionnels de la rupture de massifs en terre armée. *Revue Trav.*, No. 463 (October), pp. 46–52.
Lee, K. L. (1969). Reinforced earth. Unpublished Report, UCLA.
Lee, K. L. (1976). Reinforced earth – an old idea in a new setting. *New Horizons in Constr. Mater.*, Pensylvania: Envo Publ. Co., Inc., vol. 1, pp. 655–682.

Lee, K. L., Adams, B. D. & Vagneron, J. J. (1972). Reinforced earth walls. Rep. No. UCLA–ENG–7233.

Lee, K. L., Adams, B. D. & Vagneron, J. J. (1973). Reinforced earth retaining walls. *J. SMFE Div. Proc. ASCE*, **99,** No. SM10, 745–764 (Discussion, **100,** No. GT8, 958–966).

Levisalles, J. F. (1979). Application de la terre armée a la construction d'habitations. *Proc. Int. Conf. Soil Reinforcement*, Paris, vol. 2, pp. 311–315.

Lizzi, F. & Carnevale, G. (1979). Les réseaux de pieux racines pour la consolidation des sols. Aspects théoretiques et essais sur modèles. *Proc. Int. Conf. Soil Reinforcement*, Paris, vol. 2, pp. 317–324.

Long, N. T. (1977). Some aspects about fill material in reinforced earth. *Proc. TRRL/Heriot–Watt Univ. Symp. Reinforced Earth and Other Techniques*, pp. 246–249.

Long, N. T., Guegan, Y. & Legeay, G. (1972). Étude de la terre armée a l'appareil triaxial. *Rapp. de Recherche*, No. 17, LCPC.

Long, N. T., Schlosser, F., Guegan, Y. & Legeay, G. (1973). Étude des murs en terre armée sur modeles reduits bidimensionnels. *Res. Rep.* No. 30, LCPC.

Maagdenberg, A. C. (1977). Fabrics below sand embankments over weak soils, their technical specifications and their applications in a test area. *Proc. Int. Conf. Fabrics in Geot.*, Paris, vol. 1, pp. 77–82.

Magyarne, J. M., Radnoti, G., Scharle, P. & Szalatay, I. (1979). Numerical and experimental examination of the reinforced earth wall in Fenyeslitke. *Proc. Int. Conf. Soil Reinforcement,* Paris, vol. 2, pp. 563–567.

Mamujee, F. (1974). Reinforced earth. M.Sc. dissertation, Leeds Univ.

Marec, M., Baguelin, F. & Vincentelli, A. (1971). Données sur les murs en terre armée constuits sur l'autoroute de Menton. *Bull. de Liais. LRPC* (Spec. edn, *Autoroute de Menton*).

McGown, A., Andrawes, K. Z. & Al-Hasani, M. M. (1978). Effect of inclusion properties on the behaviour of sand. *Geot.*, **28,** No. 3, 327–346.

McKeand, E. & Sissons, C. R. (1978). Textile reinforcements – characteristic properties and their measurements. *Ground Engng*, **11,** No. 7, 13–22.

McKittrick, D. P. (1978). Reinforced earth – application of theory and research to practice. *Proc. Symp. Soil Reinforcing and Stabilising Techniques*, NSWIT/NSW Univ. (separate volume).

McKittrick, D. P. & Darbin, M. (1979). World-wide development and use of reinforced earth structures. *Ground Engng*, **12,** No. 2, 15–21.

McKittrick, D. P. & Wojciechowski, L. J. (1979). Examples of design and

construction of seismically resistant reinforced earth structures. *Proc. Int. Conf. Soil Reinforcement*, Paris, Vol. 1, pp. 95–100.

Mevellec, P. (1977), Étude de l'adhérence sol-armature dans la terre armée. Thesis, LCPC.

Ministère de L'Équipement (1975). *Dimensionnement des ouvrages en terre armée – murs et culées de ponts.* LCPC/ENPC. (Also published by Assoc. des Anciens Eleves de ENPC.)

Ministère des Transports (1979). *Les ouvrages en terre armée. Recommandations et règles de l'ait.*

Munoz, A. (1974), Use of reinforced earth to correct the 'Heart O'the Hills' slide. *Proc. 12th Ann. Engng Geol. & Soils Engng Symp.*, Boise, Idaho.

Murray, R. T. (1977), Research at the TRRL to develop design criteria for reinforced earth. *Proc. TRRL/Heriot–Watt Univ. Symp. Reinforced Earth and Other Composite Soil Techq.* TRRL Suppl. Rep. 457 (1979), pp. 55–87.

Murray, R. T. & Boden, J. B. (1979), Reinforced earth wall constructed with cohesive fill. *Proc. Int. Conf. Soil Reinforcement,* Paris, vol. 2, pp. 569–577.

Murray, R. T., Carder, D. R. & Krawczyk, J. V. (1979). Pull-out tests on reinforcements embedded in uniformly graded sand subject to vibration. *Proc. Euro. Conf. SMFE,* vol. 3, pp. 115–120.

Naylor, D. J. & Richards, H. (1977). Slipping strip analysis of reinforced earth. University of Wales – Swansea, Civ. Engng Report C/R/295/77.

Oriani, M. (1971). Road embankment stabilisation by reticulated walls. *Civ. Engng publ. Wks. Rev.,* September, p. 992.

Perloff, W. H. & Pombo. L. E. (1969). End restraint effects in the triaxial test. *Proc. 7th ICSMFE,* vol. 1, pp. 327–333.

Phan, T. L., Sergrestin, P., Schlosser, F. & Long, N. T. (1979). Étude de la stabilité interne et externe des ouvrages en terre armée par deux méthodes de cercles de rupture. *Proc. Int. Conf. Soil Reinforcement,* Paris, vol. 1, pp. 119–123.

Pickett, G. (1944). Application of the Fourier method to the solution of certain boundary problems in the theory of elasticity. *J. Appl. Mech. ASME,* **11,** A-176.

Ponce, V. M. & Bell, J. M. (1971). Shear strength of sand at extremely low pressures. *J. SMFD Proc. ASCE,* **97.** SM4, 339–353.

Price, D. I. (1975). Aspects of reinforced earth in the UK. *Ground Engng,* **8,** No. 2, 19–24.

Razani, R. & Behpour, L. (1970). Some studies on improving the properties of earth materials used for construction of rural earth houses in

seismic regions of Iran. *Proc. Roorkee Conf. Earthq. Engng,* pp. 82–89.

Reddy, D. V., Bobby, W. & Mahrenholtz, O. (1979). Ultimate load behaviour of 'cut and cover' underground nuclear containments with reinforced earth backfill. *Proc. Int. Conf. Soil Reinforcement,* Paris, vol. 2, pp. 347–350.

Reina, P. (1975). The battle over reinforced earth. *NCE,* 20 February.

Reinforced Earth Co. (1978). Reinforced earth speeds mine construction (Ed: J. D. Wiedmer), *Mining engng,* August.

Richardson, G. N. (1976). The seismic design of reinforced earth walls. Rep. No. UCLA–ENG–7586.

Richardson, G. N. & Lee, K. L. (1974). Response of model reinforced earth walls to seismic loading conditions. Rep. No. UCLA–ENG–7412.

Romstad, K. M., Al-Yassin, Z., Herrmann, L. R. & Shen, C. K. (1978). Stability analysis of reinforced earth retaining structures. *Proc. ASCE Symp. Earth Reinforcement,* Pittsburgh, pp. 685–713.

Royster, D. L. (1974). Construction of a reinforced earth fill along Interstate 40 in Tennessee. *Proc. 25th Ann. Highw. Geol. Symp.,* Raleigh, N. Carolina.

Sanglerat, G. (1971). Masiffs de terre armée. *Revue Tech.,* July–September, pp. 1–9.

Santini, C. & Long, N. T. (1978). Le terre armée étudié par modèles photo-élastiques. *Bull. de Liais. LCPC,* No. 97, pp. 121–131.

Saran, S., Talwar, D. V. & Vaish, U. S. (1978). Some aspects of engineering behaviour of reinforced earth. *Proc. Symp. Soil Reinforcing and Stabilising Techq.* NSWIT/NSW Univ., pp. 40–49.

Schlosser, F. (1970). Mur expérimental en terre armée d'Incarville. *Bull. de Liaise LCPC,* No. 33.

Schlosser, F. (1972). La terre armée – récherches et réalisations. *Bull. de Liais. LCPC,* No. 62, 79–92.

Schlosser, F. (1972). La terre armée dans l'échangeur de Sete. *Revue gén. Routes et Aérodr.,* No. 480, October.

Schlosser, F. (1973). La terre armée dans l'échangeur de Sete. *Bull. de Liais. LCPC,* No. 63.

Schlosser, F. (1976). Reinforced earth. Note D'Information, LCPC, April.

Schlosser, F. (1978). La terre armée, historique dévelopment actuel et Futur. *Proc. Symp. Soil Reinforcing and Stabilising Techq.,* NSWIT/NSW Univ., pp. 5–28.

Schlosser, F. & Elias, V. (1978). Friction in reinforced earth. *Proc. ASCE Symp. Earth Reinforcement,* Pittsburgh, pp. 735–762.

Schlosser, F. & Long, N. T. (1970). Expérimentation sur le mur en terre armée d'Incarville. Internal report., LCPC.

Schlosser, F. & Long, N. T. (1973). Étude du comportement du materiau terre armée. *Annles de l'Inst. Techq. du Batiment et des Trav. Publ.* Suppl. No. 304. Sér. Matér. No. 45.

Schlosser, F. & Long, N. T. (1974). Recent results in French research on reinforced earth. *J. Const. Div. Proc. ASCE,* **100,** No. CO3, 223–237.

Schlosser, F. Mandagaran, B. & Ricard, A. (1971). Comportement de graves argileuses artificielles. *Bull. de Liais. LPC,* Comité Francais de Mécanique de Sols et des Fondation, Journées Nationales.

Schlosser, F. & Vidal, H. (1969). La terre armée. *Bull. de Liais. LRPC,* No. 41 (November), pp. 101–144.

Schneebeli, G. (1957). Une analogie mécanique pour l'étude de la stabilité des ouvrages en terre a deux dimensions. *Proc. 4th ICSMFE,* vol. 2, pp. 228–232.

Scott, C. P. (1974). Reinforced earth structure in Tennessee. *Highw. Focus,* **6,** No. 3, 37–52.

Shockley, W. G. & Ahlvin, R. G. (1960). Nonuniform conditions in triaxial test specimens. *Proc. Res. Conf. Shear Strength of Cohesive Soils, ASCE,* pp. 341–357.

Simons, N. E. (1975). Discussion. *Proc. ASCE Cons. Div.,* vol. **101.** CO1, pp. 444–446.

Sims, F. A. & Jones, C. J. F. P. (1979). The use of soil reinforcement in highway schemes. *Proc. Int. Conf. Soil Reinforcement,* Paris, vol. 2, pp. 361–366.

Smith, A. C. S. (1979). Reinforced earth in the mining industry in Southern Africa. *Proc. Int. Conf. Soil Reinforcement,* Paris, vol. 2, pp. 367–372.

Smith, A. K. C. S. (1977). Experimental and computational investigations of model reinforced earth retaining walls. Ph.D. Thesis, Cambridge Univ.

Smith, A. K. C. S. & Bransby, P. L. (1976). The failure of reinforced earth walls by overturning. *Geot.* 26, No. 2, 376–381.

Smith, A. K. C. S. & Wroth, C. P. (1977). The failure of model reinforced earth walls. *Proc. TRRL/Heriot–Watt Univ. Symp. Reinforced Earth and Other Techniques.* TRRL Sup. Rep. 457 (1979), pp. 109–131.

Smith, A. K. C. S. & Wroth, C. P. (1978). The failure of model reinforced earth walls. *Proc. ASCE Symp. Earth Reinforcement,* Pittsburgh, pp. 794–855.

Smith, G. N. & Birgisson, G. I. (1979). Inclined strips in reinforced earth walls. *Civil Engng,* June, pp. 52–63.

Snaith, M. S., Bell, A. L. & Dubois, D. D. (1979). Embankment construc-

tion from marginal material. *Proc. Int. Conf. Soil Reinforcement,* Paris, vol. 1, pp. 175–180.

Stefani, C. & Long, N. T. (1979a). Comportement de semelles sur un massif armée semi-infini. *Proc. Int. Conf. Soil Reinforcement,* Paris, vol. 1, pp. 185–190.

Stefani, C. & Long, N. T. (1979b). Étude sur modèles réduits des radiers en terre armée a la rupture. *Proc. Int. Conf. Soil Reinforcement,* Paris, vol. 1, pp. 191–196.

Steiner, R. S. (1975). Reinforced earth bridges highway sinkhole. *Civil Engng,* ASCE, July, pp. 54–56.

Symons, I. F. (1973). Reinforced earth retaining walls. *Highw. and Road Constr.* (October), pp. 13–18.

Taylor, J. P. & Drioux, J. C. (1979). Utilisation de la terre armée dans le domaine des barrages. *Proc. Int. Conf. Soil Reinforcement,* Paris, vol. 2, pp. 373–378.

Uezawa, H. & Nasu, M. (1973). Anti-earthquake measures for embankment on a weak ground. *Proc. 5th World Conf. – Earthq. Engng.*, pp. 346–355.

Vagneron, J. J. (1972). Reinforced Earth Walls I. M.Sc. Thesis, No. 3919.

Van Leeuwen, J. H. (1977). New methods of determining the stress strain behaviour of woven and non-woven fabrics in the laboratory and in practice. *Proc. Int.Conf. Fabrics in Geotechnics,* Paris, vol. 2, pp. 299–304; vol. 3, p. 102.

Verma, B. P. & Char, A. N. R. (1978). Triaxial tests on reinforced sand. *Proc. Symp. Soil Reinforcing and Stabilising Techq.* NSWIT/NSW Univ., pp. 29–39.

Vidal, H. (1966). La terre armée *Annles Inst. Tech. du Bâtim.* Suppl., vol. 19, No. 223–224. Serie Matériaux 30.

Vidal, H. (1969a). The principle of reinforced earth. *Highw. Res. Rec.,* No. 282, pp. 1–16.

Vidal, H. (1969b). La terre armée. *Annles Inst. Tech. du Bâtim.* Suppl., vol. 22, No. 259–260. Série Matériaux 38.

Vidal, H. (1970). Reinforced earth steel retaining wall. *Civil Engng,* ASCE (February), pp. 72–73.

Vidal, H. (1972). Reinforced earth. *Annles Inst. Tech. du Bâtim.,* Suppl. No. 299, Serie Matériaux 43.

Volman, W., Krekt, L. & Risseeuw, P. (1977). Armature de traction en textile, un nouveau procède pour améliorer la stabilité des grands remblais sur sols mous. *Proc. Int. Conf. Fabrics in Geot.,* Paris, vol. 1, pp. 55–60.

Wager, O. & Holtz, R. D. (1976). Reinforcing embankments by short sheet piles and tie rods. *New Horiz. in Constr. Mater.*, vol. 1. Pennsyl-

vania: Envo Publ. Co. Inc.

Walkinshaw, J. L. (1975). *Reinf. earth constr.* Report No. FHWA–DP–18, Dept. of Transportation, Arlington, Virginia.

Watkins, R. K. (1973). Reinforced soil bridges – they're here. *Proc. XIth Ann. Engng Geol. & Soils Engng Symp.*, Pocatello, Idaho, pp. 55–71.

Westergaard, H. M. (1938). *A problem of elasticity suggested by a problem in soil mechanics, soft material reinforced by numerous strong horizontal sheets.* Stephen Timoshenko 60th Anniversary Volume. New York: Macmillan.

Yamanouchi, T. (1970). Experimental study on the improvement of the bearing capacity of soft ground by laying a resinous net. *Proc. Symp. Founds. on Interbedded Sands.* Australia: Commonwealth Scien. & Indus. Res. Orgn., pp. 144–150.

Yamanouchi, T. (1975). Resinous net applications in earthworks. *Proc. Conf. Soil Stabilisation and Compaction.* Univ. of NSW, pp. 5.1–5.16.

Yang, Z (1972). Strength and deformation characteristics of reinforced sand. Ph.D. Thesis, UCLA.

Index